This is to certify that the
thesis entitled

INVESTIGATIONS ON THE RESPONSE OF KNEE JOINT CARTILAGE TO BLUNT IMPACT IN A SMALL ANIMAL MODEL

presented by

DANIEL I. ISAAC

has been accepted towards fulfillment
of the requirements for the

M.S. degree in Engineering Mechanics

Roger C. Haut
Major Professor's Signature

03/26/09
Date

INVESTIGATIONS ON THE RESPONSE OF KNEE JOINT CARTILAGE TO BLUNT IMPACT IN A SMALL ANIMAL MODEL

By

Daniel I. Isaac

A THESIS

Submitted to
Michigan State University
in partial fulfillment of the requirements
for the degree of

MASTER OF SCIENCE

Engineering Mechanics

2009

ABSTRACT

INVESTIGATIONS ON THE RESPONSE OF KNEE JOINT CARTILAGE TO BLUNT IMPACT IN A SMALL ANMIAL MODEL

By

Daniel I. Isaac

History of joint injury due to participation in SRE, particularly to the knee or hip, increases the risk of developing a chronic joint disease, osteoarthritis. OA is one of the most common and widespread rheumatic diseases responsible for deterioration of articular cartilage, subchondral bone and synovium, ultimately leading to the failure of synovial joints. Experimental studies with animal models have sought to understand the association between acute joint trauma and the development of OA. The research presented in the current thesis makes use of an *in vivo* rabbit model to examine the acute and chronic responses of articular cartilage and subchondral bone to blunt force trauma. Chapter 2 addressed the issues of acute damage to chondrocytes following a single, severe insult to the flexed TF joint. Chapter 3 describes chronic studies where a single impact was again delivered to the TF joint of anesthetized rabbits and the changes in the mechanical and histological properties of the articular cartilage were evaluated six months and one year following trauma. Chapter 4 documented the development of an *in vivo* model of traumatic ACL rupture. Chapter 5 evaluated the efficacy of a mild non-ionic surfactant, poloxamer 188 (P188), in 'repairing' damaged cells after an *in vivo* impact to the rabbit TF joint. Future studies can utilize the data presented to investigate the progression of chronic joint disease and the efficacy of various intervention methods.

DEDICATION

I would to thank my parents and siblings for their continued guidance and support throughout my education. Without their constant guidance and support this would have never been possible.

ACKNOWLEDGMENTS

I would like to acknowledge my professor and mentor Dr. Roger Haut. I am extremely grateful for his support and guidance throughout my graduate education. I am grateful to Dr. Mike Shingles and Dr. Seungik Baek for serving on my committee. I would like to express gratitude towards Cliff Beckett for his technical support and willingness to share his knowledge with me. I would also like to thank Jean Atkinson and Jane Walsh for their constant support, hard work and dedication. Without their assistance in these studies none of this would be possible. Finally, I would like to acknowledge my fellow graduate students for their help and most importantly their friendship: Nurit Golenberg, Tim Baumer, Eric Meyer, Brian Powell, Feng Wei, Jerrod Bramen, and Mark Villwock.

TABLE OF CONTENTS

LIST OF TABLES

LIST OF FIGURES

RESEARCH PUBLICATIONS

PEER REVIEWED MANUSCRIPTS

Isaac DI, Meyer EG, Haut RC, 2008, Chondrocyte damage and contact pressures following impact on the rabbit tibiofemoral joint. Journal of Biomechanical Engineering, 130(4): 041018 1-5

Isaac DI, Golenberg N, Haut RC, 2008, Acute repair of chondrocytes using P188 surfactant in the rabbit tibiofemoral joint following blunt impact. In Preparation.

Isaac DI, Meyer EG, Guillou RP, Dejardin LM, Haut RC, 2008, A traumatic anterior cruciate ligament rupture model: A preliminary study using the rabbit model. Journal of Surgical Research, In Review

Killian ML, Isaac DI, Haut RC, Dejardin LM, Leetun D, Haut Donahue TL, 2008, Traumatic anterior cruciate ligament tear and its implications on meniscal degradation: A preliminary novel lapine osteoarthritis model. Journal of Surgical Research, In Press.

PEER REVIEWED ABSTRACTS

Isaac DI, Meyer EG, Kepich E, Haut RC, Acute chondrocyte damage and chronic changes in the rabbit tibiofemoral joint after impact. 54th Annual Meeting of the Orthopaedic Research Society, 2008

Killian MK, Lepinski NM, Haut RC, Isaac DI, Haut-Donahue TL, *In vivo* changes in glycosaminoglycan content in knee meniscal tissue following traumatic injury. 55th Annual Meeting of the Orthopaedic Research Society, 2009

Lepinski NM, Killian ML, Isaac DI, Haut RC, Haut-Donahue TL, Meniscus tissue response following tibia-femoral impact. 55th Annual Meeting of the Orthopaedic Research Society, 2009

Lepinski NM, Killian ML, Isaac DI, Haut RC, Haut-Donahue TL, Characterizing lapine meniscal tissue: A regional comparison between normal medial and lateral menisci. ASME Bioengineering Conference, 2009, In Review.

Killian ML, Haut RC, Isaac DI, Dejardin LM, Leetun D, Haut Donahue TL, Traumatic anterior cruciate ligament tear and its implications on meniscal degradation: A preliminary novel lapine osteoarthritis model. ASME Bioengineering Conference, 2009, In Review.

Killian ML, Haut RC, Isaac DI, Lepinski, NM, Regional glcosaminoglycan coverage of healthy rabbit menisci, ASME Bioengineering Conference, 2009, In Review.

CHAPTER ONE

INTRODUCTION AND LITERATURE REVIEW

Musculoskeletal and joint injuries in the U.S. have reached epidemic proportions, costing approximately $300 billion annually. Lower extremity injuries account for approximately $21.5 billion each year in treatment, rehabilitation and lost work expenses (Miller, 1995). Furthermore, these injuries are possibly the most predominate cause of disability resulting from automobile accidents. A recent analysis of the National Accident Sampling System (NASS) database shows that knee injuries account for nearly 10% of total injuries resulting from automobile accidents each year (Atkinson, 2000). Injuries can involve gross fracture of bone (States, 1970; States, 1986; Fife et al., 1984), or so-called subfracture injuries, such as microtrauma to bone and cartilage (Atkinson & Haut, 2001; Newberry et al., 1998; Taga et al., 1993; Loomer et al., 1993). As suggested by the NASS, 75% of knee injuries from automobile accidents are these subfracture types, involving no gross fracture of bone (Atkinson, 2000). These injuries are clinically relevant to the long-term health of the joint tissues, as both fracture producing injuries as well as less severe, subfracture types have both been shown to precipitate post-traumatic joint degeneration (States, 1970; Nagel & States, 1977; Colpin et al., 1990; Upadhyay et al., 1983).

Osteoarthritis (OA) is one of the most common and widespread rheumatic diseases responsible for deterioration of articular cartilage, subchondral bone and synovium, ultimately leading to the failure of synovial joints (Peyron et al., 1984; Badley, 1995; Sangha, 2000). Articular cartilage is a connective tissue that lines the ends of bones in diarthroidial joints and acts as a "frictionless" surface over which bones can glide.

Articular cartilage consists of a solid organic matrix and free interstitial fluid (primarily water). The major constituents of the organic matrix of cartilage are collagen (Type II) and proteoglycans (PGs) (Mow, 1990). Imbedded in the solid matrix are cartilage cells known as chondrocytes (Figure 1.1). Chondrocytes are responsible for the synthesis and degradation of the solid matrix constituents. The solid phase (chondrocytes, collagen and proteoglycans) accounts for 15-30% of the weight of articular cartilage. The remaining 70-85% of the weight is water that maintains the pressurized state of the cartilage. Collagen provides structural support for the surface tension that is developed by the pressurized cartilage.

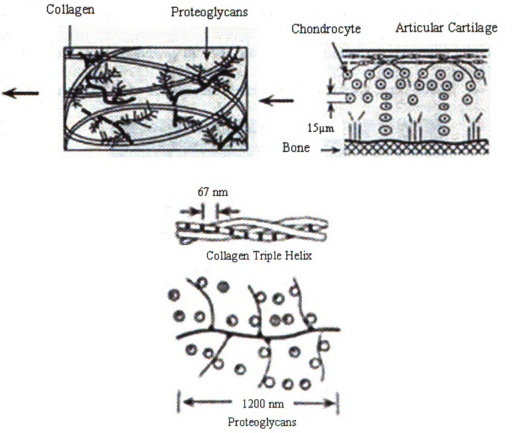

Figure 1.1. Articular cartilage is made up of a solid organic matrix and free intersititial fluid. The solid matrix consists of Type II collagen and proteoglycans with chondrocytes imbedded in the matrix.

While the etiology of OA is currently unknown, the literature suggests that a breakdown in the homeostasis of the solid matrix and chondrocyte death may contribute to the progression of this chronic disease. Biomechanically the cartilage material properties, such as tensile, compressive and shear moduli, change in disease. The hydraulic permeability of cartilage also changes due to degradation of collagen that causes an increase in the water content of the tissue and excessive swelling. Clinically, OA is characterized by joint pain and narrowing of the joint space (Figure 1.2), as diagnosed by radiological examination (Flores and Hochber, 1998). Pathologically, the disease exhibits loss of cartilage and sclerosis of underlying subchondral bone. Although acute injury to cartilage is currently thought to be a factor associated with the development of OA, the pathway that leads from a blunt impact load on the joint cartilage to the development of a chronic disease is yet unknown (Lewis et al., 2003).

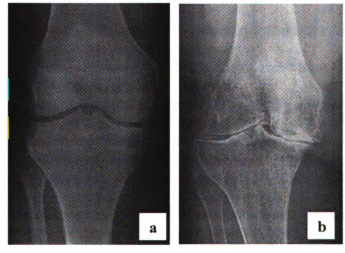

Figure 1.2. Radiograph of a normal (a) and osteoarthritic (b) knee joint showing significant narrowing of the joint space, a clinical sign of OA.

Experimental studies with animal models have sought to understand the potential association between acute joint injury and the development of OA. For example, a recent

study shows that a single, 6 J impact can be delivered to the flexed patello-femoral (PF) joint of the Flemish Giant rabbit leading to progressive degradation of the retro-patellar surface as well as thickening of the underlying subchondral bone (Ewers et al., 2002). Radin et al. (1984) has also shown that cyclic loading of the rabbit tibiofemoral (TF) joint leads to deep fibrillation of articular cartilage along with a stiffening of the underlying subchondral bone. Furthermore, a study by Rundell et al. (2005) indicates that a single 6 J of energy impact to the rabbit PF joint results in lesions on the surface of the retro-patellar cartilage that is associated with a significant number of damaged chondrocytes surrounding the lesions.

Previous studies have hypothesized that damage to chondrocytes following traumatic injury to cartilage may play a key role in the long term development of OA. Cartilage function is believed to deteriorate as a result of chondrocyte death (Blanco et al., 1998). Since chondrocytes are required for matrix repair, and chondrocyte death eventually leads to matrix loss (Simon et al., 1976), chondrocyte death either by apoptosis or necrosis has become a focus of OA research and more recently, cartilage trauma research. Necrotic cell death occurs when a cell is severely injured by physical stress. Damage to the plasma membrane prevents the cell from controlling its fluid and ion balance. Therefore, a defining feature of necrotic cells is swelling and ultimately, rupture (Duke et al., 1996). Conversely, apoptosis is programmed cell death in which the cell undergoes biochemical changes leading to death (Hashimoto et al., 1998). Simon and Green (1971), studying the short-term effects of chondrocyte death induced by freezing, noted a significant loss of stainable proteoglycans without altered collagen content or surface fibrillation. After one year the articular cartilage of rabbit knees showed

biochemical and morphological changes typical of degenerative joint disease (Simon et al., 1976). Normal chondrocytes respond to moderate or low-amplitude dynamic compression by upregulating biosynthetic activity, a property that may contribute to a tissue's ability to withstand compressive loading (Palmoski et al., 1978; Parkkinnen et al., 1992; Sah et al., 1991). Injured chondrocytes may not respond to dynamic mechanical stimulation, either because the cells have lost the ability to do so, or because damage to the extracellular matrix has disrupted the ability for the cells to respond to physical signals, which stimulate biosynthetic activity (Kurz et al., 2001). These data suggest that preventing chondrocyte death and/or matrix damage after excessive levels of blunt loading may help maintain the mechanical integrity of the cartilage; and thereby, helping to mitigate the onset of post-traumatic OA.

With increasing emphasis on physical fitness and a healthy lifestyle in all age groups, participation in sports, recreation and exercise (SRE) is increasingly popular and widespread in American culture. History of joint injury, particularly to the knee or hip increases the risk of chronic joint disease, particularly OA. Two specific acute injuries are strongly associated with development of knee OA; cruciate ligament damage and meniscal tears (Felson, 2004) (Figure 1.3). The anterior cruciate ligament (ACL) is a ligament on the interior of the knee joint that restricts anterior motion of the tibia relative to the femur.

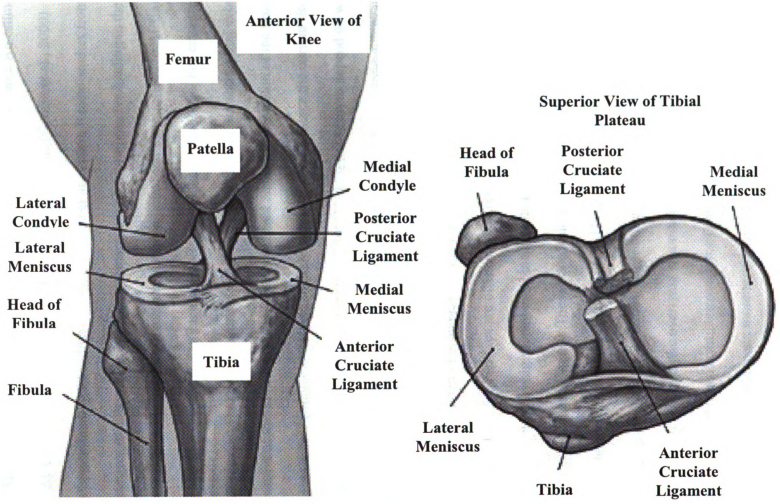

Figure 1.3. Anatomical structures of the knee joint.

The ACL is the most frequently injured ligament in the knee joint. An estimated 80,000 ACL tears occurred in the year 2000 in the U.S. alone (Griffin et al., 2000) costing approximately $2 billion annually (Hewett et al., 2006). Recent studies from our laboratory on ACL tear mechanisms document that high compressive loading in the human knee joint, such as that generated during a jump landing, may lead to ACL rupture with subsequent damage to cartilage and underlying subchondral bone. For example, in a recent study using isolated human cadaver knees our laboratory has shown that excessive compression of the TF joint resulted in a significant anterior subluxation of the tibia causing ACL tear (Meyer and Haut, 2005; Meyer et al., 2008). Since the current literature suggests that the occurrence of post-trauma joint OA does not seem to depend on whether the ACL is reconstructed or not (Myklybust and Bahr, 2005), this "micro-trauma" to subchondral bone and acute cartilage damage may play a large role in the long term progression of chronic joint disease.

Clinically, ACL ruptures are often associated with subchondral bone lesions thought to be caused by significant axial loads transmitted through the cartilage and subchondral bone during injury. These bone lesions are thought to be the basis for geographic bone bruises which are documented in over 80% of patients suffering knee ligament injury (Johnson et al., 1998). These bone injuries are also associated with visible damage to chondrocytes in the overlying articular cartilage. Vellet et al. (1991) documents an overt loss of cartilage overlying these geographic bone bruises in 48% of ACL rupture patients within six months of injury. These occult microcracks of subchondral and/or trabecular bone are thought to be caused by compressive loading during the acute ligamentous injury. A recent study evaluates the acutely ACL injured

knee with MRI and documents that 57% of all knees suffered from at least one cortical depression fracture due to large compressive loading in the joint during the acute ligament injury (Frobell et al., 2008). This study concludes that these cortical depression fractures, likely to be hallmarks of strong compressive forces, indicate severe injury to the cartilage and subchondral bone after ACL injury and may represent risk factors for OA development in the ACL injured knee. Thus, the increased risk of knee OA after ACL injury might, in part, be dependent on the initial trauma as a contributing cause, explaining the lack of success in reducing post-trauma OA by surgical interventions (Frobell et al., 2008).

Currently, the most widely used experimental model of OA is joint instability via anterior cruciate ligament transection (ACLT) (Batiste et al., 2004; Yoshioka et al., 1996; Sah et al., 1997; Vignon et al., 1987; Tiraloche et al., 2005). ACLT has been shown to lead to progressive changes in the morphology, histopathology, and biochemistry of articular cartilage and subchondral bone in the rabbit model (Batiste et al., 2004; Vignon et al., 1987; Tiraloche et al., 2005). Furthermore, MRI evaluation of rabbit knee joints after ACLT shows mild joint effusion (Batiste et al., 2004). This joint instability model of OA has proven effective in generating chronic joint changes consistent with post-traumatic joint disease; however, the model fails to address acute damage to cartilage cells and subchondral bone as a result of large compressive loads generated in the joint during the acute injury, as documented in the clinical literature. Acute chondrocyte damage, subchondral bone lesions and/or instability of the joint generated as a result of acute ACL rupture are suspected factors in the progression of chronic joint disease.

Understanding the mechanisms that lead from acute cartilage damage and the chronic progression of OA are essential in future developments of therapeutic methods to either prevent or treat joint degeneration. The research presented in this thesis makes use of an *in vivo* rabbit model to examine the acute and chronic responses of articular cartilage and subchondral bone to blunt force trauma. Chapter 2 addresses the issue of acute damage to chondrocytes following a single, severe insult to the flexed TF joint. The study hypothesized that a single insult delivered to the flexed rabbit TF joint, without gross fracture to bone or ligament, would result in significant damage to chondrocytes. Chapter 3 describes chronic studies where a single impact was again delivered to the TF joint of anesthetized rabbits and the changes in the mechanical and histological properties of the articular cartilage were evaluated six months and one year following trauma. Chapter 4 documents the development of a "Bona Fide model" for *in vivo,* traumatic ACL rupture. This "first of its kind" model is compared to the widely used ACLT method. This study hypothesized that compressive loads generated in the joint during traumatic ACL rupture would result in significantly more damage to articular cartilage and subchondral bone compared to the conventional ACLT model. Chapter 5 evaluates the efficacy of a mild non-ionic surfactant, poloxamer 188 (P188), in 'repairing' damaged cells after an *in vivo* impact to the rabbit TF joint.

The research presented in this thesis provides useful data in regards to the response of articular cartilage to blunt impact loading in the *in vivo* setting. Furthermore, a therapeutic treatment has been investigated and found to be effective in preventing damage to chondrocytes following traumatic injury, which may prevent long term degradation of articular cartilage. A "Bona Fide" model of *in vivo*, traumatic ACL

rupture has also been developed to address the long term implications of damage to articular cartilage and subchondral bone during the acute ligamentous injury. Future studies can utilize the data presented to investigate the progression of chronic joint disease and the efficacy of various intervention methods to mitigate post-trauma OA following rupture of the ACL.

REFERENCES

Atkinson PJ, Haut RC, 2001, "Injuries Produced by Blunt Trauma to the Human Patellofemoral Joint Vary with Flexion Angle of the Knee," J Orthop Res, **19,** 827-833.

Atkinson T, Atkinson P, 2000, "Knee Injuries in Motor Vehicle Collisions: A Study of the National Accident Sampling System Database for the Years 1979- 1995," Acc. Anal. Prev., **32,** pp. 779-786.

Bahr R, Myklebust G, 2005, "Return to Play Guidelines after Anterior Cruciate Ligament Surgery," Br J Sports Med, **39,** pp. 127-131.

Batiste, D., Kirkley, A., Laverty, S., Thain, L., Spouge, A., Holdsworth, D., 2004. *Ex vivo* characterization of articular cartilage and bone lesions in a rabbit ACL transection model of osteoarthritis using MRI and micro-CT. OA Cart. 12, 986-996.

Blanc FJ, Guitian R, Vazquez-Martul E, DeTorro FJ, Galdo F, 1998, "Osteoarthritis Chondrocytes Die by Apoptosis: A Possible Pathway for Osteoarthritis Pathology," Arth Rheum, **41,** pp. 284-289.

Duke RC, Ojcius DM, Young JD, 1996, "Cell Suicide in Health and Disease," Scientific American, **275,** pp. 80-87.

Ewers BJ, Weaver BT, Sevensma ET, Haut RC, 2002, "Chronic Changes in Rabbit Retro-Patellar Cartilage and Subchondral Bone after Blunt Impact Loading of the Patello-Femoral Joint," J Orthop Res, **20,** pp.545-550.

Felson D, 2004, "An Update on the Pathogenesis and Epidemiology of Osteoarthritis," Radiologic Clinics North Am, **42,** pp. 1-9.

Flores R, Hochber M, 1998, "Definition and Classification of Osteoarthritis," Brandt K, Doherty M, Lohmander S, editors. Osteoarthritis. Oxford: Oxford University Press, pp. 1-12.

Frobell RB, Roos HP, Roos EM, Hellio Le Graverand MP, Buck R, Tamez-Pena J, Totterman S, Boegard T, Lohmander LS, 2008, "The Acutely ACL Injured Knee Assessed by MRI: Are Large Volume Traumatic Bone Marrow Lesions a Sign of Severe Compression Injury?," Osteoarthritis and Cartilage, **16,** pp. 829-836.

Griffin L, Agel J, Albohm M, 2000, "Non-contact Anterior Cruciate Ligament Injuries: Risk Factors and Prevention Strategies," J Am Acad Orthop Surg, **8,** pp. 141-150.

Hashimoto S, Ochs R, Komiya S, Lotz M, 1998, "Linkage of Chondrocyte Apoptosis and Cartilage Degradation in Human Osteoarthritis," Arth Rheum, **41,** pp. 1632-1638.

Hewett T, Myer G, Ford K, 2006, "Anterior Cruciate Ligament Injuries in Female Athletes: Part 1, Mechanisms and Risk Factors," Am J Sports Med, **34,** pp. 299-311.

Johnson DL, Urban WP, Carbon DNM, Vanarthos WJ, Carlson CS, 1998, "Articular Cartilage Changes Seen with Magnetic Resonance Imaging-Detected Bone Bruises Associated with Acute Anterior Cruciate Ligament Rupture," Am J Sports Med, **26**, pp. 409-414.

Kurz B, Jin M, Patwari P, Cheng DM, Lark MW, Grodzinsky AJ, 2001, "Biosynthetic Response of Mechanical Properties of Articular Cartilage after Injurious Compression," J Orthop Res, **19**, pp. 1140-1146.

Lewis JL, Deloria LB, Oyen-Tiesma M, Thompson RC Jr., Ericson M, Oegema TF Jr., 2003, "Cell Death after Cartilage Impact Occurs Around Matrix Cracks," J Orthop Res, **21**, 881-887.

Meyer E, Baumer T, Slade J, Smith W, Haut R, 2008, "Tibiofemoral Contact Pressures and Osteochondral Microtrauma During ACL Rupture due to Excessive Compressive Loading and Internal Torque of the Human Knee," Am. J. Sports Med, **36**, pp. 1966-1977.

Meyer E, Haut R, 2005, "Excessive Compression of the Human Tibio-Femoral Joint Causes ACL Rupture," J Biomech, **38**, pp. 2311-2316.

Miller TR, Martin PG, Crandell JR, 1995, "Cost of Lower Limb Injuries in Highway Crashes," Proc ICPLEI, pp. 47-57.

Mow VC, 1990, "Fundamentals of Articular Cartilage and Meniscus Biomechanics," Articular Cartilage and Knee Joint Function: Basic Science and Arthroscopy, J.W. Ewing, ed., Raven Press, Ltd., New York, pp. 1-18.

Nagel WN, States J, 1977, "Dashboard and Bumper Knee-Will Arthritis Develop?," AAAM21, pp. 272-278.

Newberry WN, Garcia JJ, Mackenzie CD, Decamp CE, Haut RC, 1998, "Analysis of Acute Mechanical Insult in an Animal Model of Post-Traumatic Osteoarthritis," J Biomech Eng, **120**, pp. 704-9.

Parkkinen JJ, Lammi MJ, Helminen HJ, Tammi M, 1992, "Local Stimulation of Proteoglycan Synthesis in Articular Cartilage Explants by Dynamic Compression In Vitro," J Orthop Res, **10**, pp. 610-620.

Radin EL, Martin RB, Burr DB, Caterson B, Boyd RD, Goodwin C, 1984, "Effects of Mechanical Loading on the Tissues of the Rabbit Knee," J Orthop Res, **2**, pp. 221-234.
Rundell SA, Baars DC, Phillips DM, Haut, RC., 2005, "The Limitation of Acute Necrosis in Retro-Patellar Cartilage after a Severe Blunt Impact to the In-Vivo Rabbit Patello-Femoral Joint," J Orthop Res, **23**, pp.1363-1369.

Sah RL, Yang AS, Chen AC, Hant JJ, Halili RB, Yoshioka M, Amiel D, Coutts RD, 1997, "Physical Properties of Rabbit Articular Cartilage after Transection of the Anterior Cruciate Ligmaent," J Orthop Res, **15**, pp. 197-203.

Simon WH, Richardson S, Herman E, Parsons JR, Lane J, 1976, "Long-term Effects of Chondrocyte Death on Rabbit Articular Cartilage In Vivo," J Bone Joint Surg Am, **58**, pp. 517-526.

States J, 1986, "Adult Occupant Injuries of the Lower Limb," Proc Symp Biomech, pp. 97-107.

States JD, 1970, "Traumatic Arthritis: A Medial Dilemma," Proc 14th Ann Conf Am Assoc Automotive Med, **14**, pp. 21-28.

Tiraloche G, Girard C, Chouinard L, Sampalis J, Moquin L, Ionescu M, Reiner A, Polle AR, Laverty S, 2005, "Effect of Oral Glucosamine on Cartilage Degradation in a Rabbit Model of Osteoarthritis," Arth Rheum, **54**, pp. 1118-1128.

Vellet AD, Marks PH, Fowler PJ, Munro TG, 1991, "Occult Posttraumatic Osteochondral Lesions of the Knee: Prevalence, Classification, and Short-Term Sequelae Evaluated with MR Imaging," Radiology, **178**, pp. 271-276.

Vignon, E., Bejui, J., Mathiew, P., Hartmann, J., Ville, G., Evreux, J., Descotes, J., 1987. Histological cartilage changes in a rabbit model of osteoarthritis. J. Rheum. 14, 104-106

Yoshioka, M., Coutts, R., Amiel, D., 1996. Characterization of a model of osteoarthritis in the rabbit knee. OA and Cart. 4, 87-98.

CHAPTER TWO

CHONDROCYTE DAMAGE AND CONTACT PRESSURES FOLLOWING IMPACT ON THE RABBIT TIBIOFEMORAL JOINT

ABSTRACT

Epidemiological studies show that tibial plateau fractures comprise about 10% of all below-knee injuries in car crashes. Studies from this laboratory document that impacts to the tibiofemoral (TF) joint at 50% of the energy producing gross fracture can generate cartilage damage and micro-cracks at the interface between calcified cartilage and underlying subchondral bone in the tibial plateau. These injuries are suggestive of the initiation for a long term chronic disease, such as osteoarthritis. The disease process may be further encouraged by acute damage to chondrocytes in the cartilage overlying areas of occult micro-cracking. The hypothesis of the current study was that significant damage to chondrocytes in tibial plateau cartilage could be generated in areas of high contact pressure by a single impact delivered to the rabbit TF joint, without a gross fracture of bone. Three rabbits received a single, 13 J of energy blunt insult to the tibiofemoral joint, while another three animals were used as controls. Cell viability analyses compared chondrocyte damage in impacted versus control cartilage. Two additional rabbits were impacted to document contact pressures generated in the tibiofemoral joint. The study showed high contact pressures in uncovered areas of the plateau, with a trend for higher pressures in the lateral versus medial facets. A significantly higher percentage of damaged chondrocytes existed in impacted versus the opposite, non-impacted limbs. Additionally, more chondrocyte damage was documented in the superficial zone (top 20% of cartilage thickness) of the cartilage compared to

middle (middle 50% of thickness) and deep (bottom 30% of thickness) zones. This study showed that a single blunt insult to the *in situ* rabbit TF joint, generating large areas of contact pressure exceeding 20MPa produce significant chondrocyte damage in the tibial articular cartilage, esp. in the superficial zone, without gross fracture of bone. Future studies will be needed to investigate the long term, chronic outcome of this blunt force joint trauma.

INTRODUCTION

Injuries to the lower extremity are possibly the most predominant cause of disability resulting from automobile accidents. Analysis of the National Automotive Sampling System/Crashworthiness Data System (NASS) shows that knee injuries account for approximately 10% of the total injuries resulting from automobile accidents each year (Atkinson & Atkinson, 2000). Epidemiological studies show that tibial plateau fractures comprise about 10% of all below-knee injuries in car crashes (Taylor et al., 1997; Sherwood et al., 1999). These injuries carry a poor prognosis because they disrupt the articular cartilage in a weight-bearing joint, which can lead to long-term complications such as malunion and osteoarthritis (Funk et al., 2000). The NASS data also suggests that 75% of knee injuries result in no gross bone fracture (Atkinson & Atkinson, 2000). Previous studies on cadaver joints indicate impacts on the tibiofemoral (TF) joint at 50% of the fracture energy can generate micro-cracks at the cement line under the tibial plateau (Banglmaier et al., 1999). Interestingly, automobile accident victims reporting knee pain with no gross bone fracture show bone bruises in approximately 25% of cases (Atkinson et al., 2008). Bone bruises are also documented in over 80% of patients suffering knee ligament injury (Johnson et al., 1998). These bone injuries are also associated with visible damage to chondrocytes in the overlying articular cartilage. Since the current literature indicates these patients will likely generate a chronic disease in the injured joint, whether they are reconstructed or not (Bahr & Myklebust, 2005), a working hypothesis of this laboratory is that compressive loads generated in the knee during ACL rupture may initiate a chronic disease due to acute damage of chondrocytes in joint cartilage. The objective of the current study was to develop a small

animal model for study of the potential for chronic disease following impact loading of the TF joint, without causing gross bone fracture, that generates significant cartilage cell damage.

Our laboratory has previously developed an *in vivo* impact model using the patello-femoral (PF) joints of Flemish Giant rabbits (Ewers et al., 2002). Softening of the retro-patellar cartilage and thickening of the underlying subchondral bone has been observed within one year. Significant histological changes, such as the loss of proteoglycan staining, ossification and erosion of the retro-patellar cartilage have also been observed in the impacted limbs within three years. These changes are consistent with early stages of osteoarthritis (Pritzker, 1998). A recent study by this laboratory has also indicated that lesions produced on the surface of retro-patellar cartilage are associated with a significant number of damaged chondrocytes (Rundell et al., 2005). Acute damage to these cells is currently thought to be associated with the long term development of osteoarthritis (Colwell et al., 2001; Blanco et al., 1998). The hypothesis of the current study was that a single, severe level of blunt force delivered to the rabbit TF joint could produce high contact pressures and a significant number of damaged chondrocytes in the articular cartilage overlying the tibial plateau, without gross fracture of bone in the joint. The future plan is then to use this model to study long term consequences of an acute blunt force trauma in a live animal.

MATERIALS AND METHODS

Eight skeletally mature Flemish Giant rabbits (5.7 ± 0.1 kg) were used in the study. The investigation was approved by the Michigan State University All-University Committee on Animal Use and Care. All animals were housed in individual cages (152 x

152 x 36 cm) prior to the study. Three rabbits received a blunt force insult to the left TF joint using a previously described drop tower (Ewers et al., 2002; Rundell et al., 2005), with a newly designed restraint system. All animals were sacrificed with 85.9 mg/kg BW Pentobarbital I.V., prior to impact. Three non-impacted animals served as controls. Another two animals were used to measure joint contact pressures developed during the impact.

The drop tower used a sled that was arrested electronically after one impact. A pre-crushed, deformable impact head (Hexcel, 3.76 MPa crush strength) was used to ensure uniform loading over the femur (Figure 2.1).

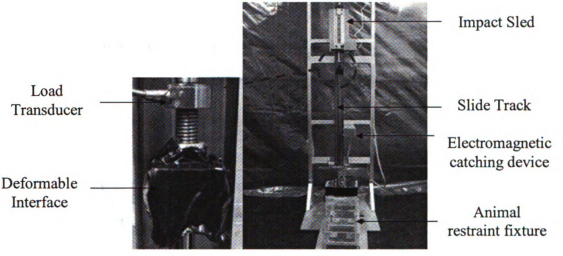

Figure 2.1. The drop tower fixture consisted of a slide track designed to prevent rotation of the dropped sled during impact. After a single impact the sled was arrested electronically by an electromagnetic catching device. The impact interface was a pre-crushed, deformable surface (Hexcel, 3.76 MPa crush strength) mounted in front of a 1000-pound load transducer.

The impact interface was mounted in front of a 4.45 kN (1000 lb) load transducer (model AL311CV, 1000lb capacity, Sensotec, Columbus, OH). Pilot studies with a 1.33 kg mass dropped from 0.7 m (9.1 J of potential energy) generated approximately 737 ± 68.9 N of impact force on the joint, but it did not alter the mechanical properties of TF joint

cartilage (Meyer, 2004). In the current study the impact mass was increased to 1.75 kg, and it was dropped from 0.75 m (~13 J).

The animal was laid supine in the fixture (Figure 2.2). The knee was flexed 90°. The foot was fixed in a boot with three Velcro straps. Two Velcro straps were crossed over the femur. The tibia was constrained to limit anterior motion of the tibia during impact. The leg was positioned so that the dropped mass struck the distal femur and axially loaded the tibia.

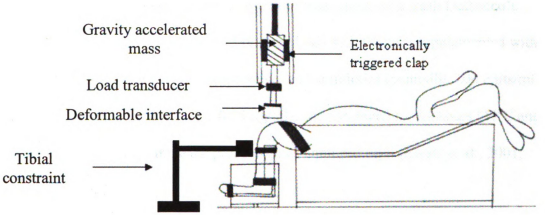

Figure 2.2. Impact experiments were performed by dropping a gravity-accelerated mass onto the flexed tibial-femoral joint with approximately 13 J of potential energy. The rabbit was oriented such that the deformable interface struck the distal femur with impact forces oriented axially in the tibia.

Hind limbs of another two animals were used to measure TF contact pressures and contact areas from the impact. Pressure sensitive film packets (Prescale, Fuji Film Ltd., Tokyo, Japan) were inserted through anterior and posterior joint capsules. After impact the film was removed from the packet and scanned (Scanmaker MRAS-1200E6, Microtek, Taiwan). The entire area of contact was digitized (Photostyler, version 1.1A, Aldus Co., Seattle, WA) at 150 dpi in 8-bit gray scale. The gray scale was converted to pressure (Scion Image 2.0, 2005) and the average pressure, total contact area and total

area having pressure over 20 MPa were determined using established protocols (Atkinson et al., 1998).

For the three impact-control and the three control-control specimens, the knee joints were cleaned and the articular capsule was opened. The meniscal location on the tibial plateau was photographed. A diamond saw (Isomet 11-1180 Low Speed Saw, Buehler, Lake Bluff, IL.) was used to split the tibial plateau into medial and lateral compartments. The facets were then undercut leaving 1-2 mm of bone and rinsed 3 times with culture media before being placed in separate wells filled with fresh Dulbecco's modified Eagle's medium (DMEM): F12 (Gibco, USA #12500-062) supplemented with 10% fetal bovine serum, additional amino acids, and antibiotics (penicillin 100 units/ml, streptomycin 1μg/ml, amphotericin B 0.25 μg/ml), and incubated for 24 hours (37°C and 95% humidity) to help maximize the percentage of damaged cells (Ewers et al., 2001; Phillips et al., 2004).

Following incubation, the specimens were prepared for cell viability analyses. The posterior half of each facet was fixed to a rectangular aluminum block (Figure 2.3) attached to a rotary microtome (Model 45; Lipshaw Mfg., Detroit, MI) using glue (*Zap-A-Gap*, Pacer Tech., Rancho Cucamonga, CA). After 7-10 minutes, while the specimen was sprayed with phosphate buffered saline (PBS), approximately 18 slices, 150 μm thick were cut and placed in individual wells with fresh media.

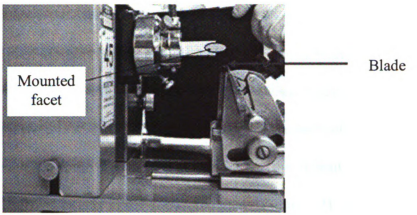

Figure 2.3. The posterior half of the subchondral bone was glued to a rectangular aluminum block which was attached to a rotary microtome. Approximately 7-10 minutes of drying time was allowed, as PBS was continually applied to the cartilage surface. Approximately 18 slices, each 150 μm thick, was taken from each facet for analysis.

The cell viability analyses followed previous procedures (Rundell et al., 2005). Briefly, four slices from each facet were rinsed with PBS and stained with calcein AM and ethidium homodimer (EthD-1), according to the manufacturer's specifications (Live/Dead Cytotoxicity Kit, Molecular Probes, Eugene, OR). Prior to imaging, each sample was rinsed three times with PBS. Viable cells were distinguished by the presence of fluorescent (green) calcein AM. Damaged cells were distinguished by a bright red fluorescence. The number of green and red cells was manually counted with an image analysis program (Image J, National Institutes of Health, 2004).

The number of total cells and the percentages of damaged (red) cells in opposite limbs were compared. Data from four slices on each facet were averaged, and the data from each of the three animals was combined. Two factors (limbs, facet) repeated measures ANOVA (Sigma Stat, SPSS Inc., Chicago, IL) compared the percentage damaged cells in opposite limbs and as a function of facet. Paired t-tests were used to evaluate differences in contact pressures and areas between facets. Statistically significant differences were indicated at $p<0.05$.

RESULTS

Examination of joints after impact indicated no gross bone fractures or ligament damage. The meniscus was always intact. The average peak, inertially-compensated load and impact duration were 1175 ± 29.8 N and 23.0 ± 0.2 ms, respectively (n=3).

Post-test mapping of the pressure film location onto the plateau indicated high contact pressures centered largely in the uncovered areas (Figure 2.4). The average contact pressures on the medial and lateral facets were 19.6 ± 1.2 MPa (n=4) and 23.9 ± 3.7 MPa (n=4), respectively. While the pressure on the lateral facet was approximately 18% higher than on the medial facet, this difference was not significant (p=0.25). The average maximum peak pressures on the medial and lateral facets were 43.1 ± 5.8 MPa and 45.4 ± 7.2 MPa, respectively.

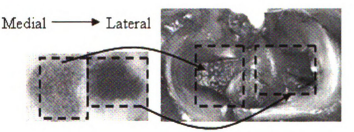

Figure 2.4. Impact induced contact pressure distributions and contact areas in the tibial femoral joint were measured by pressure sensitive film. Mapping the pressure distributions onto the tibial plateau showed that the location of highest contact pressures was largely in the area not covered by the meniscus.

Analysis of contact area having pressures between 20 to 49 MPa showed no difference (p=0.24) between the lateral and medial facets, being approximately 17.1 ± 1.2 mm^2 and 13.7 ± 4.4 mm^2, respectively.

No significant differences existed in the percentage of viable cells (n = 3) between right and left control limbs (p=0.21). No significant differences were measured between right and left limbs in the lateral (p=0.54) or medial (p=0.24) facets. Therefore, these data

were combined. The percentages of damaged cells in the lateral and medial facets were 24.9 ± 12.3% and 22.4 ± 9.7%, respectively.

Cell viability analyses in each facet indicated significant differences in the percentages of damaged cells in impacted versus unimpacted limbs for the medial ($p=0.01$) and lateral ($p<0.001$) compartments (Figure 2.5). There was also a trend ($p=.067$) for more damaged cells in the lateral than medial facets of impacted limbs.

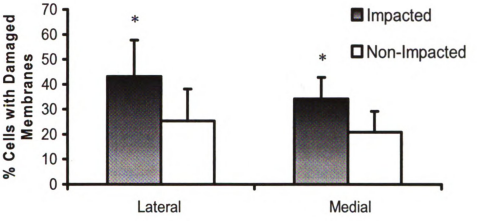

Figure 2.5. The percentage of cells with damaged membranes was manually quantified using an image processing and analysis program. Significantly more damaged cells were observed in both the medial and lateral facets of the impacted samples when compared to the opposite, non-impacted limbs. Statistical differences in the percentage of cells with damaged membranes are denoted by an asterisk. Statistical differences were found using a two factors repeated measures ANOVA with $p<0.05$ for statistical significance.

Finally, slices from impacted limbs were photographed and the cartilage layer was divided into three zones: superficial (top 20%), middle (middle 50%), and deep (bottom 30%) (Figure 2.6).

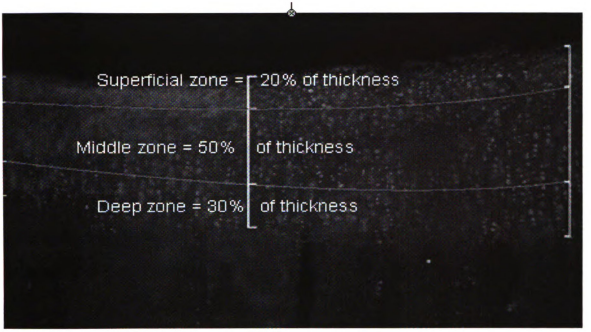

Figure 2.6. The stained osteochondral explants were imaged and divided into three zones: superficial, middle, and deep. Cell viability was measured in the thin sections of cartilage and bone.

Significantly more damaged cells existed in the superficial layer of the lateral facet compared to the middle ($p<0.001$) and deep ($p<0.001$) zones (Figure 2.7). In contrast, in the medial facet the superficial zone had more damaged cells than the deep zone ($p=0.043$), but not more than the middle zone ($p=0.13$).

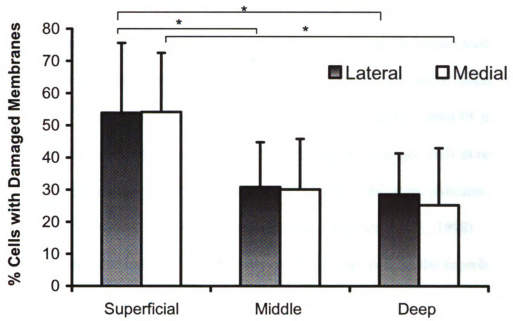

Figure 2.7. Significantly more damaged cells were observed in the superficial layer of the lateral facet when compared to the middle and deep zones. Also, significantly more damaged cells were observed in the superficial zone of the medial facet when compared to the deep zone; however, no difference was observed when the superficial zone was compared to the middle zone. Statistical differences in the percentage of dead cells were denoted by an asterisk. The statistical analyses were based on two-factor ANOVA's with $p<0.05$ for statistical significance.

DISCUSSION

This study showed that high intensity impacts produced contact pressures on the medial and lateral tibial facets of approximately 20 MPa and 24 MPa, respectively. Furthermore, the 13 J of impact potential energy produced significant chondrocyte damage in articular cartilage overlying the tibial plateau. These data were consistent with Torzilli et al. (1999) using bovine chondral explants where significant necrosis was documented at contact pressures of 15-20 MPa. Repo and Finlay (1977), on the other hand, show that contact pressures greater than 25 MPa generate significant chondrocyte necrosis using *in vitro* human osteochondral explants. The current study also showed a tendency for higher contact pressures and more contact area with pressures $\geq$ 20 MPa in

the lateral versus medial facet. These data correlated with a statistical trend for a greater percentage of damaged cells in lateral versus medial facets (Figure 6). Impact loading also increased the percentage of damaged chondrocytes in lateral and medial facets by approximately 18% and 14%, respectively. In a similar study using the rabbit PF joint, a 6 J impact, with a rigid interface, resulted in a 15% increase in damaged cells in retro-patellar cartilage (Rundell et al., 2005). Another study by this laboratory indicates that the PF contact pressures were ~ 27 MPa for similar impacts (Newberry et al., 1998).

Our findings also indicated significantly more damaged cells in the superficial (top 20% of cartilage thickness) than in the middle and deep zones. Other studies document significant damage to chondrocytes in the superficial and middle zones of bovine chondral explants subjected to low rate (35MPa/s) unconfined compression at contact pressures of 15-20 MPa (Torzilli et al., 1999). At pressures greater than or equal to 20 MPa, the former study also documents cell death throughout the entire thickness of the explants. Krueger et al. (2003) documents that high rate (~500 MPa/s), unconfined compression experiments to 25 MPa on bovine chondral and osteochondral explants yield approximately 50% and 30% cell death in the superficial zones, respectively. The former study also documents cell death throughout the middle zone, but not the deep zone of either chondral or osteochondral explants. The current study generated contact pressures of approximately 1000 MPa/s, and it also showed that the deep zone had significantly less cell death than the superficial zone. A recent study, using an open joint with a rigid impact interface on the rabbit femoral condyle, documents cell death initiating in the superficial layer of cartilage at ~ 20MPa (for 420MPa/s) near the edges of the impactor and more uniformly across the entire contact area at 25MPa . Thus, the distribution of

cell death through the cartilage thickness in the current *in situ* study generally paralleled with the findings of Krueger et al (2003) on osteochondral explants and Milentijevic et al (2005) using an open joint, *in situ* rabbit model. The former study also showed that cell death increases in depth with increasing contact pressures (2.8 ± 2% thickness/MPa), until full thickness death at contact pressures ≥ 40 MPa (Milentijevic et al., 2005). Based on these *in situ* studies, the investigators conducted *in vivo* experiments at 35MPa (for 420 MPa/s) and document "arthritic" changes in the joint by 3 weeks post injury.

There were a number of limitations in the current study. One limitation was the potential effect on joint contact mechanics of inserting Fuji Film packets into the rabbit joint. Theoretical studies have shown that the measured contact pressures may be in error by 14-28 percent (Wu et al., 1998). But, by using the Fuji Film method, we are able to compare the current results with previous studies by this laboratory from the *in situ* rabbit and the human PF (Atkinson and Haut, 2001) and TF joints (Banglmaier et al., 1999). Another limitation of the current study was that we did not accurately locate the position of each slice on the facet with respect to the meniscus. These data would have provided more information to correlate the exact distribution of damaged cells with respect to the overlying contact pressure. The sample size of the current study was also small leading to relatively large standard deviations in chondrocyte viability data. This may have contributed to a low statistical power between zonal data, for example. While significant cell damage was documented in both impact and non-impacted slices, we discounted co-culturing with bone as the problem since we previously co-cultured osteochondral explants for a longer period without a problem (Krueger et al., 2003). Rather, while we attempted to optimize our cutting methods, we still believe the baseline cell damage in all

sections was likely due to a cutting artifact in the making of thin slices of cartilage on bone. But, this existed in all slices and we were still able to measure a statistical effect due to impact loading. We were further concerned that removal of the thin tibial cartilage from the underlying bone across a complex contour of the plateau might also cause significant damage to chondrocytes, especially in the deep zone.

While 22-25% cell death in unimpacted, control specimens may seem quite high it does seem to be in accordance with current literature documenting baseline chondrocyte death in a variety of animal models. Particularly, Gulata et al and Rundell et al (2005) document approximately 19% dead cells in unloaded rabbit femoral condyle articular cartilage and 12% cell death in unloaded rabbit patella, respectively. To the authors knowledge, there currently exists no literature documenting baseline cell death percentages in the unloaded rabbit tibial plateau. Furthermore, we do not believe there to be 100% viable cells in unloaded articular cartilage, possibly due to the fact that there is no blood supply to provide the agents for rapid removal of damaged cells, as in may other types of tissue (Roach and Clarke, 2000). Most importantly, however, is that this study does document a statistical increase in the percentage of dead cells in the impacted articular cartilage when compared to the unloaded controls.

A major outcome of the current study was the establishment of a "closed joint" model for *in vivo* loading of the TF joint. The model will be utilized in future investigations to study potential correlations of acute cell damage with the pathogenesis of a post-traumatic OA in the joint. Studies can then proceed, for example, to investigate the long term efficacy of intervention methods to acutely repair damaged cell membranes in the impacted articular cartilage (Phillips et al., 2004).

REFERENCES

Atkinson PJ, Cooper TG, Anseth SM, Walter NE, Kargus R., Haut RC, 2008, "Knee Bone Bruies Frequencies Vary with Time Post-Injury and Type of Soft Tissue Injury," Orthop., **31**, pp. 440.

Atkinson PJ, Haut RC, 2001, "Impact responses of the flexed human knee using a deformable impact interface," J. Biomech.Eng., **123(3)**:205-211.

Atkinson PJ, Newberry WN, Atkinson TS, Haut RC, 1998, "A Method to Increase the Sensitive Range of Pressure Sensitive Film," J. Biomech., **31**, pp. 855-859.

Atkinson T, Atkinson P, 2000, "Knee Injuries in Motor Vehicle Collisions: A Study of the National Accident Sampling System Database for the Years 1979- 1995," Acc. Anal. Prev., **32**, pp. 779-786.

Bahr R, Myklebust G, 2005, "Return to Play Guidelines after Anterior Cruciate Ligament Surgery," Br. J. Sports Med., **39**, pp. 127-131.

Banglmaier RF, Dvoracek-Driksna D, Oniang'o TE, Haut RC, 1999, "Axial Compressive Load Response of the 90° Flexed Human Tibiofemoral Joint," 43rd Stapp Car Crash Conf. Proc., pp. 127-139.

Blanco FJ, Guitian R, Vazquez-Martul E, DeToro FJ, Galdo F, 1998, "Osteoarthritis chondrocytes die by apoptosis-a possible pathway for OA pathology," Arth. Rheum., 41(2), pp. 284-289.

Colwell CW, D'Lima DD, Hoenecke HR, Fronek J, Pulido P, Morris BA, Chung C, Resnick D, Lotz M, 2001, "In vivo changes after mechanical injury," Clin. Orthop. Rel. Res., **391S**, pp. S116-S123.

Ewers B, Krueger J, Dvoracek-Dricksna D, Orth M, Haut R, 2001, "Chondrocyte viability decreases over 24 hours post-impact in a mechanically traumatized cartilage explant," 47th Mtging Orthop. Res. Society, 2001.

Ewers BJ, Weaver BT, Sevensma ET, Haut RC, 2002, "Chronic Changes in Rabbit Retro-Patellar Cartilage and Subchondral Bone after Blunt Impact Loading of the Patello-Femoral Joint," J. Orthop. Res., **20**, pp. 545-550.

Funk JR, Tourret LJ, Crandall JR, 2000, "Experimentally Produced Tibial Plateau Fractures," Int. Res. Council Biomech. Injuries, pp. 171-182.

Johnson DL, Urban WP, Caborn DNM, Vanarthos WJ, Carlson CS, 1998, "Articular Cartilage Changes Seen With Magnetic Resonance Imaging-Detected Bone Bruises Associated With Acute Anterior Cruciate Ligament Rupture," Am. J. Sports Med., **26**, pp. 409-414.

Krueger JA, Thisse P, Ewers BJ, Dvoracek-Driksna D, Orth MW, Haut RC, 2003, "The Extent and Distribution of Cell Death and Matrix Damage in Impacted Chondral Explants Varies with the Presence of Underlying Bone," J. Biomech. Eng., **125**, pp. 1-6.

Meyer EG, 2004, "Biomechanical response of tissues to various blunt impact orientations," M.S. Thesis, Michigan State University, East Lansing, MI.

Milentijevic D, Rubel IF, Liew ASL, Helfet DL, Torzilli PA, 2005, "An in vivo rabbit model fro cartilage trauma. A preliminary study of the influence of impact stress magnitude on chondrocyte death and matrix damage," J. Orthop. Trauma, **19**, pp 466-473.

Newberry WN, Garcia JJ, Mackenzie CD, Decamp CE, Haut RC, 1998, "Analysis of Acute Mechanical Insult in an Animal Model of Post-Traumatic Osteoarthrosis," J. Biomech. Eng., **120**, pp. 704-709.

Phillips DM, Haut RC, 2004, "The Use of a Non-Ionic Surfactant (P188) to Save Chondrocytes from Necrosis Following Impact Loading of Chondral Explants," J. Orthop. Res., **22**, pp. 1135-1142.

Pritzker KPH, 1998, "Pathology of osteoarthritis," In Osteoarthritis, Edited by Brandt, K.D., Doherty, M., Lohmander, L.S., Oxford University Press. Chapter 5, pp. 50-61.

Repo R, Finlay J, 1977, "Survival of Articular Cartilage after Controlled Impact," J. Bone Jt. Surg., **59-A (8)**, pp. 1068-1076.

Rundell SA, Baars DC, Phillips DM, Haut RC, 2005, "The Limitation of Acute Necrosis in Retro-Patellar Cartilage after a Severe Blunt Impact to the In-Vivo Rabbit Patello-Femoral Joint," J. Orthop. Res., **23**, pp. 1363-1369.

Sherwood C, O'Neill B, Hurwitz S, 1999, "Lower extremity Causation in Frontal Crashes," Proc. 1999 Int. Conf. Biomech. Impact, Sitges, Spain, pp 513-524.

Taylor A, Morris A, Thomas P, Wallace A, 1997, "Mechanisms of Lower Extremity Injuries to Front Seat Car Occupants – An in Depth Accident Analysis," Proc. 1997 Int. Conf. Biomech. Impact, Hannover, Germany, pp 53-72.

Torzilli PA, Grigiene R, Borrelli J Jr, Helfet DL, 1999, "Effect of Impact Load on Articular Cartilage: Cell Metabolism and Viability, and Matrix Water Content," J. Biomech. Eng., **121**, pp. 433-441.

Wu JZ, Herzog W, Epstein M, 1998, "Effects of Inserting Pressensor Film into Articular Joints on the Actual Contact Mechanics," J. Biomech. Eng., **120**, pp. 655-659.

CHAPTER THREE

CHRONIC CHANGES IN THE MECHANICAL AND HISTOLOGICAL PROPERTIES OF RABBIT ARTICULAR CARTILAGE FOLLOWING TIBIOFEMORAL IMPACT

ABSTRACT

Characteristic osteochondral lesions have been strongly correlated with ACL trauma, as well as in the clinical literature of patients with no reported ligamentous injury. These lesions are associated with occult microcracks of subchondral and/or trabecular bone. Of concern in today's clinical literature is that there is evidence of acute injury to articular cartilage overlying these bone bruises, which may predispose the tissue to degenerative changes. Previous studies using the rabbit patellofemoral (PF) joint have shown that a single impact to the flexed rabbit knee results in significant damage to articular cartilage and subchondral bone, reminiscent of early stage OA. Given the frequency of bone bruising in the tibial plateau and femoral condyles in patients reporting knee injury, the implications of blunt trauma to articular cartilage in the tibiofemoral (TF) joint has become an area of interest. The current study investigated the chronic changes in articular cartilage and underlying bone due to a single, severe impact to the flexed rabbit TF joint. The hypothesis of this investigation was that a single compressive impact to the rabbit knee would lead to alterations in the mechanical and histological properties of the articular cartilage within 1 year. Forty eight (24 test, 24 control) animals received a single insult to the flexed knee. The animals were sacrificed at 6 months (n=24) and 1 year (n=24) post-trauma, and mechanical and histological properties were documented. The study showed no significant difference in the mechanical properties of the articular cartilage from the impacted versus contralateral, control TF joint at either 6 months or 1

year post-trauma. However, a change in the stiffness of cartilage was documented in the medial uncovered region between 6 months and 1 year. Histological evaluations revealed significant differences in the morphology of subchondral bone between impacted and contralateral, control joints as well as differences in the proteoglycan content of the articular cartilage 1 year post-trauma. Future studies should investigate the longer-term implications of these histological effects on the mechanical integrity of the articular cartilage, as well as the long-term implications of cartilage stiffening with time post-trauma.

INTRODUCTION

Long term participation in vigorous physical activities increases the risk of acute and chronic injuries, such as ligament sprains or osteoarthritis (OA), respectively (Lane, 1996). Axial compressive loading of the knee joint is a key component during a majority of anterior cruciate ligament (ACL) injuries. Acute injury to the ACL has been shown to lead to characteristic osteochondral lesions in the postero-lateral aspect of the tibia and/or antero-lateral aspect of the lateral femoral condyle (Atkinson et al., 2008; Mink & Deutsch et al., 1989; Speer et al., 1992; Spindler et al., 1993). These lesions are associated with occult microcracks of subchondral and/or trabecular bone (Speer et al., 1992; Rangger et al., 1998). Although strongly correlated with ACL trauma, bone bruises have also been documented in the clinical literature in patients with no ligamentous damage (Wright et al., 2000; Davies et al., 2004). Since the current literature seems to suggest that even following ACL reconstruction as many as 50% of patients will develop radiological degenerative changes within 10-15 years (Myklebust & Bahr, 2007) the initial injury to articular cartilage and subchondral bone may play a large role in initiating chronic joint disease.

Of concern in today's clinical literature is that there is evidence of acute injury to articular cartilage overlying these bone bruises, which may predispose the knee to degenerative changes (Mankin, 1982; Thompson et al., 1991; Faber et al., 1999). Recent studies have focused on the long-term implications of cartilage and subchondral bone damage generated during the acute joint injury. However, establishing a cause and effect relationship between acute joint injury and the chronic development of OA has been difficult. Our laboratory has previously developed a model using the patellofemoral (PF)

joint of the Flemish Giant rabbit in which a 6 J energy blunt impact was delivered to the flexed knee. Acute studies using this model document significant damage to chondrocytes as well as impact induced lesions on the retropatellar surface. Chronic studies using this PF rabbit model document significant changes in the mechanical and histological properties of the retropatellar cartilage including a 30% reduction in cartilage stiffness, a significant thinning of the cartilage and an increase in its permeability 36 months post-trauma. Ewers et al. (2000) also document a significant softening of the retropatellar cartilage within 12 months following blunt trauma to the rabbit PF joint. However, given the frequency of bone bruising in the tibial plateau and femoral condyles of patients reporting knee injury, the implications of blunt trauma to articular cartilage in the tibiofemoral joint (TF) has become an area of active interest.

Vellet et al. (1991) document an overt loss of cartilage overlying geographic bone bruises in 48% of patients within 6 months of the reported injury. In order to investigate the pathogenesis that leads from the acute bone bruise to this overt cartilage loss animal models have been developed. Radin et al. (1984), for example, document severely fibrillated cartilage, horizontal and vertical microcracks and the interface between calcified cartilage and bone, and a stiffening of underlying subchondral bone 3 weeks after impulsive loading to the rabbit TF joint. These authors also conclude that in this model early bone changes precede changes in articular cartilage. Our laboratory has recently developed an *in vivo* traumatic injury model involving the rabbit TF joint. We have shown that a single, severe impact to the flexed rabbit knee results in average contact pressures of approximately 20 MPa and 24 MPa, with corresponding increases of 22% and 25% in the percentage of cells with damaged plasma membranes in the medial

and lateral facets, respectively (Isaac et al., 2008). And, acute trauma to cells has been thought to be associated with the long-term development of osteoarthritis (Colwell et al., 2001).

The objective of the current study was to use this newly developed TF impact model (Isaac et al., 2008) to investigate chronic changes in articular cartilage and underlying bone due to a single, severe impact. Based on the results of previous studies on the PF joint by our laboratory, the hypothesis of the current study was that a single, severe compressive impact on the flexed rabbit knee would lead to alterations in the mechanical and histological properties of the articular cartilage in the TF joint within 1 year. Such a model could then be used to study the efficacy of various methods of intervention including repair of acutely damaged chondrocytes or addressing trauma to subchondral and/or trabecular bone.

MATERIALS AND METHODS

Forty eight skeletally mature Flemish Giant rabbits (average mass = 5.5 ± .08 kg, 9-12 months of age) were used in this study. This investigation was approved by the Michigan State University All-University Committee on Animal Use and Care. A licensed veterinary technician (J.A) cared for the animals. All animals were housed in individual cages (60 x 60 x 14 in) throughout the duration of the study. Twenty-four animals were randomly selected for the chronic impact study. These animals received a single, high-intensity blunt impact to the left TF joint, per the protocol described below. Twelve animals were selected for either a 6 or 12 month study. Another 24 animals served as unimpacted, controls for the study and were split into two groups that for either the 6 or 12 month study.

The blunt impact experiments have been described in an earlier study (Isaac et al., 2008). Briefly, a 1.75 kg mass was dropped from a height of 75 cm (~ 13 J of potential energy) onto the left TF joint of anesthetized rabbits (2% Isoflurane and Oxygen). Each animal was laid supine in the test fixture, and the knee was flexed 90 degrees. Two Velcro straps were crossed over the femur, and the tibia was constrained in order to limit anterior motion of the tibia during impact (Figure 3.1). A pre-crushed deformable interface (Hexcel, 3.76 MPa) was used to ensure uniform loading over the anterior surface of the femur. The mass was arrested electronically after the first impact, preventing multiple impacts. After trauma the animals received one injection of Buprenorphine (.03 ml/kg BW) for early post-impact pain.

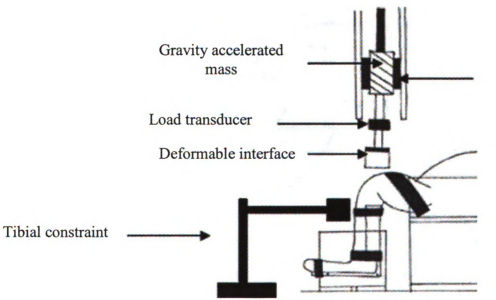

Figure 3.1. Impact experiments were performed by dropping a gravity-accelerated mass onto the flexed tibial-femoral joint with approximately 13 J of potential energy. The rabbit was oriented such that the deformable interface struck the distal femur with impact forces oriented axially in the tibia. The tibia was constrained so as to limit anterior subluxation and prevent ligament damage.

After either six months (n=24) or 1 year (n=24), in which the animals were monitored daily for any abnormal movements or behavior, the animals were sacrificed with an overdose of Pentobarbital I.V. (85.9 mg/kg BW). Immediately following sacrifice the hind limbs were opened, removed and examined for abnormalities. The meniscus was also examined for abnormalities. It was then removed after marking its location on the surface of the tibial plateau. The material properties of the articular cartilage were documented at four specific locations sites the medial and lateral facets using an indentation relaxation test (Ewers et al., 2002). Sites 1 and 3 on the medial and lateral facets, respectively, were near the edge of the meniscus in uncovered areas. Sites 2 and 4 were slightly posterior to these sites and located in regions covered by the medial and lateral meniscus, respectively (Figure 3.2).

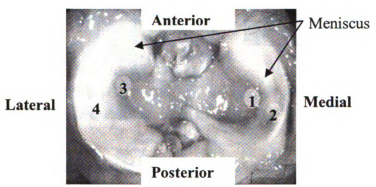

Figure 3.2. Indentation relaxation tests were performed across the tibial plateau in regions covered and uncovered by the meniscus. Sites 1 and 3 correspond to regions uncovered by the meniscus on the medial and lateral facet, respectively. Sites 2 and 4 are located in covered regions on the medial and lateral facet, respectively.

The tibial plateau was mounted in a specialized clamp attached to a 3-dimensional camera mounting fixture and bathed in room temperature phosphate buffered saline (PBS) (pH = 7.2). Prior to indentation testing a needle was slowly penetrated into the cartilage to measure thickness at two locations around each indentation site. This measurement was made based on an analysis of the force time plot that showed the

needle touching the surface of the cartilage followed by the appearance of a sudden rise in force as the needle contacted the deep layer of calcified cartilage (Athanasiou et al., 1991). At each site the surface of the tibial plateau was positioned perpendicular to the indenter probe (Figure 3.3).

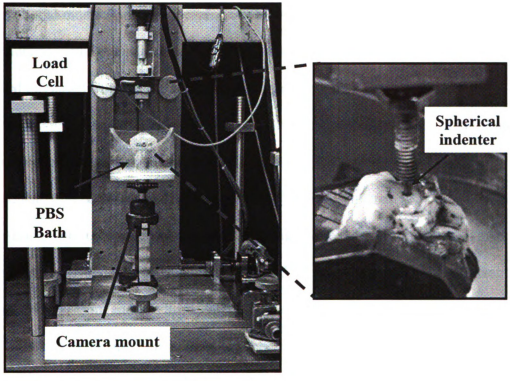

Figure 3.3. Indentation relaxation testing was performed using a custom built step-motor device. The tibial plateau was fixed in a specialized camera mounting fixture and the cartilage was position perpendicular to the spherical indenter.

At each of the previously marked sites a 1.06 mm diameter, spherical nonporous probe was pressed into the cartilage to 40% of the cartilage thickness for approximately 30 minutes using a custom built stepper motor driven device (Physic Instruments, Waldbronn, Germany, Model M-168.3). The resistive loads were measured (Data Instruments, Acton MA, Model JP-25), amplified and sampled at 1000 Hz for the first second and at 20 Hz thereafter. After indentation, the cartilage was left to rest for 30

minutes. The indenter probe was then replaced with the needle and thickness measurements were taken at the indentation site, following the procedure described above.

The load relaxation curves were fit with a fibril-reinforced, biphasic computational model (Golenberg et al., 2008) with an assumed Poisson's ratio of 0.3. In this model of cartilage tissue attached to bone, a linear variation of voids ratio which was assumed increased from 70% fluid at the cartilage-bone interface to 85% in the superficial zone (Lipshitz et al., 1975). The model allowed for finite deformations and was implemented in a commercial finite element analysis package (ABAQUS v.6.3, Hibbitt, Karlsson & Sorensen, Inc., Pawtucket, RI, USA). The matrix modulus (E_m), fiber modulus (E_f) and tissue permeability (k) of cartilage were determined from this model with a custom-written, Gauss-Newton constrained nonlinear least square minimization procedure (Lindstrom and Wedin, 1993).

Following the mechanical tests, the specimens were prepared for histological evaluations. The plateaus were bathed in 10% buffered formalin for one week and decalcified in 20% formic acid for an additional week. Cornoal tissue blocks were then cut in the medial to lateral direction across the plateau. The blocks were processed in paraffin and sequential sections, 8 microns thick, were prepared for examination. The sections were stained with Safranin O-Fast Green and examined under light microscopy. The thickness of the subchondral plate was determined by averaging across the facets with a calibrated eyepiece. The overlying articular cartilage was also scored using a previously established system (Weaver and Haut, 2005; Columbo et al., 1983; Mazieres et al., 1987) (Figure 3.4).

Surface Geometry	Normal	0	Tide Mark	Present 0
	Slightly Irregular	1		Multiple 1
	Moderately Disrupted	2		Focal Loss 2
	Focally Disrupted	3		Diffuse Loss 3
	Extensively Disrupted	4		Total Loss 4
Articular Cartilage Fissures	None	0	Calcified Cartilage Spiculae	Normal 0
	1-3 Surface	1		Slight 1
	1-2 Mid-zone	2		Moderate 2
	3-4 Mid-zone	3		Focally Excessive 3
	4+ Mid-zone	4		Excessive 4
	1+ Deep zone	4		
Proteoglycan Stain	Normal	0	Calcified Cartilage Stain	Normal 0
	Slight Loss	1		Slight 1
	Moderate Loss	2		Moderate 2
	Focally	3		Dark 3
	Total Loss	4		
Articular Cartilage Cells	Normal	0	Subchondral Bone Morphology	Dense 3
	Some Clones	1		Some Small Spaces 1
	Many Clones	2		Moderate Spaces 2
	Some Clusters	3		Some Splits 2
	Many Clusters	4		Numerous Splits 4
	Path Cells	4		
Articular Cartilage Disruptions	None	0		
	Compression Ridges	2		
	Horizontal Splits	4		
	Vertical Splits	4		
Articular Cartilage Thickness			Subchondral Bone Thickness	
Calcified Cartilage Thickness				

Figure 3.4. Histological scoring system used to quantify the characteristics for cartilage across the tibial plateau.

A two-factor ANOVA (limb, group) with post hoc Student-Newman-Keuls (S-N-K) tests was used in order to evaluate the differences in mechanical properties between the impacted and control limbs, as well as for differences between the 6 month and 1 year data. A one-factor (limb) ANOVA on Ranks was used to test for differences between

histological parameters in the impacted and control limbs, as well as between the 6 month and 1 year groups. A statistically significant effect was indicated for $p<0.05$.

RESULTS

The average peak, inertially-compensated impact load and impact duration were 1070 ± 107 N and 23.0 ± 0.2 ms in the study. During the post-trauma period no limping or swollen knee joints were observed in any animal. Some animals did develop a slight bruise at the impaction site following the insult, but no subsequent consequences were evident thereafter. Upon necropsy no significant joint pathology such as synovitis, hardening of the joint capsule, cartilage erosion, etc. were noted in any rabbit. Additionally, no ligament or meniscal damages were documented in any animal during dissection of the joints.

No significant differences were documented in any mechanical parameter between the right and left limbs of the control animals; therefore, these data were averaged for this study. Additionally, no significant differences in any mechanical parameter were documented between the contralateral, control limbs and the combined control rabbits at any site across the plateau in either group of animals; therefore, the current study compared the impacted limbs to the contralateral, control (right).

Analysis of the data from indentation relaxation tests revealed no significant differences in any mechanical parameter between the left and right limbs in the 6 month, impacted group. Similarly, the 1 year, impacted group also showed no significant differences in any mechanical property between the left and right limbs. Analysis of indentation data from the impacted limb between 6 months and 1 year, however, showed a significant increase in both the matrix ($p=0.009$) and fiber ($p=0.025$) moduli at site 1. In

addition, a significant decrease in tissue permeability was also noted at site 1 in the 1 year groups compared to the 6 month group ($p=0.002$). Interestingly, the contralateral, control limb also exhibited an increase of approximately 33% and 50% in the matrix and fiber modulus, respectively, at site 1. These differences, however, did not rise to the level of statistical significance. No such differences were noted at site 1, or any other site, between 6 months and 1 year for the unimpacted, control animals (Figure 3.5).

Table 3.1. The mechanical properties (average (± *standard deviation*)) were extracted from the relaxation indentation testing across the medial and lateral facet (Site 1 – medial uncovered, Site 2 – medial covered, Site 3 – lateral uncovered and Site 4 – lateral covered). Statistical differences between the between the 6 month and 1 year group are indicated (^{b}).

6 Month Group					
		Site 1	**Site 2**	**Site 3**	**Site 4**
Impacted	*Em*	0.65 (± 0.14)^b	0.62 (± 0.20)	0.82 (± 0.21)	1.91 (± 1.12)
	Ef	4.4 (± 1.84)^b	2.82 (± 1.08)	12.62 (± 3.89)	31.88 (± 16.37)
	k	22.7 (± 8.03)^b	10.8 (± 4.09)	5.55 (± 3.32)	2.3 (± 1.32)
Control Limb	*Em*	0.61 (± 0.17)	0.71 (± 0.23)	0.96 (± 0.37)	2.09 (± 1.42)
	Ef	3.2 (± 1.21)	4.87 (± 3.48)	15.53 (± 4.42)	36.35 (± 19.51)
	k	25.8 (± 8.68)	8.35 (± 3.10)	5.52 (± 1.93)	2.27 (± 1.24)
Control Rabbit	*Em*	0.60 (± 0.12)	0.81 (± 0.38)	0.90 (± 0.24)	1.62 (± 0.75)
	Ef	4.42 (± 2.01)	6.66 (± 4.66)	14.58 (± 8.03)	31.23 (± 22.09)
	k	21.0 (± 6.07)	8.05 (± 2.74)	5.58 (± 2.15)	2.24 (± 0.69)
1 Year Group					
		Site 1	**Site 2**	**Site 3**	**Site 4**
Impacted	*Em*	0.81 (± 0.12)^b	0.71 (± 0.13)	0.88 (± 0.09)	1.58 (± 0.45)
	Ef	6.5 (± 2.2)^b	3.98 (± 3.36)	12.7 (± 3.98)	49.0 (± 23.8)
	k	12.7 (± 5.18)^b	10.0 (± 3.66)	6.26 (± 2.68)	2.12 (± 0.49)
Control Limb	*Em*	0.81 (± 0.15)	0.76 (± 0.15)	1.10 (± 0.29)	1.50 (± 0.58)
	Ef	5.12 (± 1.4)	5.89 (± 4.52)	16.1 (± 4.06)	42.7 (± 21.1)
	k	14.9 (± 5.05)	7.94 (± 3.08)	4.73 (± 0.99)	2.24 (± 0.79)
Control Rabbit	*Em*	0.69 (± 0.15)	0.91 (± 0.25)	1.11 (± 0.29)	1.57 (± 0.47)
	Ef	4.07 (± 2.05)	4.97 (± 2.07)	14.6 (± 4.09)	37.0 (± 17.7)
	k	19.5 (± 7.18)	8.88 (± 2.42)	5.46 (± 1.02)	2.28 (± 0.66)

The analysis of histological sections from the right and left limbs of the unimpacted, control rabbits showed no significant differences in either the medial or

lateral aspects of the plateau for either the 6 month or 1 year group. Additionally, no statistical differences were noted between the contralateral, control limb and the control animals; therefore, the impacted limbs were compared to the contralateral limbs for this study.

Histological analysis of sections from the 6 month group indicated a significant increase in the number of surface lesions on the medial aspect of the impacted plateau ($p=0.04$) versus the contralateral limb; however, no significant increase was found in the lateral aspect. The number of vertical and horizontal micro-cracks at the interface between articular cartilage and subchondral bone was also documented in the histological sections. A significant increase in the frequency of microcracks was evident in the medial ($p=0.003$) and lateral ($p=0.005$) aspects of the impacted limbs, with a slightly higher frequency of microcracks in the lateral versus medial aspects. A significant loss of Safranin-O stain was also evident in the medial ($p=0.017$) and lateral ($p=0.039$) aspects of the impacted plateau. No significant change in subchondral bone thickness was documented for the 6 month group in either aspect of the plateau (Figure 3.6).

Analysis of histological sections from the 1 year group also revealed findings similar to those of the 6 month group. A significant increase in the number of surface fissures was documented in the medal ($p=0.025$) aspect of the impacted limb compared to the contralateral. The frequency of vertical and horizontal microcracks was also found to be significantly greater in the medial ($p=0.001$) and lateral ($p=0.037$) aspects of the impacted plateau versus the contralateral limb (Figure 3.7). In contrast to the 6 month group, a significant increase in subchondral bone thickness was documented in the medial ($p=0.029$) and lateral ($p<0.001$) aspects of the plateau for the impacted versus

control limbs in the 1 year group. A statistical decrease in the Safranin-O stain was also documented in the impacted cartilage at 1 year compared to the control limbs for both the medial ($p<0.001$) and lateral ($p=0.003$) aspects of the tibial plateau (Figure 3.6).

When comparing the data from histological sections of impacted limbs between the 6 month and 1 year groups there was also a statistical trend for a higher frequency of microcracks in the medial aspect of the plateau ($p=0.092$) of impacted limbs. A significant increase in subchondral bone thickness was also shown in the medial ($p=0.100$) and lateral ($p=0.05$) aspects of the impacted plateaus. The lateral aspect of the plateau also showed a significant decrease in the Safranin-O stain ($p=0.017$) in the 1 year compared to the 6 month groups.

Table 3.2. Histological evaluations of the impacted and control osteochondral sections of the medial and lateral tibial plateau indicated significant increases in surface fissures, subchondral bone thickness, disruptions (i.e. microcracks) and PG stain. Statistical differences between the impacted and contralateral, control limbs are indicated for the 6 month and 1 year group (^{a}) and between the 6 month and 1 year groups (^{b}).

6 Month									
		SB Thick		Fissures		Disruptions		PG Stain	
		Average	SD	Average	SD	Average	SD	Average	SD
Left	M	26.58	3.94	2.92[a]	1.68	2.92[a]	2.02	1.00	0.85
	L	29.00	5.10	0.58	0.79	3.17[a]	2.76	0.33	0.49
Right	M	24.42	3.58	1.25	1.06	0.58	0.67	0.09	0.39
	L	26.83	5.64	0.67	0.98	0.67	0.98	0.00	0.00
Control	M	27.23	4.42	1.41	0.78	0.68	0.56	0.36	0.39
	L	29.00	5.64	0.18	0.25	0.14	0.23	0.14	0.23
1 Year									
		SB Thick		Fissures		Disruptions		PG Stain	
		Average	SD	Average	SD	Average	SD	Average	SD
Left	M	28.50[a,b]	3.44	3.20[a]	1.99	4.70[a]	2.71	0.90[a]	0.32
	L	33.55[a,b]	5.39	1.27	1.42	2.73[a]	2.45	1.36[a]	1.12
Right	M	25.00	2.24	1.18	1.17	0.36	0.50	0.00	0.00
	L	25.18	2.82	0.36	0.67	0.64	1.29	0.00	0.00
Control	M	24.45	1.48	1.20	0.75	0.55	0.55	0.10	0.21
	L	24.40	2.28	0.35	0.41	0.25	0.35	0.10	0.21

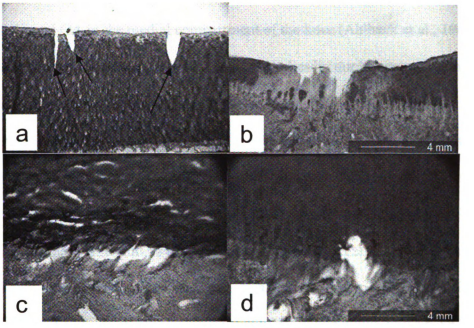

Figure 3.5. Histological analysis showed a significant increase in surface lesions for both the 6 month and 1 year groups (a) and a loss of proteoglycan staining in the 1 year group (b) compared to unimpacted, control limbs. An increase in the frequency of vertical (d) and horizontal (c) microcracks at the interface of articular cartilage and subchondral bone was also documented in both groups compared to controls.

DISCUSSION

The current study documented the mechanical and histological properties of articular cartilage on the rabbit tibial plateau 6 months and 1 year following blunt trauma to the TF joint. Mechanical tests showed no significant differences in the mechanical properties between the impacted limb and the contralateral, control limbs at any of the sites on the medial or lateral tibial plateau. However, the study documented a statistical increase in both the matrix and fiber moduli, as well as a decrease in the permeability, of the articular cartilage in the medial uncovered region of the impacted limb between the 6 month and 1 year group. The medial uncovered region of the tibial plateau has been shown to exhibit statistically more baseline damage than its lateral counterpart (Golenberg et al., 2008).

This "baseline" damaged cartilage has also been thought to be similar to a higher prevalence of clinical OA in the medial compartment of the knee (Ahlback et al., 1968). These results are in contrast with those from previous studies by our laboratory on the PF joint which document a significant softening of the retropatellar cartilage 3 years following impact (Ewers et al., 2000). Previous investigations on the pathogenesis of OA have shown deposition of calcium in degenerative cartilage (Radin et al., 1984). Weaver and Haut (2005) also document histological ossification/calcification in the rabbit PF joint 2 years after impact. The authors of the latter study conclude that this ossification may lead to a stiffening of the impacted cartilage. It is possible that the articular cartilage from the 1 year group may also have exhibited some calcification which could have lead to the observed stiffening.

An interesting finding of the current study was the response of the contralateral, control limb in the medial uncovered region of the impacted animal groups. Although not statistically significant, the contralateral limb also showed a slight stiffening of cartilage between the 6 month and 1 year groups. In contrast, the unimpacted, control rabbits did not show any changes in mechanical properties between 6 months and 1 year. There are a number of possible explanations for stiffening of cartilage in the medial uncovered region of both the impacted and contralateral limbs in these animals. It is possible that these rabbits simply had different baseline material properties. However, the rabbits were randomly assigned to groups, and it seems unlikely that rabbits with different cartilage properties were all placed in the same group. It does seem possible, however, that altered gait as a result of injury could have lead to an increased loading of the contralateral limb. During normal gait higher loads have been shown to pass through the medial

compartment of the rabbit knee joint (Mansour et al., 1998) particularly in the uncovered regions. This could result in a more advanced disease process in the medial compartment of these animals. On the other hand, Gaushe et al., (2005) suggests that higher loads pass through the lateral compartment for the rabbit. This could suggest that medial compartment OA in the rabbit is largely due to an unloading effect, which could have also been additionally provoked by trauma to the opposite, impacted limb. Future studies will be needed to better understand the loading pathways through the rabbit knee, and alterations that could be due to trauma in on of the limbs.

The current study also documented significant histological differences between the impacted and contralateral limbs in both the 6 month and 1 year groups. Impact trauma was found to significantly increase the frequency of vertical and horizontal microcracks at the interface between calcified cartilage and subchondral bone, with a higher frequency noted in the 1 year group compared to the 6 month group. Furthermore, a trend for higher frequency of these disruptions were noted in the lateral compartment of the tibial plateau at 6 months compared to the medial compartment. A recent study by Batiste et al. (2004) indicates that the bone mineral density (BMD) is significantly higher in the medial tibial plateau. This could possibly explain why slightly fewer microcracks are seen in the medial than lateral compartments 6 months following trauma. A previous study by Ewers et al. (2002) documents a significant softening of the retropatellar cartilage with no subsequent microtrauma at the articular cartilage subchondral bone interface in the rabbit PF joint following single, severe impact. Initiation of cartilage damage and progression to end stage OA has been shown to depend on pathophysiology of cartilage and bone (Burr and Schaffler, 1997). Therefore, the occult bone trauma

documented in the current TF impact model and not the previous studies using the rabbit PF joint could have lead to a more accelerated degeneration and therefore, calcification and stiffening of the articular cartilage.

There were a number of limitations of the current study. In particular, histological analysis of osteochondral sections did not allow for evaluation of calcium deposition in the articular cartilage, which we have implied may possibly have lead to a stiffening of the articular cartilage at site 1 in the 1 year group. Additionally, although a statistical increase in articular cartilage stiffness was documented between 6 months and 1 year in the medial uncovered regions of the impacted limb it is not yet conclusive as to whether this increase was due, in part, to an increase in the mechanical parameters of the contralateral limbs or to impact itself. Although there were no statistical differences between the contralateral limbs of the two groups there did seem to be a trend for an increase in both the matrix and fiber moduli in the 1 year compared to the 6 month control limbs. Altered loading mechanics due to injury of the impacted limb could have affected the contralateral limb. However, post-trauma gait and cage activity was not quantified. Future studies should investigate the implications of this change in the properties of the contralateral limb.

While the current study indicated significant changes in the mechanical and histological properties of articular cartilage and subchondral bone in the rabbit TF joint, the mechanical property changes that were potentially due to impact trauma seem to be in contrast to those documented in previous studies on the rabbit PF joint. Future studies should investigate the mechanism of cartilage stiffening to determine if it may be associated with a more end stage disease. Longer-term studies should also be performed

in order to understand the relationship between articular cartilage degeneration and subchondral bone remodeling in this model. Investigations can then proceed to study the efficacy of therapeutic agents aimed at preventing damage to cartilage and subchondral bone following traumatic loading to the joint.

ACKNOWLEDGEMENTS

This study was supported by a grant from the Centers for Disease Control and Prevention, Center for Injury Control & Prevention (CE000623). The contents of this manuscript are solely the responsibility of the authors and do not necessarily represent the official views of the Center for Injury Control and Prevention. The authors wish to acknowledge Ms. Jean Atkinson (JA) for her assistance in animal care, Ms. Jane Walsh (JW) for her assistance with histological evaluations and Mr. Clifford Beckett for his technical support.

REFERENCES

Ahlback S, 1968, "Osteoarthorosis of the knee: A radiographic investigation," Acta Radiologica Supplementum, **277**, pp. 7-72.

Athanasio KA, Rosenwasser MP, Buckwalter JA, Malinin TI, Mow VC, 1991, "Interspecies Comparison of In Situ Intrinsic Mechanical Properties of Distal Femoral Cartilage," J Orthop Res, **9(3)**, pp. 330-340.

Atkinson P, Cooper T, Anseth S, Walter N, Kargus R, Haut RC, 2008, "Association of Knee Bone Bruise Frequency with Time Postinjury and Type of Soft Tissue Injury," Orthp, **31**, pp. 440

Bahr R, Myklebust G, 2005, "Return to Play Guidelines after Anterior Cruciate Ligament Surgery," Br J Sports Med, **39**, pp. 127-131.

Batiste D, Kirkley A, Laverty S, Thain L, Spouge A, Holdsworth D, 2004, "*Ex Vivo* Characterization of Articular Cartilage and Bone Lesions in a Rabbit ACL Transection Model of Osteoarthritis Using MRI and Mirco-CT," OA Cart, **12**, pp. 986-996.

Colombo C, Butler M, O'Byrne E, Hickman L, Swartzendruber D, Selwyn M, Steinetz B, 1983, "A New Model of Osteoarthritis in Rabbits. I. Development of Knee Joint Pathology Following Lateral Meniscectomy and Section of Fibular Collateral and Sesamoid Ligaments'," Arth Rheum, **26(7)**, pp.875-886.

Colwell CW, D'Lima DD, Hoenecke HR, Fronek J, Pulido P, Morris BA, Chung C, Resnick D, Lotz M, 2001, "In Vivo Changes after Mechanical Injury," Clin Orthop Rel Res, **391S**, pp. S116-S123.

Davies NH, Niall D, King LJ, Lavelle J, Healy JC, 2004, "Magnetic Resonance Imaging of Bone Bruising in the Acutely Injured Knee. Short-Term Outcome," Clin Radiol, **59**, pp. 439-445.

Ewers BJ, Haut RC, 2000, "Polysulphated Glycosaminoglycan Treatments can Mitigate Decreases in Stiffness of Articuar Cartilage in a Traumatized Joint," J Orthop Res, **18**, pp. 756-761.

Ewers BJ, Weaver BT, Sevensma ET, Haut RC, 2002, "Chronic Changes in Rabbit Retro-Patellar Cartilage and Subchondral Bone after Blunt Impact Loading of the Patello-Femoral Joint," J Orthop Res, **20**, pp.545-550.

Faber K, Dill J, Amendola A, Thain L, Spouge A, Fowler P, 1999, "Occult Osteochondral Lesions after Anterior Cruciate Ligament Rupture Six-Year Magnetic Resonance Follow-Up Study," Am J Sports Med, **27(4)**, pp. 489-494.

Golenberg N, Kepich E, Haut RC, 2008, "Histomorphological and Mechanical Property Correlations in Rabbit Tibial Plateau Cartilage Based on a Fibril-Reinforced Biphasic Model," Int J Exp Comp Biomech, **1(1)**, pp. 58-

Gushe DL, Houck J, Lerner AL, 2005, "Rabbit knee joint biomechanics: Motion analysis and modeling of forces during hoping," J Orthop Res, **23(4)**, pp. 735-742.

Isaac DI, Meyer EG, Haut RC, 2008, "Chondrocyte Damage and Contact Pressures Following Impact on the Rabbit Tibiofemoral Joint," J Biomech Eng, **130**, 0410180.

Lane N, 1996, "Physical Activity at Leisure and Risk of Osteoarthritis," Annals Rheumatic Disease, **55**, pp. 682-684.

Lindstrom P, Wedin PA, 1993, "A Method of Gauss-Newton Type for Nonlinear Least-Squares Problems with Nonlinear Constraints," Technical Report UMINF-133.87, Inst Of Information Processing, University of Umea, Umea Sweden.

Lipshitz H, Etheridge R, Glimcher MJ, 1975, "In Vitro Wear of Articular Cartilage," J Bone Joint Surg, **57(4)**, pp. 527-537.

Mankin J, 1982, "The Response of Articular Cartilage to Mechanical Injury," J Bone Joint Surg Am, **64**, pp. 460-466.

Mansour JM, Wentorf FA, Degoede DM, 1998, "In vivo kinematics of the rabbit knee in unstable models of osteoarthritis," Annals of Biomedical Eng, **26**, pp. 353-360.

Mazieres B, Blanckaert A, Thiechart M, 1987, "Experimental Post-Contusive Osteoarthritis of the Knee: Quantitative Microscope Study of the Patella and the Femoral Condyles'," J Rheum, **14**, pp. 119-121.

Mink J, Deutsch A, 1989, "Occult Cartilage and Bone Injuries of the Knee: Detection, Classification, and Assessment with MR Imaging," Radiology, **170**, pp. 823-829.

Radin E and Rose R, 1986, "Role of Subchondral Bone in the Initiation and Progression of Cartilage Damage," Clin Orthop Rel Res, **213**, pp. 34-40.

Radin EL, Martin RB, Burr DB, Caterson B, Boyd RD, Goodwin C, 1984, "Effects of Mechanical Loading on the Tissues of the Rabbit Knee," J Orthop Res, **2**, pp. 221-234.

Rangger C, Kathrein A, Freund M, Klestil T, Kreczy A, 1998, "Bone Bruise of the Knee: Histology an Cryosections in 5 Cases," Acta Orthop Scand, **69**, pp. 291-294.

Speer K, Spritzer C, Basset F, Feagin J, Garrett W, 1992, "Osseous Injury Associated with Acute Tears of the Anterior Cruciate Ligament," Am J Sports Med, **20**, pp. 382-389.

Spindler K, Schils J, Bergfeld J, Andrish J, Weiker G, Anderson T, Piraino D, Richmond B, Medendrop S, 1993, "Prospective Study of Osseous, Articular, and Mensical Lesions in Recent Anterior Cruciate Ligament Tears by Magnetic Resonance Imaging and Arthroscopy," Am J Sports Med, **21**, pp. 5551-557.

Thompson R, Oegema T, Lewis J, Wallace L, 1991, "Osteoarthritic Changes after Acute Transarticular Load," J Bone Joint Surg, **73**, pp. 990-1001.

Vellet AD, Marks PH, Fowler PJ, Munro TG, 1991, "Occult Posttraumatic Osteochondral Lesions of the Knee: Prevalence, Classification, and Short-Term Sequelae Evaluated with MR Imaging," Radiology, **178**, pp. 271-276.

Weaver BT, Haut RC, 2005, "Enforced Exercise after Blunt Trauma Significantly Affects Biomechanical and Histological Changes in Rabbit Retro-Patellar Cartilage," J Biomech, **38(5)**, pp. 1177-1183.

Wei F, Golenberg N, Kepich ET, Haut RC, 2008, "Effect of Intermittent Cyclic Preloads on the Response of Articular Cartilage Explants to an Excessive Level of Unconfined Compression," J Orthop Res, **26**, pp.1636-1642.

Wright RW, Phaneuf M, Limbird TJ, Spindler KP, 2000, "Clinical Outcome of Isolated Subcortical Trabecular Fractures (Bone Bruise) Detected on Magnetic Resonance Imaging in Knees," Am J Sports Med, **28**, pp. 663-667.

CHAPTER FOUR

A TRAUMATIC ANTERIOR CRUCIATE LIGAMENT RUPTURE MODEL: A PRELIMINARY STUDY USING THE RABBIT MODEL

ABSTRACT

Axial compressive loading of the knee is a key component during a majority of anterior cruciate ligament (ACL) injuries and severe tibiofemoral (TF) contact pressures have been documented during these events. Clinically, there are characteristic osteochondral lesions with cellular damage in overlying articular cartilage that occurs in the tibial plateau and femoral condyles in over 80% of ACL injury cases. A hypothesis of this study was that compressive loading of the rabbit knee would result in ACL rupture along with significant damage in articular cartilage and underlying subchondral bone.. A second hypothesis of this study was that this traumatic ACL rupture model (ACLF) would result in relatively more joint degeneration than a surgical transection model of ACL injury (ACLT). Six Flemish giant rabbits were anesthetized and received a blunt force insult to the left TF joint resulting in ACL rupture. One of the animals had pressure sensitive film inserted into the TF joint prior to impact to record the acute magnitude and contact pressure distribution over the medial and lateral plateaus during rupture of the ACL. Two other animals were sacrificed immediately following impact to document acute cartilage and chondrocyte damages. An additional three animals underwent unilateral surgical transection of the ACL.The final three ACLF animals and the three ACLT animals were sacrificed at 12 weeks. The degre of chronic degeneration was evaluated based on the extent of surface fissureing and morphological changes in articular cartilage and underlying subchondral bone. Vertical and horizontal microcracks at the articular cartilage subchondral bone interface were manually quantified in

histological sections. The maximum contact pressures in the tibiofemoral joint were approximately 50 MPa on both plateaus. Acute surface fissures on articular cartilage were also documented, especially in the medial femoral condyle. There was acute damage to the meniscus in all ACLF animals, primarily in the lateral meniscus. There were significantly more chondrocytes with damaged plasma membranes in the medial and lateral tibial plateaus and femoral condyles in the impacted than contralateral, control limbs. At 12 weeks there was full thickness erosion of the articular cartilage as well as severe damage to the menisci in all three of the ACLF animals. Only one of the ACLT animals had moderate cartilage erosion and meniscal degeneration. Histological sections revealed significantly more vertical and horizontal micro-cracks at the articular cartilage-subchondral bone interface in the ACLF group than the ACLT group. The ACLT animal model for post-traumatic osteoarthritis fails to address the acute injuries, such as bone micro-cracks, that occur in most clinical cases of ACL rupture and may have important implications in the long-term development of joint disease. The proposed ACLF model is more directly relevant to the clinical cases of traumatic ACL rupture by incorporating acute histological microtrauma at the articular cartilage subchondral bone interface and meniscal damage that leads to chronic cartilage erosion and joint remodeling after 12 weeks.

INTRODUCTION

Participation in sports, recreation and exercise is increasingly popular and widespread in American culture. Long-term participation in vigorous physical activities increases the risk of acute and chronic injuries, such as ligament injury or post-traumatic osteoarthritis (OA), respectively (Lane, 1996). Two specific types of injuries are strongly associated with subsequent knee OA: cruciate ligament damage and meniscal tears (Felson, 2004). In the year 2000 approximately 80,000 anterior cruciate ligament (ACL) tears occurred in the U.S. alone (Griffin et al., 2000), with a total cost of nearly $2 billion (Hewitt et al., 2006).

Many clinical studies have focused on documenting mechanisms that cause injury to the ACL. Noncontact ACL injuries occur more frequently than injuries involving player-to-player contact (Griffen et al., 2000), and these injuries often involve landing from a jump on one or both legs (Boden et al., 2000). The axial load distribution in injured legs at the time of injury is estimated to be more than 65%, and in most cases 100% of the total ground reaction force (Olsen, 2004). Axial compressive loading of the knee during landing from a jump can be approximately six times body weight for males (Hewett et al., 1996). The tibial plateau has an inherent posterior slope of 10°-15° (Li et al., 1998) which can produce an anterior shift of the tibia under tibiofemoral (TF) compressive loading (Torzilli et al., 1994). Since the ACL provides 85% of the retaining ligamentous force during anterior tibial subluxation (Butler et al., 1989), TF compression may be an important component in the mechanism of clinical ACL injury. Our laboratory has confirmed that a pure TF compressive load can generate an isolated ACL injury in human cadaver knees at knee flexion angles between 30-120° (Meyer et al., 2005; Meyer

et al., 2008). Another group reports similar results using porcine knees at 70° of flexion (Yeow et al., 2008).

Clinically, in over 80% of ACL injury cases a characteristic osteochondral lesion occurs in the postero-lateral aspect of the tibia and/or antero-lateral aspect of the lateral femoral condyle, as these regions are aligned and in contact (Atkinson et al., 2008; Mink & Deutsch, 1989; Speer et al., 1992; Spindler et al., 1993). A number of clinical studies have also described osteochondral lesions existing in the postero-medial tibial plateau after ACL rupture (Chan et al., 1999; Kaplan et al., 1999). Vellet et al. (1991) provides a classification for these osteochondral lesions using magnetic resonance imaging (MRI), documenting an overt loss of cartilage overlying geographic bone bruises in 48% patients within 6 months of injury. These lesions are associated with occult micro-cracks near the interface between calcified cartilage and subchondral bone (Speer et al., 1992; Rangger et al., 1998). These lesions may play a role in pain after joint trauma (??). Also, of concern in today's clinical literature is that there is evidence of injury to articular cartilage and chondrocytes overlying these bone bruises, which may predispose the knee to degenerative changes (Mankin, 1982; Thompson et al., 1991; Faber et al; 1999; Frobell et al., 2008). Fang et al. (2001) suggests that damage to articular cartilage overlying MRI detected bone bruises in patients with ACL rupture may be due to excessive compressive forces generated in the joint during the acute injury.

Our laboratory has previously shown histological microfractures of subchondral bone in isolated, flexed human knees under high compressive loads that produce 18 to 21 MPa of contact pressure in the TF joint (Banglmaier et al., 1999; Meyer et al., 2008). Articular cartilage surface lesions and cell death have also been documented in TF impact

studies with the rabbit that generate contact pressures of approximately 20 MPa and 24 MPa on the medial and lateral tibial plateaus, respectively (Isaac et al., 2008). Surgical transection of the ACL (ACLT) in the rabbit has been used to investigate the pathogenesis of OA in the knee joint (Yoshioka et al., 1996; Chang et al., 1997; Batiste et al., 2004; Vignon et al., 1987). These studies document formation,of osteophytes, fibrillation of cartilage and synovitis which leads to erosion of articular cartilage in the joint within 8-12 weeks (Yoshioka et al., 1996; Batiste et al., 2004). These studies, however, have not documented early damage to cartilage cells or subchondral bone which might be similar to injuries noted in the clinical literature.

The objective of the current study was to develop an animal model involving traumatic ACL failure (ACLF) that includes acute compressive trauma to cartilage and underlying bone. Since the rabbit knee joint also exhibits a posterior slope of the tibial plateau which is more pronounced than the human (Crum et al., 2003), the first hypothesis of this study was that compressive loading of the flexed rabbit knee would result in ACL rupture along with significant cartilage and underlying subchondral bone damage. A second hypothesis of the study was that this traumatic model would result in relatively more chronic joint degeneration compared to the ACLT model. The traumatic model of ACL rupture may have a more direct relevance to the clinical situation than the ACLT.

MATERIALS AND METHODS

Nine skeletally mature Flemish Giant rabbits (5.5 ± 0.1 kg) were used in the study. The investigation was approved by the Michigan State University All-University Committee on Animal Use and Care. The animals were housed in individual cages (60 x

60 x 14 in) during the study. Three rabbits received a blunt force insult to the left TF joint resulting in ACL rupture. Another three rabbits underwent unilateral, surgical transection of the ACL. Two additional animals were used to study acute cellular trauma in the cartilage, and one animal was used to document impact induced contact pressures in the TF joint during rupture of the ACL.

Animals undergoing traumatic ACL rupture (n=3) were place under general anesthesia (2% Isoflurane and oxygen). Following a previously described impact procedure (Isaac et al., 2008), a 1.75 kg mass was dropped from a height of 75 cm (~ 13 J of potential energy) striking the femoral condyle on the left leg. The sled was arrested electronically after one impact. A pre-crushed, deformable impact head (Hexcel, 3.76 MPa crush strength) was used to ensure uniform loading over the condyle. The impact interface was mounted in front of a 4.45 kN (1000 lb) load transducer (model AL311CV, 1000 lb capacity, Sensotec, Columbus, OH). Prior to impact the left limb was shaved. With the animal lying supine in the fixture, the knee was flexed 90° and the foot was fixed in a custom designed boot with three Velcro straps (Figure 4.1). An additional Velcro strap was crossed over the femur. Unlike the former study of Isaac et al. (2008), the tibia was not constrained so as to allow anterior subluxation of the tibia. In one animal, during setup, a lateral X-ray was performed on the flexed knee in the restraint fixture. All animals received buprenorphine (0.3 ml/kg BW) every 8 hours for 72 hours for post-trauma pain. The right limb served as a non-impacted, contralateral control.

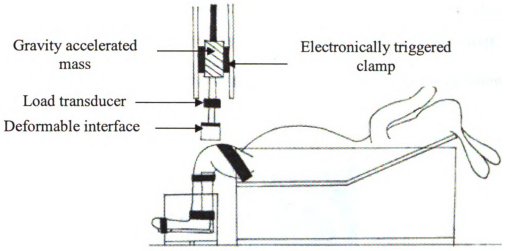

Figure 4.1. Impact experiments were performed by dropping a gravity-accelerated mass onto the flexed tibial-femoral joint with approximately 13 J of potential energy. The rabbit was oriented such that the deformable interface struck the femoral condyle with impact forces oriented axially in the tibia.

One animal was euthanized with 85.9 mg/kg BW Pentobarbital IV immediately prior to impact in order to document contact pressures in the joint during ACL rupture. The impact was administered as previously outlined, after pressure sensitive film packets (Prescale, Fuji Film Ltd., Tokyo, Japan) had been inserted through anterior and posterior joint capsules (Meyer et al., 2008). After impact, the film was removed from the packet and scanned (Scanmaker MRAS-1200E6, Microtek, Taiwan). The entire area of contact was digitized (Photostyler, version 1.1A, Aldus Co., Seattle, WA) and the average pressure, total contact area and the area having pressures over 20 MPa were determined using an established protocol (Atkinson et al., 1998).

Two additional animals were sacrificed immediately following ACL rupture in order to document acute cartilage and chondrocyte damage via a cell viability assay. A 6 mm trephine (TREPH-6, Salvin Dental Specialties, Charlotte, NC) was used to core a region of the medial and lateral tibial plateau in areas not covered by the meniscus, as

these areas were exposed to high contact pressures during impact (Figure 4.2) (Isaac et al., 2008). A diamond saw (Isomet 11-1180 Low Speed Saw, Buehler, Lake Bluff, IL.) was used to then undercut the cores leaving approximately 0.5-1 mm of bone below the articular cartilage.

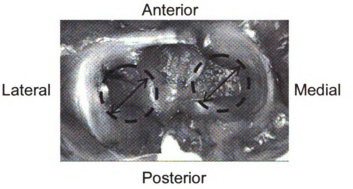

Figure 4.2. 6 mm osteochondral explants were taken in regions uncovered by the meniscus for cell viability analyses.

Similarly, the femurs were fixed in the diamond saw and sagittal slices were cut across the medial and lateral condyles leaving approximately 0.5-1 mm of underlying bone. All explants were rinsed 3 times with culture media before being placed in separate wells filled with fresh Dulbecco's modified Eagle's medium (DMEM): F12 (Gibco, USA #12500-062) supplemented with 10% fetal bovine serum, additional amino acids, and antibiotics (penicillin 100 units/ml, streptomycin 1μg/ml, amphotericin B 0.25 μg/ml), and incubated for 24 hours (37ºC and 95% humidity). This incubation period has been found to be required to allow the perfusion of dye in damaged cells post-impact (Ewers et al., 2001; Phillips et al., 2004).

Following incubation, the specimens were prepared for cell viability analyses. Full depth sections of the femoral and tibial cartilage and subchondral bone were cut using a specialized cutting device (Ewers et al., 2001). The cell viability analyses

followed previous procedures (Rundell et al., 2005). Briefly, slices from medial tibia (MT), lateral tibia (LT), medial femur (MF) and lateral femur (LF) were rinsed with phosphate buffered saline (PBS) and stained with calcein AM and ethidium homodimer (EthD-1), according to the manufacturer's specifications (Live/Dead Cytotoxicity Kit, Molecular Probes, Eugene, OR). Prior to imaging, each sample was rinsed three times with PBS. Viable cells were distinguished by the presence of fluorescent (green) calcein AM. Damaged cells were distinguished by a bright red fluorescence. The number of green and red cells was manually counted with an image analysis program (Image J, National Institutes of Health, 2004).

Another three animals underwent unilateral transection of the ACL. Both rear legs of the animals were shaved from the hock to the hip. The area was prepared using 70% Betadine scrub and 70% alcohol, alternatively. Once scrubbed, the rabbits were moved to a sterile surgery suite. The left TF joint was then exposed through a medial parapatellar incision. Following a medial arthrotomy, the patella was dislocated laterally, exposing the ACL. With the knee in full flexion the ACL was sharply transected. The joint capsule and reticulum was sutured immediately after transection using 3/0 PDS. The sub-cuticular layer and skin was closed in sequence using 4/0 PDS and staples, respectively. A sham operation was performed on the right limb. The rabbits were monitored closely by a licensed veterinary technician (JA) for signs of pain. Post-surgery pain medication (Buprenorphine 0.3ml/kg BW) was administered every 8 hours for 72 hours following the procedure. MRI was taken of the ACLT and ACLF animals within 1 week post-injury in order to verify complete transection or rupture of the ACL.

The three ACLF and three ACLT animals were sacrificed 12 weeks after injury. The surfaces of the tibial plateaus and femoral condyles were stained with India ink to highlight surface fissures, cartilage degeneration, and other irregularities. The surfaces were digitally photographed (Polaroid DMC2, Polaroid Corp., Waltham, MA) under a dissecting microscope at 12X and 25X (Wild TYP 374590, Heerbrugg, Switzerland). Gross morphological assessments were made according to the following criteria, after the application of India ink using the following grading scale (Yoshioka et al., 1996).

Grade 1: Intact cartilage with the surface appearing normal with no ink retention;

Grade 2: Cartilage with few surface lesions that appears normal before staining, but retains some ink;

Grade 3: Cartilage with moderate fibrillation that retains intense black patches of ink; and

Grade 4: Cartilage with full thickness erosion exposing underlying bone.

After a morphological assessment, the plateaus and condyles were placed in 10% buffered formalin for one week and decalcified in 20% formic acid for another week. Tissue blocks were then cut medial to lateral across both the plateau and femoral condyles. Tissue blocks were processed in paraffin and six sequential sections, 8 microns thick, were prepared for analysis. The sections were stained with Safranin O-Fast Green and examined under light microscopy at 12-40X. The thicknesses of the articular cartilage, the zone of calcified cartilage and the subchondral plate were determined with a calibrated eyepiece at 25X by visually averaging across the entire sample by three readers (JW, DI, EM). These readers also independently scored the cartilage and underlying subchondral bone using a system documented in the literature and previous studies from

our laboratory (Columbo et al., 1983; Weaver et al., 2005). The number of surface fissures and micro-trauma (vertical and horizontal cracks at the ZCC/SB interface) were manually quantified in one histological section from each animal. Proteoglycan content was scored by the uptake of Safranin-O stain with normal uptake of stain receiving a 0 and total loss of stain receiving a 4 (Golenberg et al., 2008).

A two-factor, repeated measures ANOVA (limb, plateau) with one-tailed post hoc Student-Newman-Keuls (S-N-K) tests was used to compare the cell viability data from the left impacted, limbs with the contralateral, controls. A two-factor ANOVA (plateau/condyle, ACLF/ACLT) with a post-hoc S-N-K test was used to compare the frequency of microcracks in the tibial plateaus and femoral condyles of the ACLT and ACLF groups. Morphological scores from the ACLT and ACLF groups were compared using a one-factor ANOVA. The contralateral, control limb was analyzed using the same procedures and statistical analyses as the test limbs. Statistical significance was indicated at $p<0.05$ in all tests.

RESULTS

At 90° of flexion the rabbit's tibial plateau displayed a distinct posterior slope on the order of 20° from the horizontal (Figure 4.3). The average impact force was 931 ± 27 N. In each case rupture of the ACL and damage to the meniscus were evident either acutely within one week after trauma in an MRI scan of the joint. The average contact pressures generated on the medial and lateral plateau were 22.7 MPa and 27.5 MPa, respectively in the single animal tested (Table 4.1). The peak pressures on the medial and lateral plateaus were 50.9 and 48.4 MPa, respectively.

Table 4.1. Analysis of pressure sensitive film revealed high contact pressures in the medial compartment of the TF joint during ACL trauma, and even higher pressures in the lateral facet.

	Medial	Lateral
Average Pressure (MPa)	22.7	27.5
Maximum Pressure (MPa)	48.4	50.9
Area over 20 MPa (mm^2)	18.5	19.7

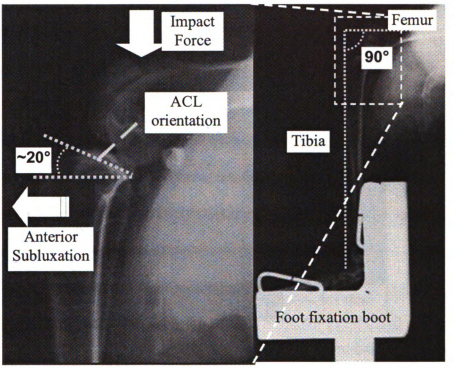

Figure 4.3. Radiograph of the rabbit lower extremity orientation for impacts. The posterior slope of the tibial plateau creates anterior subluxation of the tibia to cause ACL rupture.

As a result of traumatic ACL rupture acute surface fissures were noted, especially on cartilage covering the medial femoral condyle (Figure 4.4). Cell viability analyses of cartilage/bone slices taken from this region also showed a large percentage of cells with damaged membranes (stained in red), particularly in regions adjacent to surface fissures (Figure 4.4).

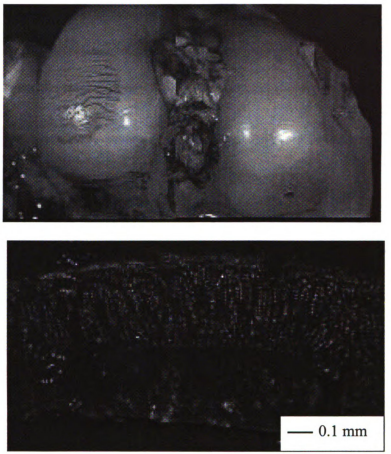

Figure 4.4. India ink staining revealed acute fissuring and a significant amount of damaged chondrocytes (red) in regions surrounding these surface lesions on the medial femoral condyle following traumatic ACL rupture.

Statistical analysis of the cell viability data revealed a significantly larger percentage of damaged chondrocytes in the MF compartment of impacted versus control limbs ($p=0.08$). While the same trend was noted at other locations, no site had statistically more damaged cells than the contralateral, control (Figure 4.5).

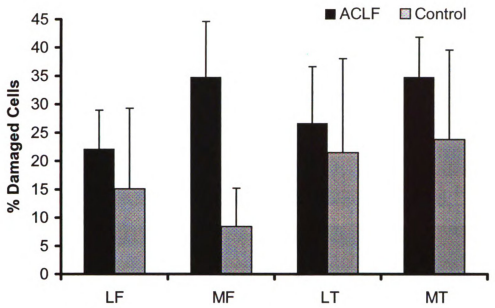

Figure 4.5. Cell viability analysis showed an increase in the percentage of cells with damaged plasma membranes in the ACLF joints in all compartments (lateral femur (LF), medial femur (MF), lateral tibia (LT) and medial tibia (MT)) compared to the contralateral joint tissue.

The ACLF group showed severe degenerative changes that included severely discolored and viscous synovial fluid, erosion of cartilage on the femoral trochlear ridges, and the development of periarticular joint osteophytes. Morphological assessment of the ACLF group at 12 weeks showed full thickness erosion of articular cartilage on the medial femoral condyle in all specimens. Cartilage erosion was also noted in the posterior aspect of the medial tibial plateau in these animals. The animals from the transected group also showed signs of synovitis including an increase in synovial fluid viscosity with discoloration as well as osteophyte formation on the femoral trochlear ridges (Figure 4.6). ACLT animals showed severe fibrillation of cartilage on the medial femoral condyle of one animal, but no full-thickness erosion of cartilage. Comparative morphological

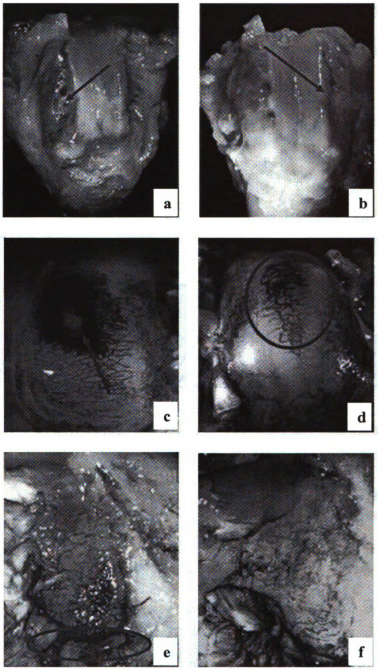

Figure 4.6. Severe cartilage erosion was noted on the femoral trochlear ridges in the traumatic group (a), while only mild erosion was documented in the transected animals (b). The arrows denote joint osteophytes. The medial femoral condyles also showed full thickness ulceration of articular cartilage in the traumatic group (c), but only fibrillation in the transected group (d). The medial tibial plateau showed cartilage erosion in the posterior aspect of the compartment in the traumatic group (e), while the transected rabbits (f) showed no such erosion in the tibial plateau.

assessments of the two groups indicated statistically significant higher grades of degeneration in the MT, the MF and the LT for the ACLF animals compared to the ACLT animals (Figure 4.7).

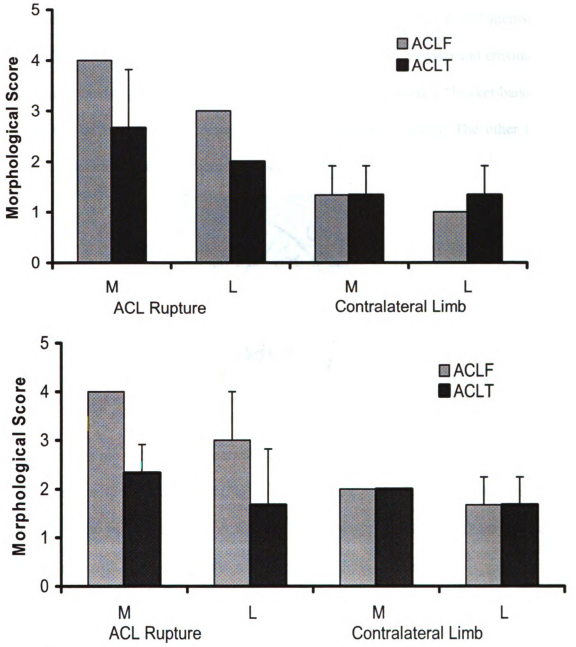

Figure 4.7. Gross morphological analysis of the medial (M) and lateral (L) (a) femoral condyle, and (b) tibial plateau after staining with India ink revealed more cartilage defects in the traumatically injured rabbits.

Both acute and chronic groups of animals showed injury to the menisci (Figure 4.8). The lateral meniscus of the acute animals displayed longitudinal tears located in posterior regions. One acute animal displayed medial meniscal damage. All 12 week ACLF animals showed gross morphological changes to the medial and lateral meniscus that included fibrillation, degeneration of the central portion of the menisci and erosion of the cranial and caudal horns. One 12 week ACLT animal displayed a "bucket-handle" tear of the medial meniscus and degeneration of the lateral meniscus. The other two ACLT animals lacked significant meniscal degeneration.

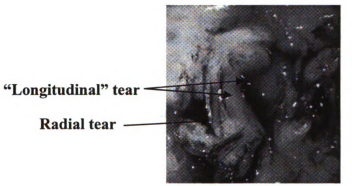

Figure 4.8. India ink staining of the lateral menisci highlight meniscal damage as a result of traumatic ACL injury.

Significantly more occult microcracks appeared in all compartments of the ACLF limbs compared to the ACLT limbs (Figure 4.9). Histological sections of both groups showed significant surface fibrillation in articular cartilage on the medial and lateral femoral condyles with significant losses of proteoglycan stain.

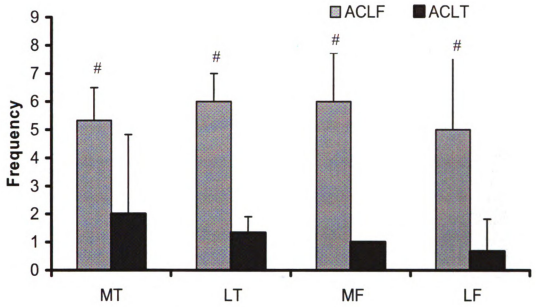

Figure 4.9. Histological sections showed a significant increase in the number of vertical and horizontal microcracks at the articular cartilage/subchondral bone interface, where (#) denotes statistical significance between models.

Severe cartilage fibrillation and erosion were documented in all of the ACLF medial femoral condyles and in two of the lateral femoral condyles (Figure 4.10). One of the ACLT animals showed excessive histological fibrillation and cartilage erosion. The medial tibial plateau displayed more surface fissuring in the ACLF animals compared to the ACLT animals.

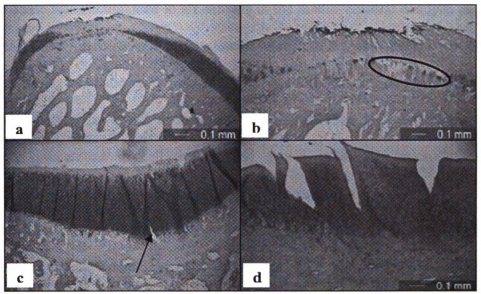

Figure 4.10. Histological sections of the medial femoral condyles (a & b) and medial tibial plateau (d) revealed severe surface fibrillation and fissures, respectively. Proteoglycan loss was noted completely in the femoral sections (a & b) and at the surface in the medial tibial plateau (c & d). Horizontal and vertical micro-cracking was also noted at the ZCC/SB interface as pointed out.

DISCUSSION

The current study has outlined data from the development of a small animal model to study traumatic ACL rupture and the potential for post-traumatic OA. ACLT is widely used to investigate the pathogenesis of OA, but the traumatic model involves more acute injuries that precipitate a more aggressive disease process (Burr and Schaffler, 1997). Rabbit models involving ACLT have documented localized cartilage erosion accompanied by bone remodeling and osteophyte formation (Yoshioka et al., 1996; Chang et al., 1997; Batiste et al., 2004; Vignon et al., 1987). A previous study by Batiste et al. (2004) documents cartilage fibrillation and full thickness erosion in 22% and 59% of the TF joints 12 weeks post-ACLT, respectively. These studies always document that the most extensive area of degeneration is the medial femoral condyle (Yoshioka et al., 1996; Chang et al., 1997; Batiste et al., 2004). In the traumatic ACL rupture model

grade 4 disease was documented in all animals in the medial femoral condyle, as well as the medial tibial plateau. While the lateral compartment did experience cartilage fibrillation in the traumatic model, no full thickness defects were noted. Studies on the rabbit ACLT model have also documented histological changes that include cartilage hypertrophy, reductions in cell density and matrix alterations preceding cartilage fibrillation at 12 weeks (Vignon et al., 1987). In previous studies, our laboratory has shown that blunt trauma at 6 J of energy to the *in vivo* rabbit patellofemoral (PF) joint leads to a significant increase in the percentage of acutely damaged chondrocytes (Rundell et al., 2005). Furthermore using the same model, Ewers et al. (2002) documents surface lesions, progressive degradation of retropatellar cartilage and thickening of the underlying subchondral bone 3 years post-trauma. The current study documents an increase in the percentage of cells damaged acutely in tibial plateaus and femoral condyles following ACLF. These acute injuries may have contributed to the rapid degeneration of cartilage that has been documented in the current study. Hashimoto et al. (1998) also suggests that acute injuries to cartilage and cells may play critical role in the long term progression of chronic joint degeneration in humans.

A significant result from the ACLF model was the histological appearance of numerous vertical and horizontal microcracks at the interface between articular cartilage and subchondral bone, without signs of gross fracture in either the tibial plateau or femoral condyles. The ACLT models have not documented these acute damages to underlying subchondral bone, but the clinical literature does describe these injuries after ACL rupture (Frobell et al., 2008) and, while these mechanisms are not well understood, these osteochondral lesions have been strongly implicated in the development of a post-

traumatic OA (Frobell et al., 2008; Fang et al., 2001; Burr and Radin, 2003; Tambyah et al., 2008). The current study also documented a higher frequency of microcracks in the lateral than medial plateau. This could possibly be due to slightly higher contact pressures in the lateral facet, or because of differences in the material properties of the two plateaus. In a previous study by Batiste et al. (2004), the bone mineral density (BMD) of the rabbit TF joint was found to be significantly higher in the medial femoral condyle and medial tibial plateau than in the lateral compartments. The human literature also documents the BMD of the tibial plateau for a young, non-osteoarthritic population to be approximately 15% higher in the medial compartment than in the lateral compartment (Hurwitz et al., 1998). The lower BMD in the lateral compartment may correspond to an approximately 50% lower ultimate failure stress for trabecular bone (Goldstein et al., 1983). This may explain why bone bruises are more commonly documented in the lateral compartment in clinical studies, as well as in the current ACLF model. Future studies with this newly developed model may be able to help clarify the role of underlying bone trauma on the development of degeneration in overlying articular cartilage.

One limitation of the current study was a small sample size for cell viability analysis, which may have limited statistical significance in the study. However, histological scoring did show significant differences between the ACLT and ACLF groups in the MT, LT, MF and LF, as well as statistical differences in the morphological scores for the MT, LF and LT. Additionally, the study was conducted for a 12 week period. A recent study by Papaioannou et al. (2004) suggests 2 phases in the ACLT model. The early degeneration phase is from 0-8 weeks, followed by a late phase of regeneration or repair from 8-16 weeks. Batiste et al. (2004) also documents a decrease in

the volumetric BMD (vBMD) at 4 and 8 weeks post-ACLT, with a return to control values at 12 weeks. These studies support the notion of degenerative and regenerative phases following ACLT. Future work on the ACLF model should be conducted for various time periods in order to more accurately document the disease process in this new model.

While previous ACLT models have allowed investigators to study the pathogenesis of OA, they have failed to address the acute injuries that occur in a clinical setting; such as damage to underlying subchondral bone, meniscus and cartilage. These injuries may have significant implications in the long-term development of disease. The current investigation has outlined a model of traumatic ACL rupture which ultimately may have direct relevance to the clinical setting. Future investigations can then focus on the importance of addressing acute injury to articular cartilage, as well as the efficacy of various therapeutic agents. The long-term efficacy of intra-articular ACL replacements should also be investigated in the future with the new model.

ACKNOWLEDGMENTS

This study was supported by a grant from the Centers for Disease Control and Prevention, Center for Injury Control & Prevention (CE000623). The contents of this manuscript are solely the responsibility of the authors and do not necessarily represent the official views of the Center for Injury Control and Prevention. The authors wish to acknowledge Ms. Jean Atkinson (J.A.) for her assistance in animal care, Ms. Jane Walsh (J.W.) for her assistance with histological evaluations and Dr. Julien Cabassu for his assistance in the surgical procedures.

REFERENCES

Atkinson P, Cooper T, Anseth S, Walter N, Kargus R, Haut R, 2008, "Association of knee bone bruise frequency with time postinjury and type of soft tissue injury," Orthop, **31**, pp. 440.

Atkinson P, Newberry W, Atkinson T, Haut R, 1998, "A method to increase the sensitive range of pressure sensitive film," J. Biomech, **41**, pp. 284-289.

Banglmaier R, Dvoracek-Driksna D, Oniang'o T, Haut R, 2001, "Axial compressive load response of the 90° flexed human tibiofemoral joint," Stapp Conf Proc, **42**, pp. 127-140.

Batiste D, Kirkley A, Laverty S, Thain L, Spouge A, Holdsworth D, 2004, "*Ex vivo* characterization of articular cartilage and bone lesions in a rabbit ACL transection model of osteoarthritis using MRI and micro-CT," OA Cart, **12**, pp. 986-996.

Boden B, Dean G, Feagin J, Garrett W, 2000, "Mechanisms of anterior cruciate ligament injury," Orthop, **23**, pp. 573-578.

Burr D, Radin E, 2003, "Microfractures and microcracks in subchondral bone: are they relevant to osteoarthritis?" Rhem. Dis. Clin. North Am, **29**, pp. 675-685.

Butler D, 1989, "Anterior cruciate ligament; its normal response and replacement," J Orthop Res, **7**, pp. 910-921.

Chan K, Resnick D, Goodwin D, Seeger L, 1999, "Posteromedial tibial plateau injury including avulsion fracture of the semimembranous tendoninsertion site: Ancillary sign of anterior cruciate ligament tear at MR imaging," Radiology, **211**, pp. 754-758.

Chang D, Iverson E, Schingal R, Sonoda M, Amiel D, Coutts D, Sah R, 1997, "Quantitation and localization of cartilage degeneration following the induction of osteoarthritis in the rabbit knee," OA Cart, **5**, pp. 357-372.

Colombo C, Butler M, O'Byrne E, Hickman L, Swartzendruber D, Selwyn M, Steinetz B, 1983, "A new model of osteoarthritis in rabbits. I. Development of knee joint pathology following lateral meniscectomy and section of fibular collateral and sesamoid ligaments," Arth Rheum, **26**, pp. 875-886.

Crum J, LaPrade R, Wentorf F, 2003, "The anatomy of the posterolateral aspect of the rabbit knee," J Orthop Res, **21**, pp. 723-729.

Ewers B, Weaver B, Sevensma E, Haut R, 2002, "Chronic changes in rabbit retro-patellar cartilageand subchondral bone after blunt impact loading of the patello-femoral joint," J Orthop Res, **20**, pp. 545-550.

Ewers B, Krueger J, Dvoracek-Dricksna D, Orth M, Haut R, 2001, "Chondrocyte viability decreases over 24 hours post-impact in a mechanically traumatized cartilage explant," 47th Mtging Orthop Res Society.

Faber K, Dill J, Amendola A, Thain L, Spouge A, Fowler P, 1999, "Occult osteochondral lesions after anterior cruciate ligament rupture six-year magnetic resonance follow-up study," Am J Sports Med, **27 (4)**, pp. 489-494.

Fang C, Johnson D, Leslie MP, Calson C, Robbins M, Cesare P, 2001, "Tissue distribution and measurement of cartilage oligomeric matrix protien in patients with magnetic resonance imaging-detected bone bruises after acute anterior cruciate ligament tears," J Orthop. Res, **19**, pp. 634-641.

Felson D, 2004, "An update on the pathogenesis and epidemiology of osteoarthritis," Radiologic Clinics North Am, **42**, pp. 1-9.

Frobell R, Roos H, Roos E, Hellio Le Graverand M, Buck R, Tamez-Pena J, Totterman S, Boegard T, Lohmander L, 2008, "The acutely ACL injuried knee assessed by MRI: are large volume traumatic bone marrow lesions a sign of severe compression injury?" Osteo Cart, **16**, pp. 829-836.

Goldstein S, Wilson D, Sonstegard D, Matthews L, 1983, "The mechanical properties of human tibial trabecular bone as a function of metaphyseal location," J Biomech, **16**, pp. 965-969.

Griffin L, Agel J, Albohm M, 2000, "Non-contact anterior cruciate ligament injuries: risk factors and prevention strategies," J Am Acad Orthop Surg, **8**, pp. 141-150.

Hashimoto S, Ochs R, Komiya S, Lotz M, 1998, "Linkage of chondrocyte apoptosis and cartilage degredation in human osteoarthritis," Arth Rheum, **41**, pp. 1632-1638.

Hewett T, Stroupe A, Nance T, Noyes F, 1996, "Pylometric training in female athletes: Decreased impact forces and increased hamstrings torques," Am J Sports Med, **24**, pp. 765-773.

Hewett T, Myer G, Ford K, 2006, "Anterior cruciate ligament injuries in female athletes: Part 1, Mechanisms and risk factors," Am J Sports Med, **34**, pp. 299-311.

Hurwitz D, Sumner D, Andriacchi T, Sugar D, 1998, "Dynamic Knee loads during gait predict proximal tibial bone distribution," J Biomech, **31**, pp. 423-430.

Isaac D, Meyer E, Haut R, 2008, "Chondrocyte damage and contact pressures following impact on the rabbit tibiofemoral joint," J Biomech Eng ,**130**, pp. 0410180.

Kaplan P, Gehl R, Dussault R, Anderson M, Diduch D, 1999, "Bone contusions of the posterior lip of the medial tibial plateau (Countercoup injury) and associated internal derangements of the knee at MR imaging," Radiology, **211**, pp. 747-753.

Lane N, 1996, "Physical activity at leisure and risk of osteoarthritis," Annals Rheumatic Diseases, **55**, pp. 682-684.

Li G, Rudy T, Allen C, 1998, "Effect of combined axial compressive and anterior tibial loads on in situ forces in the anterior cruciate ligament: a porcine study," J Orthop Res, **16**, pp. 122-127.

Mankin J, 1982, "The response of articular cartilage to mechanical injury," J Bone Joint Surg Am, **64**, pp. 460-466.

Meyer E, Haut R, 2005, "Excessive compression of the human tibio-femoral joint causes ACL rupture," J Biomech, **38**, pp. 2311-2316.

Meyer E, Baumer T, Slade J, Smith W, Haut R, 2008, "Tibiofemoral contact pressures and osteochondral microtrauma during ACL rupture due to excessive compressive loading and internal torque of the human knee," Am J Sports Med, **36**, pp. 1966-1977.

Mink J, Deutsch A, 1989, "Occult cartilage and bone injuries of the knee: Detection, classification, and assessment with MR imaging," Radiology, **170**, pp. 823-829.

Natoli R, Athanasiou K, 2008, "P188 reduces cell death and IGF-I reduces GAG release following single-impact loading of articular cartilage," J Biomech Eng, **130**, pp. 041012-1-9.

Olsen O, Myklebust G, Engebretsen L, Bahr R, 2004, "Injury mechanism for anterior cruciate ligament injuries in team handball: A systematic video analysis," Am J Sports Med, **32**, pp. 1002-1012.

Papaioannou N, Krallis N, Triantafillopoulos I, Khaldi L, Dontas I, Lyritis G, 2004, "Optimal timing of research after anterior cruciate ligament resection in rabbits.," Contemp Topics, **43**, pp. 22-27.

Phillips D, Haut R, 2004, "The use of a non-ionic surfactant (P188) to save chondrocytes from necrosis following impact loading of chondral explants," J Orthop Res, **22**, pp. 1135-1142.

Rangger C, Kathrein A, Freund M, Klestil T, Kreczy A, 1998, "Bone bruise of the knee: Histology and cryosections in 5 cases," Acta Orthop Scand, **69**, pp. 291-294.

Rundell S, Baars D, Phillips D, Haut R, 2005, "The limitation of acute necrosis in retro-patellar cartilage after a severe blunt impact to the in vivo rabbit patello-femoral joint," J Orthop Res, **23**, pp. 1363-1369.

Speer K, Spritzer C, Basset F, Feagin J, Garrett W, 1992, "Osseous injury associated with acute tears of the anterior cruciate ligament," Am J Sports Med, **20**, pp. 382-389.

Spindler K, Schils J, Bergfeld J, Andrish J, Weiker G, Anderson T, Piraino D, Richmond B, Medendorp S, 1993, "Prospective study of osseous, articular, and meniscal lesions in recent anterior cruciate ligament tears by magnetic resonance imaging and arthroscopy.," Am J Sports Med, **21**, pp. 551-557.

Thambyah A, Shim V, Chong L, Lee V, 2008, "Impact-induced osteochondral fracture in the tibial plateau," J Biomech, **41**, pp. 1236-1242.

Thompson R, Oegema T, Lewis J, Wallace L, 1991, "Osteoarthritic changes after acute transarticular load," J Bone Joint Surg, **73**, pp. 990-1001.

Torzilli P, Deng X, Warren R, 1994, "The effect of joint-compressive load and quadriceps muscle force on knee motion in the intact and anterior cruciate ligament-sectioned knee," Am J Sports Med, **22**, pp. 105-112.

Vellet A, Marks P, Fowler P, Munro T, 1991, "Occult post-traumatic osteochondral lesions of the knee: prevalence, classification and short-term sequelae evaluated with MR imaging," Radiology, **178**, pp. 271-276.

Vignon E, Bejui J, Mathiew P, Hartmann J, Ville G, Evreux J, Descotes J, 1987, "Histological cartilage changes in a rabbit model of osteoarthritis," J Rheum, **14**, pp. 104-106.

Weaver B, Haut R, 2005, "Enforced exercise after blunt trauma significantly affects biomechanical and histological changes in rabbit retro-patellar cartilage," J Biomech, **38**, pp. 1177-1183.

Yeow C, Cheong C, Ng K, Lee P, Goh J, 2008, "Anterior cruciate ligament failure and cartilage damage during knee joint compression," Am J Sports Med, **36**, pp. 934-942.

Yoshioka M, Coutts R, Amiel D, 1996, "Characterization of a model of osteoarthritis in the rabbit knee," OA and Cart, **4**, pp. 87-98.

CHAPTER FIVE

ACUTE REPAIR OF CHONDROCYTES IN THE RABBIT TIBIOFEMORAL JOINT FOLLOWING BLUNT IMPACT USING P188 SURFACTANT

ABSTRACT

Two specific types of injuries are strongly associated with subsequent knee OA; cruciate ligament damage and meniscal tears. Damage to chondrocytes has been documented in patients suffering ACL tears. Recent studies indicate that there may be a correlation between acute chondrocyte damage and the chronic progression of OA. P188 surfactant is able to interact with the bilayer of damaged cell membranes to restore their integrity after injury. The hypothesis of the current study was that a single injection of P188 into the *in vivo* TF joint following impact would reduce the percentage of damaged chondrocytes. A single, 13 J of energy impact was delivered to the left limb of eighteen rabbits, while the right legs served as contralateral controls. Animals were divided in three groups of six; 'time zero', '4 day no P188' and '4 day P188'. The left and right limbs of the 'time zero' and '4 day no P188' animals received an injection of sterile PBS immediately following trauma. The left limbs of the '4 day P188' rabbits received an injection of P188, and right limbs received a sham saline injection. Cell viability assays were performed to quantify the percentage of cells with damaged membranes. A two-way ANOVA was used to determine statistical differences between groups, and a two-way repeated measures ANOVA was used to determine differences between limbs. In both the 'time zero' and '4 day no P188' groups, an increase in the number of damaged chondrocytes was documented in the impacted limb compared to the control. The '4 day P188' group showed a significant decrease in the percentage of damaged chondrocytes

when compared to the '4 day no P188' animals. No significant difference was found between the impacted, P188 limb and the contralateral, control. A single injection of P188 surfactant into the TF joint immediately following insult resulted in a significant reduction in the percentage of cells with damaged plasma membranes in all compartments of the TF joint. Future studies should examine the long term consequences of P188 or possibly other interventions to acutely repair cellular membranes following trauma to the knee.

INTRODUCTION

Participation in sports, recreation and exercise (SRE) is increasingly popular and widespread in American culture. Furthermore, participation in SRE increases the risk of musculoskeletal injuries. History of a joint injury, particularly to the knee or hip, increases the risk of developing chronic joint disease, such as osteoarthritis (OA). OA affects over 21 million Americans and is the leading cause of disability in the United States (US Census Bureau, 2000). Acute knee joint injury has been associated with the subsequent development of post-traumatic osteoarthritis (Gelber et al., 2000). Although acute injury to cartilage is currently thought to be a factor associated with the development of OA, the pathway that leads from a blunt impact load on the joint cartilage to the development of chronic disease is yet unclear (Lewis et al., 2003). Recent studies have indicated that there may be a correlation between acute chondrocyte damage and the chronic pathogenesis of OA in the joint (Hashimoto et al., 1998; Natoli and Athanasiou, 2008). Since chondrocytes are required for matrix repair and chondrocyte death eventually leads to matrix loss (Simon et al., 1976), chondrocyte death by either apoptosis or necrosis has become a focus of OA research, and more recently cartilage trauma research.

Two specific types of injuries are strongly associated with subsequent knee OA; cruciate ligament damage and meniscal tears (Felson et al., 2004). Clincally, in over 80% of patients suffering anterior cruciate ligament (ACL) tears, a characteristic osteochondral lesion occurs in the postero-lateral aspect of the tibia and/or antero-lateral aspect of the lateral femoral condyle (Atkinson et al., 2008; Mink et al., 1989; Speer et al., 1992; Spindler et al., 1993). These injuries are also associated with visible damage to

the chondrocytes (Johnson et al., 1998) and an overt loss of cartilage within six months (Vellet et al., 1991) overlying "geographic" bone bruises, in particular. These types of bone lesions have been associated with occult microcracks of subchondral and/or trabecular bone (Speer et al., 1992; Rangger et al., 1998). There is also evidence that acute injury to articular cartilage overlying these bone bruises may predispose the knee to degenerative changes in the joint (Mankin, 1982; Thompson et al., 1991; Faber et al., 1996). Evidence in the current clinical literature suggests that these ACL patients will likely develop chronic joint disease whether they are reconstructed or not (Bahr et al., 2005). This may be due to the acute damage of articular cartilage in the joint.

Damage to articular cartilage overlying MRI detected bone bruises in patients with ACL tears has been suggested to be caused by excessive compressive forces on cartilage and meniscus generated in the joint during the acute ligamentous injury (Fang et al., 2001). This acute injury may provide a basis for the initiation of the chronic joint disease, OA (Fang et al., 2001; Frobell et al., 2008). In a previous study, our laboratory has shown that a single, 6 J of energy blunt insult to the rabbit PF joint leads to a significant increase in the percentage of acutely damaged chondrocytes (Rundell et al., 2005), as well as acute surface fissures, progressive degradation of retro-patellar surface cartilage, and thickening of underlying subchondral bone 3 years post-trauma (Ewers et al., 2002). The authors of these previous studies hypothesized that the chronic cartilage degradation may be partly due to acute damage of chondrocytes.

Acute damage to chondrocytes, necrosis, has been shown to produce degradative changes chronically in an *in vivo* animal model (Simon et al., 1976). A defining feature of cellular necrosis is swelling of the cell due to a damaged membrane. This damage results

in the inability of the cell to maintain ionic gradients across its plasma membrane and ultimately, the necrotic cell ruptures (Duke et al., 1996). Prior to cellular lysis, these cells may develop an apoptotic pathway or produce degenerative matrix enzymes (Baars et al., 2006). Due to their amphiphilic properties, some mild surfactants are able to interact with the bilayer of cell membranes to restore their integrity after injury from physical stress (Clarke and McNeil, 1992; Papoutsakis, 1991). One such surfactant is poloxamer 188 (P188). P188 is an 8400-dalton triblock copolymer containing both hydrophobic and hydrophilic regions. Recent studies on brain trauma suggest that P188 can help 'save' neurons from developing early necrotic death following severe mechanical loading (Barbee et al., 1992; Marks et al., 2001). Furthermore, P188 has been shown to reduce cell damage after *in vivo* loading of the rabbit PF joint (Rundell et al., 2005), as well as after *in vitro* impacts to bovine chondral (Phillips and Haut, 2004) and osteochondral (Natoli and Athanasiou, 2008) explants.

A previous study, using the rabbit tibiofemoral (TF) joint, documents a significant increase in the percentage of acutely damaged chondrocytes following a single, 13 J of energy impact on the joint (Isaac et al., 2008). Using this previously developed model, the hypothesis of the current study was that a single injection of P188 surfactant into the *in vivo* TF joint immediately after impact would significantly reduce the percentage of chondrocytes in the articular cartilage with acutely damaged plasma membranes. Ultimately, administration of this therapeutic agent immediately following a suspected joint injury may aid in mitigating the onset of a chronic joint disease.

MATERIALS AND METHODS

Eighteen skeletally mature, Flemish Giant rabbits (aged 6-12 months) were used in this study after approval by an All-University Committee on Animal Use and Care. The blunt impact experiments have been described previously in detail (Isaac et al., 2008). Briefly, a 1.75 kg mass with a pre-crushed, deformable impact head (Hexcel, 3.76 MPa crush strength) was dropped onto the left, flexed TF joint of anesthetized animals (2% isoflurane and oxygen). The right limb was not impacted and used as a paired, unimpacted control. A 4.45 kN (1000 lb) load transducer (Model AL311CV, 1000lb capacity, Sensotec, Columbus, OH) was attached behind the impact interface to record peak contact load, time to peak, and total contact duration.

Six rabbits were impacted and randomly selected as "time zero" animals and received a 1.5 mL sham injection of sterile phosphate buffered saline (PBS) into the joint capsule of both the right and left limbs. These animals were then sacrificed immediately after impact. The remaining 12 animals were sacrificed 4 days post-impact. During these four days the animals were housed in individual cages (152 x 152 x 36 cm) and permitted free cage activity. Six of the 4 day old animals received a single 1.5 mL injection of an 8 mg/mL concentration of P188 surfactant in sterile phosphate buffered saline (PBS) into the traumatized TF joint capsule immediately after impact. The concentration level was established in previous studies by the laboratory (Phillips and Haut, 2004; Rundell et al., 2005; Baars et al., 2006). The right legs of these animals received a 1.5 mL sham injection of sterile PBS into the joint. The remaining six 4 day animals received sham injections of 1.5 mL sterile PBS into both the impacted left limb as well as the contralateral, right limb. The combination of P188 in PBS and PBS sham solutions were

filter sterilized prior to injection using a 0.2 mm vacuum filter (Nalgene, Nalge Nunc Int., Rochester, NY). After injection, the limb was manually flexed a number of times to distribute the P188 surfactant and PBS solutions in the joint.

Immediately following sacrifice the joint was dissected and examined for abnormalities. The surfaces of the femur and tibia were wiped with India ink to highlight surface defects and photographed using a digital camera (Polaroid DMCS, Polaroid Corporation, Waltham, MA) under a dissecting microscope (Wild TYP 374590, Heerbrugg, Switzerland). The femurs and tibiae were prepared for cell viability analyses. A 6 mm trephine (#TREPH-6, Salvin Dental Specialties, Charlotte, NC) was used to core a region of the medial and lateral tibial plateau in areas not covered by the meniscus, as these were the areas of high contact pressure during impact [29]. A diamond saw (Isomet 11-1180 Low Speed Saw, Buehler, Lake Bluff, IL.) was then used to undercut the cores, leaving approximately 0.5 mm of bone underlying the articular cartilage. The femurs were fixed parallel to the diamond saw allowing coronal slices to be taken across the medial and lateral condyles in a predetermined area of contact, also leaving approximately 0.5 mm of underlying subchondral bone. Explants were rinsed 3 times with culture media before being placed in separate wells filled with fresh Dulbecco's modified Eagle's medium (DMEM): F12 (Gibco, USA #12500-062) supplemented with 10% fetal bovine serum, additional amino acids, and antibiotics (penicillin 100 units/ml, streptomycin 1μg/ml, amphotericin B 0.25 μg/ml), and incubated for 24 hours (37°C and 95% humidity) using an established protocol (Ewers et al., 2001).

Following incubation, full depth sections of the explants were cut using a specialized cutting device (Ewers et al., 2001). The cell viability analyses followed

previous procedures (Rundell et al., 2005). Briefly, slices from each compartment of the femur and tibia were rinsed with PBS and stained with calcein AM and ethidium homodimer (EthD-1), according to the manufacturer's specifications (Live/Dead Cytotoxicity Kit, Molecular Probes, Eugene, OR). Prior to imaging, each sample was rinsed three times with PBS to remove excess stain. Viable cells were distinguished by the presence of fluorescent (green) calcein AM. Damaged cells were distinguished by a bright red fluorescence due to ethidium homodimer passing through a damaged plasma membrane. Sections were viewed using a fluorescence microscope (Leitz Dialux 20, Leitz Mikroskopie und Systeme GmgH, Wetlzar, Germany). Each slice was then photographically divided into three zones: superficial (top 20% of explant thickness), middle (middle 50%) and deep (bottom 30%) (Phillips and Haut, 2004) (Figure 5.1). Two blinded observers (MR, BP) manually counted the number of green and red cells with an image analysis program (Image J, National Institutes of Health, 2004). The total percentage of damaged cells was determined for each section (for an average of approximately 4 samples from each compartment).

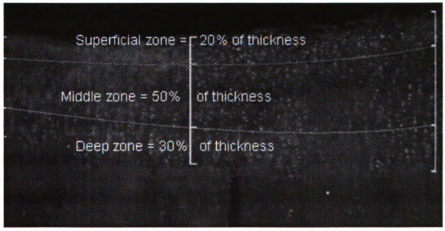

Figure 5.1. Cell viability was measured in the thin sections of cartilage and bone. The stained osteochondral explants were imaged and divided into three zones: superficial, middle, and deep.

Statistical analysis was used to evaluate the percentage of damaged cells in each compartment and zone. A two-factor, repeated measures ANOVA with a post hoc Tukey test was used to compare the left impacted limbs with the right controls in each time group for both the total percentage of damaged cells and the zonal data. A two-factor ANOVA with post hoc Tukey tests was used to compare the total and zonal data for both the impacted limbs of time zero versus 4 day no P188 group, and the 4 day no P188 versus 4 day P188 group. The control limbs of both 4 day groups were compared using a t-test. Statistical significance was indicated at $p<0.05$.

RESULTS

Gross inspection of the joints at necropsy showed no signs of joint disease and no damage to ligaments or menisci. No statistical differences were found in the times to peak impact load or the magnitudes of the peak load between treatment groups. The average peak, inertially compensated impact load and impact duration were 1102 ± 92 N and 23.0 ± 0.2 ms, respectively.

Analysis of damaged cells through the depth of the articular cartilage indicated a statistically significant increase in the percentage of damaged cells in the impacted than unimpacted joints in the medial compartment of the tibial plateau (MTP) ($p=0.003$), lateral tibial plateau (LTP) ($p=0.002$) and lateral femoral condyle (LFC) ($p=0.025$), as well as a statistical trend of a difference in the medial femoral condyle (MFC) ($p=0.08$) for the 'time zero' group. A significant increase in the total percentage of damaged cells was observed in the MTP ($p=0.003$), LTP ($p=0.004$) and LFC ($p<0.001$), as well as a statistical trend in the MFC ($p=0.069$) between the impacted '4 day no P188' and the contralateral, controls (Figure 5).

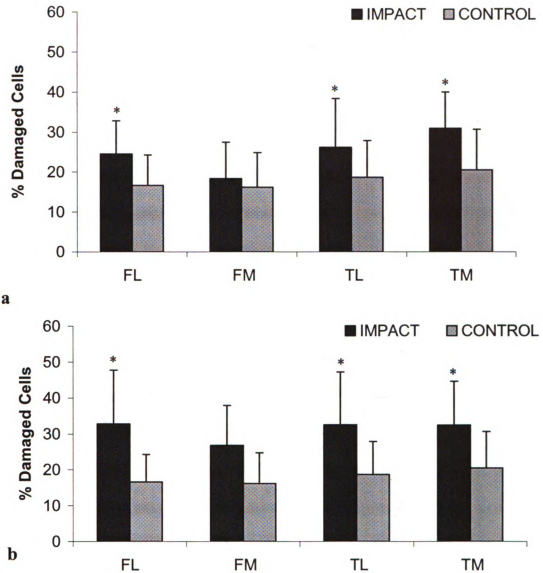

Figure 5.2. A single, blunt impact to the TF joint produced a significant increase in the percentage of damaged cells in the 'time zero' (a) and '4 day no P188' (b) groups. A '*' indicates a statistically significant difference between the impacted and control limbs.

A single injection of P188 into the TF joint immediately after impact significantly reduced the number of damaged chondrocytes in the MTP ($p=0.034$), LTP ($p<0.001$), MFC ($p<0.001$) and LFC ($p<0.001$) in the '4 day P188' group compared to the '4 day no P188 group' (Figure 5.3 & 5.4a).

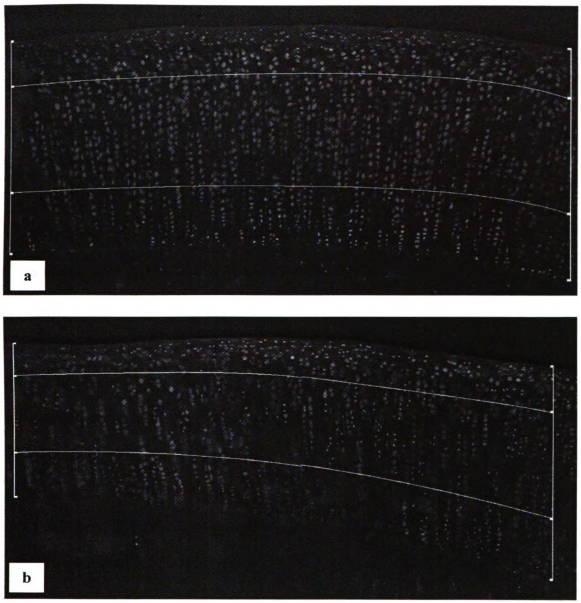

Figure 5.3. Administration of P188 significantly reduced the percentage of damaged cells in the '4 Day P188' group (a) when compared to the '4 Day No P188' group (b).

Furthermore, no significant differences were noted at any of the four locations between the '4 day P188 group' and their contralateral, control limbs (Figure 5.4b).

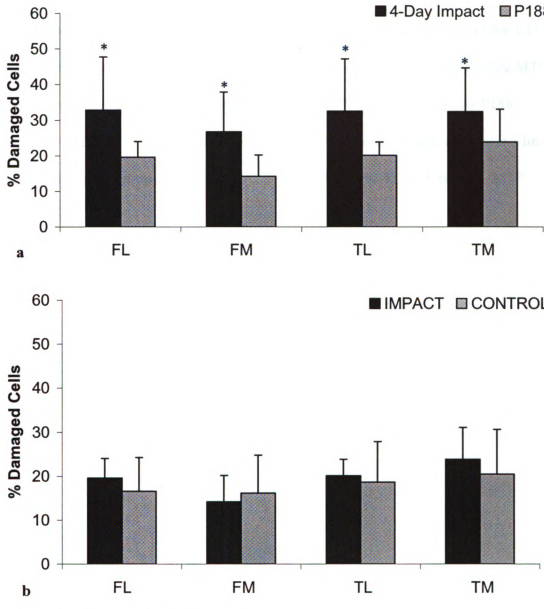

Figure 5.4. P188 reduced the number of damaged cells when compared to the '4 Day No P188' group (a), while no differences were noted between the '4 Day P188' group and the contralateral, controls (b). A '*' indicates a statistically significant difference between the impacted limbs of the '4 day no P188' and '4 day P188' groups.

Analysis of the zonal data indicated the most consistent statistical effects of impact and P188 intervention in the superficial zones. For example, significantly higher percentages of damaged cells were noted in the LFC ($p=0.002$), LTP ($p=0.004$), and MTP ($p=0.05$), with a statistical trend in the MFC ($p=0.1$) of the impacted limb when compared to the

contralateral, control limb for the '4 day no P188' group (Figure 5.5). Significantly higher percentages of damaged cells were also noted in the superficial zone of the LTP ($p=0.026$), MFC ($p=0.016$) and LFC ($p=0.002$), as well as a statistical trend in the MTP ($p=0.077$) between the impacted limbs of the '4 day no P188' and the '4 day P188' groups. However, no differences were seen between the impacted and contralateral limbs in the '4 day P188' group at any site (LFC $p=0.52$, MTP $p=0.41$, LTP $p=0.57$, MTP $p=0.91$).

Figure 5.5. Analysis of zonal data revealed a significant increase in the percentage of damaged cells in the superficial zone of the '4 Day No P188' group compared to their controls in the (a) LFC, (b) MFC, (c) LTP and (d) MTP. A'*' denotes a statistically significant difference between the impacted and contralateral limbs, while '+' denotes a significant difference between the impacted limbs of the '4-day no P188' and the '4 day P188' groups.

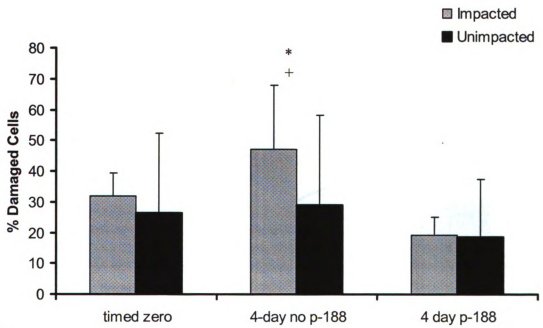

a

Figure 5.5 Continued.

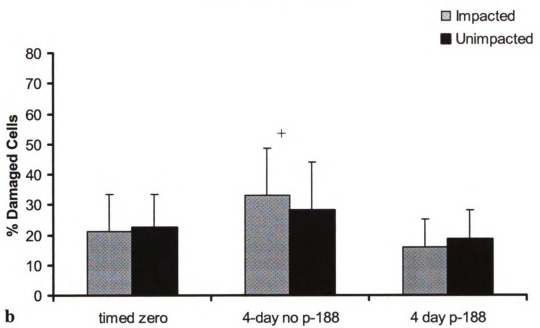

b

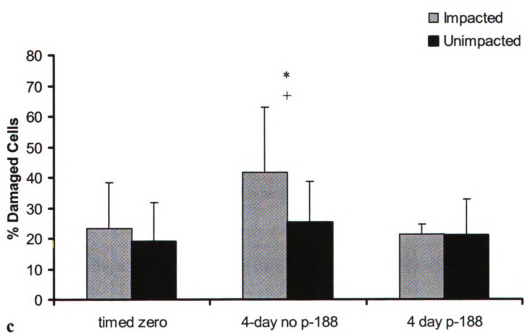

c

Figure 5.5 Continued.

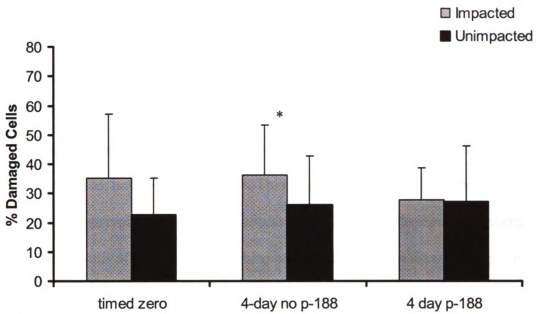

d

DISCUSSION

The objective of the current study was to determine the effect of P188 on cell viability following a single, traumatic impact to the rabbit TF joint. Impact trauma to the joint resulted in an increase in the percentage of damaged cells in the articular cartilage for all compartments. These results compared with a previous study by our laboratory documenting an increase in damaged cells in the medial (18%) and lateral (14%) tibial plateaus following a 13 J energy impact (Isaac et al., 2008). Furthermore, the current study indicated the greatest increase in the percentage of damaged chondrocytes following impact in the lateral compartments of both the femur and tibia. These results compared with those from Isaac et al. (2008) documenting slightly higher percentages of damaged cells laterally, and corresponding to a trend for higher impact induced contact pressures in the lateral compartment during impact. The results of both studies are

supported by the clinical literature in patients suffering anterior cruciate ligament (ACL) rupture where osteochondral lesions (or bone bruises) and early changes in the overlying articular cartilage are typically confined largely to the lateral compartment (Atkinson et al., 2008; Mink and Deutsch, 1989; Speer et al., 1992; Spindler et al., 1993).

Administration of P188 surfactant immediately after impact reduced the percentage of damaged cells for all locations in the TF joint. Some lack of statistical power was noted, however, in the MTP. This could be due to relatively more pre-impact, baseline damage typically in this compartment of the rabbit stifle joint (Golenberg et al., 2008). The results of the current study also compared with previous studies by our laboratory that document the ability of P188 to reduce the extent of chondrocyte damage following insult to the rabbit PF joint (Rundell et al., 2005), as well in bovine chondral explants undergoing unconfined compression for contact pressures of 25 MPa (Phillips and Haut, 2004). In a more recent study using bovine osteochondral explants Natoli and Anthanasiou (2008) also document that the administration of P188 surfactant following a 2.8 J impact reduced the percentage of cell death by nearly 75%.

Cell damage in the current study was measured by membrane disruption, documented by the ability of ethidium homodimer to pass through the plasma membrane. A defining feature of this damage, called necrosis, is cellular swelling due to the injured cell not being able to maintain ionic gradients across a damaged plasma membrane (Duke et al., 1996). Previously, Marks et al. (2001) showed that P188 surfactant specifically inserts into only the damaged areas of the cell membrane. A limitation of the current study was that the longer term response of these cells was not monitored. Chondrocyte death by apoptosis has been shown in human biopsy tissue near sites of chondral fracture

(Kim et al., 2002), as well as in canine cartilage explants following cyclic loads (Chen et al., 2001). While the mechanism of cell death following traumatic loading of articular cartilage is largely unknown, Chen et al. (2001) suggests that necrosis is observed 2 hrs after cessation of loading, whereas apoptosis (TUNEL-positive cells) is not significant until 48 or more hours after loading. These data suggest that mechanical injury to a joint may result in both necrotic and apoptotic cell death. Importantly, P188 repaired chondrocytes may ultimately die or produce excessive amounts of degeneration products after traumatic injury, via apoptosis. In fact, in a study on human chondral explants subjected to 14 MPa of unconfined compression D'Lima et al. (2001) documents 34% of chondrocytes suffered apoptosis in the longer term. The fate of these P188 repaired cells remains unknown. However, in a previous study performed by this laboratory using bovine chondral explants subjected to 25 MPa of unconfined compression, the administration of P188 surfactant was effective in reducing the percentage of cells with DNA fragmentation (as measured by TUNEL stain) 7 days following impact. Interestingly, the percentage of cells "saved" was similar to that "saved" within 1 day in previous studies using the same model (Phillips and Haut, 2004). The authors proposed that the acute damage to chondrocytes occurred by necrosis, as suggested by Chen et al (2001), and this precipitated a longer term response of the cells where apoptosis develops with the possible production of various products of matrix degradation (Baars et al., 2006).

Death of chondrocytes following traumatic injury has been associated with loss of glyosaminoglycans (GAG) from the tissue and decreased proteoglycan synthesis (Huser and Davies, 2006; Torzilli et al., 1999; Ewers et al., 2001; Jeffrey et al., 1997). These

degenerative changes have been shown to result in a loss of tissue integrity, represented by a decrease in tissue stiffness as well as an increase in tissue permeability (Kurz et al., 2001; Ewers and Haut, 2000; Ewers et al., 2002). Additionally, in a study on porcine patella Duda et al. (2001) document considerable cellular dysfunction that may act to promote the subsequent structural tissue damage. This may be particularly important because the synthesis of cartilage matrix proteins is directly dependant on cell viability (Duda et al., 2001). Cellular necrosis has been shown to generate early OA-like changes in tissue from a chronic animal model (Simon et al., 1976). With the ability of P188 to repair damaged cell membranes in the articular cartilage of the rabbit TF joint following severe blunt loading, the potential use of this surfactant should be explored as an intervention for the ACL injured patient. If P188 is capable of repairing chondrocytes, the cells may then function normally in the chronic setting. Surgical reconstruction may then yield a better long term result for the injured knee. Clinically, P188 has been used because of its lack of toxicity and has been shown to be 'squeezed out' of the cell membrane after it heals and excreted in the urine of the patient (Schmolka, 1977).

In summary, a 13 J blunt impact to the rabbit TF joint resulted in a significant increase in the percentage of damaged cells in the articular cartilage overlying femoral condyles and tibial plateaus. A single injection of P188 surfactant into the joint immediately following insult resulted in a significant reduction in the percentage of cells with damaged plasma membranes in all compartments of the joint. The long term consequences of 'saving' these cells from necrotic cell death, in terms of them becoming apoptotic and producing degradative enzymes, should be the focus of future investigations. While the exact mechanism leading from acute joint trauma to the chronic

progression of long term joint disease is currently unknown, recent evidence has shown that acute chondrocyte damage may play an important role. Therefore, future studies should examine the more long term consequences of P188, or possibly other interventions, on joint cartilage following ligamentous and other trauma to the knee and other diarthrodial joints of the human body.

ACKNOWLEDGEMENTS

This study was supported by a grand from the Centers for Disease Prevention and Control, Center for Injury Control & Prevention (CE000623). The contents of this manuscript are solely the responsibility of the authors and do not necessarily represent the official views of the Center for Injury Prevention and Control. The authors wish to acknowledge Ms. Jean Atkinson (J.A.) for her assistance in animal care, Michelle Raetz (M.R.) and Brian Powell (B.P.) for their assistance in cell viability analyses, and Eric Meyer for his assistance in the impact procedures.

REFERENCES

Atkinson PJ, Cooper TG, Anseth S, Walter NE, Kargus R, Haut RC, 2008, "Knee bone bruise frequencies vary with time post-injury and type of soft tissue injury," Orthopedics, **31**, pp. 440.

Baars DC, Rundell SA, Haut RC, 2006, "Treatment with the non-ionic surfactant poloxamer P188 reduces DNA fragmentation in cells from bovine chondral explants exposed to injurious unconfined compression," Biomech Model Mechanobiol, **5(2-3)**, pp. 133-139.

Bahr R, Myklebust G, 2005, "Return to play guidelines after anterior cruciate ligament surgery," Br J Sports Med, **39**, pp. 127-131.

Barbee K, Ford C, Blackman B, Thibault L, 1992, "Neural cell injury: characterization and treatment strategy," In 2nd Injury Prevention Through Biomechanics Symposium Proceeding, CDC. Edited by Yang K..

Chen CT, Burton-Wurster N, Borden C, Hueffer K, Bloom SE, Lust G, 2001, "Chondrocyte necrosis and apoptosis in impact damaged articular cartilage," J Orthop Res, **19**, pp. 703-711.

Clarke MSF, McNeil PL, 1992, "Syringe loading introduces macromolecules into living mammalian cell cytosol," J Cell Sci, **102**, pp. 533-541.

D'Lima DD, Hashimoto S, Chen PC, Colwell CW, Lotz MK, 2001, "Impact of mechanical trauma on matrix and cells," Clincal Orthopaedics and Related Research, **1(391)**:, pp. S90-S99.

Duda GN, Eilers M, Loh L, Hoffman JE, Kaab M, Schaser K, 2001, "Chondrocyte death precedes structural damage in blunt impact trauma," Clinical Orthopaedics and Related Research, **393**, pp. 302-309.

Duke RC, Ojcius DM, Young JD, 1996, "Cell suicide in health and disease," Scientific American, **275**, pp.: 80-87.

Ewers BJ, Dvoracek-Driksna D, Orth MW, Haut RC, 2001, "The extent of matrix damage and chondrocyte death in mechanically traumatized articular cartilage explants depends on rate of loading," J Orthop Res, **19**, pp. 779-784.

Ewers BJ, Haut RC, 2000, "Polysulphated gycosaminoglycan treatments can mitigate decreases in stiffness of articular cartilage in a traumatized animal joint," J Orthop Res, **18**, pp. 756-761.

Ewers BJ, Weaver BT, Sevensma ET, Haut RC, 2002, "Chronic changes in rabbit retro - patellar cartilage and subchondral bone after blunt impact loading of the patellofemoral joint," J Orthop Res, **20**, pp. 5545-550.

Faber K, Dill J, Thain L, Spouge A, Fowler PJ, 1996, "Intermediate follow-up of occult osteochondral lesions following ACL reconstruction," Arthroscopy: J Arthroscopic Rel Surg, **12**, pp. 370-371.

Fang C, Johnson D, Leslie MP, Carlson CS, Robbins M, Cesare PE, 2001, "Tissue distribution and measurements of cartilage oligomeric matrix protein in patients with magnetic resonance imaging-detected bone bruises after acute anterior cruciate ligament tears," J Orthop Res, **19**, pp. 634-641.

Felson DT, 2004, "An update on the pathogenesis and epidemiology of osteoarthritis," Radiol Clin North Am, **42**, pp. 1-9.

Frobell RB, Roos HP, Roos EM, Hellio Le Graverand M-P, Buck R, Tamez-Pena Gelber A, Hochberg M, Mead L, Wang N, Wigley F, Klag M, 2000, "Joint injury in young adults and risk for subsequent knee and hip osteoarthritis," Ann Intern Med, **133(5)**, pp. 321-328.

Frobell RB, Roos HP, Roos EM, Hellio LeGraverand M-P, Buck R, Tamez-Pena J, Totterman S, Boegard T, Lohmander LS, 2008, "The acutely ACL injured knee assessed by MRI: are large volume traumatic bone marrow lesions a sign of severe compression injury?" Osteoarthritis and Cartilage, **16**, pp. 829-836.

Golenberg N, Kepich E, Haut RC, 2008, "Histomorphological and mechanical property correlations in rabbit tibial plateau cartilage based on a fibril-reinforced biphasic model," Int J Exp Comp Biomech, **1(1)**, pp. 58-75.

Hashimoto S, Ochs RL, Komiya S, Lotz M, 1998, "Linkage of chondrocyte apoptosis and cartilage degredation in human osteoarthritis," Arth Rheum, **41(9)**, pp. 1632-1638.

Huser CAM, Davies ME, 2006, "Validation of an In Vitro single-impact load model of the initiation of osteoarthritis –like changes in articular cartilage," J Orthop Res, **24(4)**, pp. 725-732.

Isaac DI, Meyer EG, Haut RC, 2008, "Chondrocyte damage and contact pressures following impact on the rabbit tibiofemoral joint," J Biomech Eng, **1130**, pp.00410181-5.

Jeffrey JE, Gregory GW, Aspden RM, 1997, "Matrix damage and chondrocyte viability following a single impact load on articular cartilage," Archive of Biochemistry and Biophysics, **322(1)**, pp. 87-96.

Johnson DL, Urban WP, Carbon DNM, Vanarthos WJ, Carlson CS, 1998, "Articular cartilage changes seen with magnetic resonance imagining-detected bone bruises

associated with acute anterior cruciate ligament rupture," Am J Sports Med, **26,** pp. 409-414.

Kim HT, Lo MY, Pillarisetty R, 2002, "Chondrocyte apoptosis following intraarticular fracture in humans," Osteoarthritis and Cartilage, **10**, pp. 747-749.

Kurz B, Jin M, Patwari P, Cheng DM, Lark MW, Grodzinsky AJ, 2001,"Biosynthetic response and mechanical properties of articular cartilage after injurious compression," J Orthop Res, **19**, pp. 1140-1146.

Lewis JL, Deloria LB, Oyen-Tiesma M, Thompson RC Jr., Ericson M, Oegema TR Jr, 2003, "Cell death after cartilage impact occurs around matrix cracks," J Orthop Res, **21**, pp. 881-887.

Mankin HJ, 1982, "The response of articular cartilage to mechanical injury," J Bone Joint Surg, **64(A)**, pp. 460-466.

Marks JD, Pan CY, Bushell T, Cromie W, Lee RC, 2001, "Amphiphilic tri-block copolymers provide potent membrane-targeted neuroprotection," FASEB, **15**, pp. 1107-1109.

Mink JH, Deutsch AL, 1989, "Occult cartilage and bone injuries of the knee: detection, classification, and assessment with MRmr imaging," Radiology, **170**, pp. 823-829.

Natoli RM, Athanasiou KA, 2008, "P188 reduces cell death and IGF-I reduces GAG release following single-impact loading of articular cartilage," J Biomech Eng, **1130:0,** pp. 041012-1-9.

Papoutsakis ET, 1991, "Media additives for protecting freely suspended animal cells against agitation and aeration damage," TIBTECH, **9**, pp. 316-324.

Phillips DM, Haut RC, 2004, "The use of a non-ionic surfactant (P188) to save chondrocytes from necrosis following impact loading of chondral explants," J Orthop Res, **22,** pp. 1135-1142.

Rangger C, Kathrein A, Freund MC, Klestil T, Kreczy A, 1998, "Bone bruise of the knee; histology and cryosections in 5 cases," Acta Orthop Scand, **6 69(3)**, pp. 291-294.

Rundell SA, Baars DC, Phillips DM, Haut RC, 2005, "The limitation of acute necrosis in retro-patellar cartilage after a severe blunt impact to the in vivo rabbit patello-femoral joint," J Orthop Res, **23**, pp. 1363-1369.

Schmolka IR, 1977, "A review of block polymer surfactants," J Am Oil Chemists' Society, **54(3)**, pp. 110-116.

Simon WH, Richardson S, Herman W, Parsons JR, Lane J, 1976, "Long-term effects of chondrocyte death on rabbit articular cartilage in vivo," J Bone Joint Surg Am, **58**, pp. 517-526.

Speer KP, Spritzer CE, Bassett FH, Feagin JA, Garrett WE, 1992, "Osseous injury associated with acute tears of the anterior cruciate ligament," Am J Sports Med, **20**, pp. 382-389.

Spindler KP, Schils JP, Bergfeld JA, Andrish JT, Weiker GG, Anderson TE, Piraino DW, Richmond BJ, Medendorp SV, 1993, "Prospective study of osseous, articular, and meniscal lesions in recent anterior cruiciate ligament tears by magnetic resonance imaging and arthroscopy," Am J Sports Med, **21**, pp. 551-557.

Thompson RC, Oegema T, Lewis J, Wallace L, 1991,"Osteoarthritic changes after acute transarticular load," J Bone Joint Surg Am , **73**, pp. 990-1001.

Torzilli PA, Grigiene R, Borrelli J Jr, Helfet DL, 1999, "Effect of impact load on articular cartilage: cell metabolism and viability, and matrix water content," J Biomech Eng, **121,** pp. 433-441.

US Census Bureau, State and County Quickfacts, US Public Information Office, 2000.

Vellet AD, Marks PH, Fowler PJ, Munro TG, 1991, "Occult posttraumatic osteochondral lesions of the knee: prevalence, classification, and short-term sequelae evaluated with MR imaging," Radiology, **178**, pp. 271-276.

CHAPTER SIX

CONCLUSIONS AND RECOMMENDATIONS FOR FUTURE WORK

The previous chapters describe the results of a severe, blunt impact load to the *in vivo* rabbit tibiofemoral (TF) joint resulting in damage to cartilage and underlying subchondral bone. A novel, *in vivo* model of traumatic ACL rupture has also been developed and contrasted with conventional ACL transaction models. Additionally, the use of a potential therapeutic agent to restore membrane integrity to acutely damage chondrocytes was also explored.

In Chapter 2 a single, blunt impact to the rabbit TF joint was found to result in high contact pressures located primarily in regions uncovered by the meniscus on the medial and lateral tibial plateaus. Additionally, higher contact pressures were documented on the lateral plateau compared to the medial plateau. A single, severe impact was also found to result in a significant increase in the percentage of cells with damaged plasma membranes in the articular cartilage overlying the medial and lateral tibial plateaus. A slightly higher percentage of damaged cells was documented in the lateral plateau corresponding to slightly higher contact pressures. Acute damage to chondrocytes has been thought to lead to the progression of chronic joint disease. Future studies should investigate the longer-term implications of chondrocyte death in the pathogenesis of joint disease in order to establish a cause and effect relationship between acute trauma to cartilage and chronic joint disease.

Chapter 3 described a study on the rabbit TF joint subjected to a 13 Joule impact. In this study the chronic alterations in the mechanical and histological properties of cartilage and underlying subchondral bone at 6 months and 1 year were investigated. The

major findings of this study included the presence of vertical and horizontal microcracks at the articular cartilage and subchondral bone interface as well as an increase in the subchondral bone thickness at 1 year post-trauma. Furthermore, analysis of the mechanical properties of the cartilage showed no significant changes in any mechanical parameter at either 6 months or 1 year. However, in comparing the 6 month properties to the 1 year significant stiffening in both the matrix and fiber modulus was documented in the impacted limbs. Stiffening of the contralateral, control limb was also documented between the 2 groups; however, increase in these properties were shown in the control animals. Although not quantified in the current study, this stiffening was attributed to calcification/ossification of the articular cartilage. Future investigations should investigate the calcium content of the cartilage in this model in order to validate the ossification process. In addition, future studies should acknowledge the fact that stiffening was also observed in the contralateral limb and document the implications of altered gait following knee joint trauma. Bone trauma documented in the current study could have also lead to a more advanced progression of the disease, therefore, future studies should also investigate the implications of acute bone trauma in the chronic disease process.

Chapter 4 described the development of a traumatic anterior cruciate ligament failure model where a single, compressive load was delivered to the TF joint resulting in ACL rupture. This model was then compared to current conventional OA models via ACL transaction. Compressive loads generated in the joint during the acute ligamentous injury were found to lead to significant damage to cartilage, including acute surface lesions and chondrocyte damage, as well microcracking in subchondral bone. Since the

clinical literature documents significant damage to cartilage and underlying bone in patients suffering ACL tears, the current study may provide a more clinically relevant model for the investigation of joint trauma. Future investigations should focus on documenting the biochemical changes in the joint synovial fluid and cartilage. In addition, the current literature suggests that reconstruction of the ACL has not proven effective at mitigating the onset of post-traumatic OA, possibly due to the acute damage to cartilage and subchondral bone. However, future studies should also investigate the implications of ACL reconstruction coupled with therapeutic treatments aimed at repairing the acutely injured cartilage and subchondral bone.

Chapter 5 investigated the effects of treating acutely injured cartilage with a non-ionic surfactant, P188. The major findings of this study were the presence of acutely necrotic cells in the articular cartilage of the medial and lateral tibial plateau and a reduction in the percentage of these damaged cells with the administration of Poloxamer 188 (P188) directly into the joint immediately following impact. This study did not, however, assess the long term viability of the 'saved' cells. It is possible that these damaged cells, although repaired within 4 days post-trauma, may still have abnormal functionality and soon die via apoptotic pathways at a later time. In addition, the current study did not investigate the effects of multiple injections of P188 at various time periods. It is possible that multiple injections may help prevent cells from dying in the chronic setting. Future studies should investigate the long term viability of these acutely 'saved' cells. A different cell viability analysis in order to assess apoptotic cells should also be included in future investigations. Furthermore, the concentration of P188 in this study was chosen based on previous work done by our laboratory. Future investigations

should analyze the effects of various concentration levels and the ability to 'save' acutely injured chondrocytes. Finally, mechanical response of the cartilage matrix should also be investigated in order to determine the longer term effects of 'saving' acutely damaged chondrocytes following traumatic injury.

APPENDIX A

RAW DATA FROM CHAPTER TWO

Table A.1. Pressure film data for the right and left limbs.

LATERAL TIBIAL PLATEAU							
Specimen RSOAO4 -RIGHT		**Specimen RSOAO4 - LEFT**		**Specimen LB737 - RIGHT**		**Specimen LB737 - LEFT**	
Impact Load (N)	1264.00	Impact Load (N)	1084.00	Impact Load (N)	1084.00	Impact Load (N)	1084.00
# Pixels =	1118.00	# Pixels =	829.00	# Pixels =	1203.00	# Pixels =	1269.00
Area =	32.01	Area =	23.73	Area =	34.44	Area =	36.33
Ave Pressure =	22.60	Ave Pressure =	28.12	Ave Pressure =	19.39	Ave Pressure =	21.06
Ave Force =	723.23	Ave Force =	667.37	Ave Force =	667.74	Ave Force =	765.30
Max. Pressure	44.32	Max. Pressure	54.88	Max. Pressure	37.37	Max. Pressure	44.88
Min. Pressure	10.10	Min. Pressure	11.07	Min. Pressure	10.10	Min. Pressure	10.10
Percent of total	42.1%	Percent of total	48.9%	Percent of total	65.0%	Percent of total	58.0%
MEDIAL TIBIAL PLATEAU							
# Pixels =	1656.00	# Pixels =	1287.00	# Pixels =	526.00	# Pixels =	1027.00
Area =	47.41	Area =	36.85	Area =	15.06	Area =	29.40
Ave Pressure =	21.01	Ave Pressure =	18.92	Ave Pressure =	23.83	Ave Pressure =	18.82
Ave Force =	996.34	Ave Force =	697.29	Ave Force =	358.94	Ave Force =	553.45
Max. Pressure	49.60	Max. Pressure	36.07	Max. Pressure	41.17	Max. Pressure	45.44
Min. Pressure	10.10	Min. Pressure	10.10	Min. Pressure	10.10	Min. Pressure	10.10
Percent of total	57.9%	Percent of total	51.1%	Percent of total	35.0%	Percent of total	42.0%
Medium Total Force	1719.58	Medium Total Force	1364.66	Medium Total Force	1026.68	Medium Total Force	1318.75

Table A.2. Peak Pressures on the lateral and medial tibial plateau.

Lateral Tibial Plateau		Medial Tibial Plateau	
Rabbit	Peak Pressure (MPa)	Rabbit	Peak Pressure (MPa)
RSOA04R	44.32	RSOA04R	49.6
RSOA04L	54.88	RSOA04L	36.07
LB737R	44.88	LB737R	45.44
LB737L	37.37	LB737L	41.17
Average	45.36	**Average**	43.07
Standard Dev	7.20	**Standard Dev**	5.79

Table A.3. Cell viability data for the impact (left) and unimpacted (right) animal

	Combined Lateral Control						Combined Medial Control					
Rabbit	Sample	Live	Dead	Total	% Live	% Dead	Sample	Live	Dead	Total	% Live	% Dead
BB3	LLA5B	724	206	930	77.85	22.15	LMC4B	1205	411	1616	74.57	25.43
	LLA7B	315	179	494	63.77	36.23	LMC9B	912	236	1148	79.44	20.56
	LLA12B	606	156	762	79.53	20.47	LMC11B	986	376	1362	72.39	27.61
	LLB4B	681	269	950	71.68	28.32	LMD1B	821	705	1526	53.80	46.20
	RLC6B	816	95	911	89.57	10.43	RMA3B	748	257	1005	74.43	25.57
	RLC9B	977	108	1085	90.05	9.95	RMA9B	1327	304	1631	81.36	18.64
	RLC11B	583	70	653	89.28	10.72	RMA11B	951	464	1415	67.21	32.79
	RLD2B	755	79	834	90.53	9.47	C3LM2	647	308	955	67.75	32.25
GF5	A12LL2	772	535	1307	59.07	40.93	C6LM3	645	318	963	66.98	33.02
	A10LL3	371	469	840	44.17	55.83	C8LM2	850	410	1260	67.46	32.54
	B02LL2	653	127	780	83.72	16.28	D2LM2	696	183	879	79.18	20.82
	B04LL2	829	391	1220	67.95	32.05	E3RM1	1536	89	1625	94.52	5.48
	F5RL2	698	341	1039	67.18	32.82	E5RM1	1025	80	1105	92.76	7.24
	F7RL2	980	937	1917	51.12	48.88	E11RM2	941	207	1148	81.97	18.03
	F12RL2	755	424	1179	64.04	35.96	E8RM3	805	52	857	93.93	6.07
	G3RL2	888	291	1179	75.32	24.68	C11LM2	1092	321	1413	77.28	22.72
MG19	A4LL2	614	113	727	84.46	15.54	C7LM2	524	218	742	70.62	29.38
	A6LL2	1060	153	1213	87.39	12.61	C9LM2	996	312	1308	76.15	23.85
	A9LL2	901	314	1215	74.16	25.84	E10RM3	1196	298	1494	80.05	19.95
	A11LL2	1216	310	1526	79.69	20.31	E9RM2	997	270	1267	78.69	21.31
	G10RL2	1097	302	1399	78.41	21.59	F1RM3	1212	398	1610	75.28	24.72
	G12RL2	1238	389	1627	76.09	23.91				**Average**	76.47	23.53
	G6RL2	1046	197	1243	84.15	15.85				**Std. Dev.**	9.73	9.73
	H3RL3	1245	440	1685	73.89	26.11						
				Average	75.13	24.87						
				Std. Dev.	12.33	12.33						

Table A.4. Zonal cell viability data (% Dead Cells) for the impacted (left) and unimpacted (right) limbs

Left Lateral				Left Medial			
Sample	**Super**	**Middle**	**Deep**	**Sample**	**Super**	**Middle**	**Deep**
A5LL2	51.59	26.09	25.87	**C5LM1**	78.42	32.55	13.10
A7LL3	50.29	11.58	26.05	**C6LM2**	59.57	11.05	10.90
A11LL3	43.89	39.39	60.45	**E2LM2**	47.99	29.06	60.21
B5LL2	17.88	10.12	24.26	**LME112**	36.65	24.11	9.03
LLB42	34.43	36.85	25.55	**LMF22**	31.72	44.73	30.61
LLB62	72.17	46.87	31.28	**LMF61**	70.61	47.65	15.89
LLB82	43.86	31.90	19.50	**LMF2 2**	54.51	17.80	13.92
LLB2 2	38.46	11.44	14.44	**LMF4 3**	36.40	19.26	47.41
LLB6 2	76.47	45.14	37.92	**LMF6 2**	20.50	15.72	37.27
LLB8 2	73.82	43.34	33.33	**LMF8 2**	36.06	58.82	13.59

Right Lateral				Right Medial			
Sample	**Super**	**Middle**	**Deep**	**Sample**	**Super**	**Middle**	**Deep**
G9RL2	23.85	15.34	21.60	**D7RM2**	7.73	11.23	28.27
G12RL2	27.97	15.67	41.60	**F2RM3**	38.58	12.09	13.93
H5RL2	35.59	13.18	13.40	**RMG41**	21.05	17.19	17.92
H6RL2	48.59	34.44	40.20	**RMG71**	44.49	47.63	16.67
RLC92	26.61	6.76	19.93	**RMG31**	25.00	14.77	22.94
RLC122	29.69	17.43	31.14	**RMG10 2**	21.11	9.76	17.53
RLD22	14.42	14.39	18.10	**RMG12 3**	12.21	12.73	25.34
RLD53	41.56	21.70	34.75	**RMH2 3**	23.04	19.51	28.63
RLD2 2	65.61	38.89	51.21	**RMH4 2**	12.27	22.89	43.40
RLD4 2	42.24	40.29	35.22				
RLD6 3	30.87	30.77	42.19				

APPENDIX B

RAW DATA FROM CHAPTER THREE

Table B.1. Histology scores for the impacted (left) limb of the 6 month animals.

Rabbit	Facet	Limb	Fissures	PG Stain	Cells	Disruptions	AC Thick	Tide Mark	TM Thick	Spikes	Stain	SB Thick	Morphology
	Medial	Left	1	0	0	2	42	0	6	2	2	31	3
RSOCO4	Lateral	Left	0	0	0	4	32	0	11	2	2	35	3
	Medial	Left	7	1	0	3	52	0	7	2	3	25	1
RSOLAB	Lateral	Left	2	0	0	4	34	0	7	2	2	29	1
	Medial	Left	2	3	2	2	47	0	8	2	2	34	1
FM1	Lateral	Left	2	1	0	3	30	0	6	3	1	23	3
	Medial	Left	3	1	0	5	51	0	5	3	3	30	1
MF15	Lateral	Left	0	0	0	3	33	0	11	2	3	38	3
	Medial	Left	3	1	1	1	51	0	5	1	2	26	1
MF17	Lateral	Left	0	1	1	0	36	0	5	1	2	25	1
	Medial	Left	2	1	0	1	61	0	10	3	3	28	3
MF16	Lateral	Left	0	0	0	0	40	0	12	2	3	30	3
	Medial	Left	3	0	1	3	21	0	7	2	3	25	1
SM1	Lateral	Left	0	1	1	5	29	0	9	1	2	30	1
	Medial	Left	5	1	0	7	53	0	7	1	2	27	3
TF1	Lateral	Left	1	0	0	3	35	0	6	1	2	34	3
	Medial	Left	3	2	0	4	37	0	5	1	2	23	3
TF6	Lateral	Left	0	0	0	4	33	0	9	1	3	23	3
	Medial	Left	3	1	0	5	50	0	7	1	2	19	1
MF7	Lateral	Left	1	0	0	10	38	0	7	0	2	23	1
	Medial	Left	2	1	1	0	48	0	5	1	2	27	1
TF10	Lateral	Left	0	1	0	0	45	0	5	2	2	32	1
	Medial	Left	1	0	1	2	41	0	4	1	2	24	1
TF11	Lateral	Left	1	0	1	2	29	0	5	2	1	26	1

Table B.2. Histology scores for the contralateral, control (right) limb of the 6 month animals.

Rabbit	Facet	Limb	Fissures	PG Stain	Cells	Disruptions	AC Thick	Tide Mark	TM Thick	Spikes	Stain	SB Thick	Morphology
	Medial	Right	3	1	0	0	60	0	6	2	3	27	3
RSOCO4	Lateral	Right	0	0	1	1	40	0	11	4	3	32	1
	Medial	Right	1	0	0	0	48	0	7	1	2	29	1
RSOLAB	Lateral	Right	0	0	1	0	39	0	8	2	2	33	1
	Medial	Right	0	0	1	0	45	0	5	2	2	22	1
FM1	Lateral	Right	0	0	1	0	36	0	9	2	2	26	1
	Medial	Right	2	0	0	1	48	0	9	2	3	32	1
MF15	Lateral	Right	1	0	0	0	35	0	7	2	2	31	3
	Medial	Right	2	0	1	1	41	0	4	1	2	25	1
MF17	Lateral	Right	3	0	2	2	34	0	7	1	2	25	1
	Medial	Right	3	0	0	1	62	0	7	4	2	26	3
MF16	Lateral	Right	0	0	1	0	34	0	6	4	2	26	3
	Medial	Right	1	0	1	1	45	0	8	1	2	23	1
SM1	Lateral	Right	1	0	2	1	38	0	9	2	2	27	3
	Medial	Right	1	0	0	0	58	0	6	2	2	21	3
TF1	Lateral	Right	0	0	1	0	37	3	11	1	1	28	3
	Medial	Right	1	0	0	0	37	0	4	1	2	20	1
TF6	Lateral	Right	1	0	1	0	27	0	8	1	2	20	1
	Medial	Right	1	1	0	2	55	0	7	1	2	21	1
MF7	Lateral	Right	2	0	0	3	39	0	7	1	2	24	1
	Medial	Right	0	0	1	1	30	0	4	0	1	24	3
TF10	Lateral	Right	0	0	1	1	32	0	6	1	3	35	1
	Medial	Right	0	0	1	0	30	0	5	2	2	23	1
TF11	Lateral	Right	0	0	2	0	12	0	11	1	3	15	1

Table B.3. Histology scores for the non-impacted, control animals (left limb) of the 6 month group.

Rabbit	Facet	Limb	Fissures	PG Stain	Cells	Disruptions	AC Thick	Tide Mark	TM Thick	Spikes	Stain	SB Thick	Morphology
	Medial	Left	3	0	1	0	33	0	4	1	2	28	1
FB4	Lateral	Left	0	0	0	0	31	0	8	4	2	32	1
	Medial	Left	2	0	0	0	60	0	6	1	2	34	1
MF6	Lateral	Left	0	0	0	0	42	0	10	1	2	37	3
	Medial	Left	4	0	0	0	23	0	9	0	2	25	3
MF10	Lateral	Left	0	0	0	0	34	3	11	0	1	33	3
	Medial	Left	1	0	1	0	48	0	8	1	2	29	1
TF18	Lateral	Left	1	0	0	0	31	0	9	1	2	30	1
	Medial	Left	1	0	1	1	54	0	4	0	3	19	1
TF8	Lateral	Left	0	0	0	0	35	0	5	0	3	21	1
	Medial	Left	2	0	0	1	42	0	6	0	2	23	1
TF7	Lateral	Left	0	1	1	0	28	0	9	1	1	30	3
	Medial	Left	1	1	0	1	39	0	7	1	2	24	1
TF14	Lateral	Left	0	0	1	1	28	0	6	2	2	21	1
	Medial	Left	0	1	1	1	51	0	5	1	2	26	1
TF17	Lateral	Left	0	1	1	0	36	0	5	1	2	22	1
	Medial	Left	3	1	1	0	49	0	5	1	1	32	1
FN3	Lateral	Left	0	1	0	1	35	0	7	3	1	34	1
	Medial	Left	1	0	0	1	55	0	8	2	3	28	3
ACB71	Lateral	Left	0	0	1	0	40	0	6	2	3	35	1
	Medial	Left	2	0	1	0	48	0	6	1	2	32	3
TF25	Lateral	Left	0	0	1	0	18	1	9	3	2	26	3

Table B.4. Histology scores for the non-impacted, control animals (right limb) of the 6 month group.

Rabbit	Facet	Limb	Fissures	PG Stain	Cells	Disruptions	AC Thick	Tide Mark	TM Thick	Spikes	Stain	SB Thick	Morphology
	Medial	Right	2	1	0	1	38	0	5	0	2	23	3
FB4	Lateral	Right	0	0	0	0	27	0	5	1	2	27	1
	Medial	Right	0	0	0	1	39	0	5	1	2	29	1
MF6	Lateral	Right	0	0	0	0	32	0	9	0	2	20	1
	Medial	Right	0	0	1	1	38	0	3	0	2	22	3
MF10	Lateral	Right	0	0	1	0	33	0	13	1	2	25	3
	Medial	Right	1	0	0	0	44	0	7	0	2	24	3
TF18	Lateral	Right	0	0	0	0	34	0	6	1	2	37	3
	Medial	Right	2	0	0	1	45	0	4	0	3	24	3
TF8	Lateral	Right	1	0	1	0	35	0	5	1	3	24	1
	Medial	Right	1	1	0	0	42	0	12	1	3	28	3
TF7	Lateral	Right	0	0	0	0	23	0	8	0	2	29	3
	Medial	Right	1	1	0	1	44	0	5	1	2	22	1
TF14	Lateral	Right	0	0	0	0	30	0	6	2	2	21	1
	Medial	Right	1	0	1	1	41	0	4	1	2	25	1
TF17	Lateral	Right	0	0	2	1	34	0	7	1	2	25	1
	Medial	Right	2	1	1	0	38	0	5	1	2	25	3
FN3	Lateral	Right	1	0	0	0	32	0	7	2	2	24	3
	Medial	Right	0	0	0	1	41	0	5	1	2	27	3
ACB71	Lateral	Right	1	0	2	0	40	2	7	2	2	33	1
	Medial	Right	1	1	1	1	51	0	6	0	2	32	3
TF25	Lateral	Right	0	0	2	0	20	1	7	3	2	24	1

Table B.5. Histology scores for the impacted (left) limb of the 1 year animals.

Rabbit	Facet	Limb	Fissures	PG Stain	Cells	Disruptions	AC Thick	Tide Mark	TM Thick	Spikes	Stain	SB Thick	Morphology
	Medial	Left	3	1	0	3	50	0	6	1	2	25	1
A3	Lateral	Left	0	1	0	1	28	32	14	1	1	30	1
	Medial	Left	1	1	0	5	34	0	7	3	1	27	1
MF12	Lateral	Left	2	3	3	4	29	0	12	2	2	29	3
	Medial	Left	5	1	1	4	49	0	6	3	2	30	3
FN1	Lateral	Left	2	2	0	2	32	0	10	3	2	25	3
	Medial	Left	2	1	2	1	35	0	5	3	3	30	3
FB3	Lateral	Left	4	0	1	0	35	0	9	3	3	38	1
	Medial	Left	2	0	0	8	52	2	8	1	0	29	3
CKDOC	Lateral	Left	0	0	0	0	21	0	11	0	0	32	3
	Medial	Left	1	1	1	9	46	0	7	2	0	22	1
A2	Lateral	Left	2	3	2	7	35	0	11	4	1	26	2
	Medial	Left											
B2	Lateral	Left	3	0	1	3	38	0	8	2	2	39	3
	Medial	Left	4	1	1	7	45	0	7	2	2	30	4
TF21	Lateral	Left	0	2	3	6	42	0	8	4	1	35	4
	Medial	Left	5	1	0	5	53	0	8	3	1	29	4
MF9	Lateral	Left	0	1	2	1	32	2	10	1	0	40	2
	Medial	Left	7	1	0	1	43	0	6	1	1	28	3
CKSAM	Lateral	Left	1	1	1	5	41	0	10	1	1	37	1
	Medial	Left	2	1	1	4	37	0	5	1	0	35	2
TF24	Lateral	Left	0	2	3	1	39	0	6	1	1	38	2

Table B.6. Histology scores for the contralateral, control (right) limb of the 1 year animals.

Rabbit	Facet	Limb	Fissures	PG Stain	Cells	Disruptions	AC Thick	Tide Mark	TM Thick	Spikes	Stain	SB Thick	Morphology
	Medial	Right	0	0	0	1	47	0	8	2	3	25	3
A3	Lateral	Right	2	0	1	2	35	0	6	3	2	21	1
	Medial	Right	1	0	1	0	43	0	8	1	2	25	3
MF12	Lateral	Right	1	0	1	0	26	0	9	0	0	27	3
	Medial	Right	0	0	1	1	40	0	6	2	1	28	1
FN1	Lateral	Right	0	0	0	4	34	0	12	3	1	27	1
	Medial	Right	2	0	1	1	37	0	6	1	2	28	1
FB3	Lateral	Right	0	0	0	0	28	0	7	2	2	27	1
	Medial	Right	3	0	0	0	41	0	5	0	1	22	1
CKDOC	Lateral	Right	0	0	0	0	40	0	6	1	3	29	3
	Medial	Right	2	0	0	0	53	0	7	1	1	25	1
A2	Lateral	Right	0	0	1	0	29	0	8	1	2	20	1
	Medial	Right	0	0	0	0		0	9	1	3	23	1
B2	Lateral	Right	0	0	0	0	33	0	7	1	0	25	3
	Medial	Right	1	0	0	1	67	0	6	1	3	24	3
TF21	Lateral	Right	1	0	0	1	41	0	8	2	3	28	3
	Medial	Right	1	0	0	0	35	0	6	1	3	22	1
MF9	Lateral	Right	0	0	0	0	31	0	10	2	3	25	1
	Medial	Right	3	0	0	0	43	0	6	0	1	28	3
CKSAM	Lateral	Right	0	0	0	0	32	0	9	1	2	24	1
	Medial	Right	0	0	0	0	39	0	6	1	3	25	1
TF24	Lateral	Right	0	0	0	0	36	0	10	1	3	24	1

Table B.7. Histology scores for the non-impacted, control animals (left limb) of the 1 year group.

Rabbit	Facet	Limb	Fissures	PG Stain	Cells	Disruptions	AC Thick	Tide Mark	TM Thick	Spikes	Stain	SB Thick	Morphology
	Medial	Left	0	1	0	0	25	0	5	1	3	26	3
BCW2	Lateral	Left	1	1	1	0	28	0	9	3	2	25	3
	Medial	Left	0	0	0	0	38	0	7	2	3	22	3
GM1	Lateral	Left	0	0	0	0	33	0	7	2	3	26	3
	Medial	Left	3	0	1	0	39	0	6	1	2	23	1
AB1	Lateral	Left	0	0	0	0	28	0	6	1	2	22	1
	Medial	Left	3	0	0	1	28	0	6	0	3	25	3
FN2	Lateral	Left	0	0	1	1	26	0	6	3	1	27	3
	Medial	Left	1	0	0	0	47	0	5	1	2	24	3
TF5	Lateral	Left	1	0	0	0	35	0	5	2	2	22	1
	Medial	Left											
TF23	Lateral	Left	1	0	0	0	42	0	8	1	3	24	1
	Medial	Left	1	0	0	1	49	0	4	3	2	27	3
TF27	Lateral	Left	0	0	0	0	38	3	4	1	2	25	3
	Medial	Left	0	0	0	0	36	0	7	1	3	24	1
543RL	Lateral	Left	0	0	0	0	38	0	9	2	3	28	1
	Medial	Left	0	0	0	1	54	0	6	0	0	22	1
551RF	Lateral	Left	0	0	0	1	37	0	7	0	0	27	1
	Medial	Left											
TF35	Lateral	Left											
	Medial	Left	1	0	0	1	54	0	10	2	2	20	3
TF26	Lateral	Left											

Table B.8. Histology scores for the non-impacted, control animals (right limb) of the 1 year group.

Rabbit	Facet	Limb	Fissures	PG Stain	Cells	Disruptions	AC Thick	Tide Mark	TM Thick	Spikes	Stain	SB Thick	Morphology
	Medial	Right	1	0	1	0	42	0	6	0	2	24	3
BCW2	Lateral	Right	0	0	2	1	30	0	7	1	2	22	1
	Medial	Right	1	1	0	1	46	0	8	2	2	22	1
GM1	Lateral	Right	0	1	1	0	31	0	5	1	2	19	3
	Medial	Right	1	0	0	0	40	0	6	1	2	26	3
AB1	Lateral	Right	0	0	1	0	34	0	6	2	3	25	1
	Medial	Right	2	0	0	1	46	0	7	1	2	27	3
FN2	Lateral	Right	2	0	2	1	34	0	7	2	2	27	1
	Medial	Right	2	0	1	0	57	2	7	1	2	26	3
TF5	Lateral	Right	1	0	2	0	35	0	6	1	2	27	3
	Medial	Right	1	0	0	1	55	0	8	0	2	26	1
TF23	Lateral	Right	0	0	0	1	34	0	7	1	2	25	1
	Medial	Right	1	0	0	2	53	0	5	2	2	20	3
TF27	Lateral	Right	1	0	0	0	33	0	3	2	2	20	3
	Medial	Right	3	0	0	0	44	0	6	1	1	27	3
543RL	Lateral	Right	0	0	1	0	34	0	5	1	0	26	1
	Medial	Right	0	0	0	0	60	0	8	1	3	28	3
551RF	Lateral	Right	0	0	0	0	40	0	6	1	3	29	3
	Medial	Right											
TF35	Lateral	Right											
	Medial	Right	2	0	0	1	46	0	7	1	1	24	3
TF26	Lateral	Right	0	0	0	0	44	0	8	2	1	21	1

Table B.9. Mechanical indentation data for medial uncovered (site 1) 6 month group.

Rabbit	Limb	Thickness (mm)	E_m (MPa)	E_f (MPa)	k_0 ($m^4/(Ns)^* 10^{-12}$)
RSOCO4	Left	0.97	0.65	5.01	20.58
RSOLAB	Left	0.90	0.57	2.15	22.83
FM1	Left	0.92	0.84	6.21	12.54
MF15	Left	1.02	0.56	5.15	26.15
MF17	Left	0.74	0.75	2.51	21.43
MF16	Left	0.87	0.41	3.64	23.17
SM1	Left	1.10	0.66	2.52	42.07
TF1	Left	0.93	0.84	7.01	14.88
TF6	Left	0.77	0.47	3.48	23.70
MF7	Left	0.98	0.78	4.52	28.39
TF10	Left	0.91	0.59	2.96	24.82
TF11	Left	0.77	1.01	7.67	12.04
RSOCO4	Right	0.86	0.54	3.00	25.19
RSOLAB	Right	0.94	0.67	5.11	16.91
FM1	Right	0.88	0.90	4.50	13.72
MF15	Right	0.86	0.53	3.37	25.52
MF17	Right	0.91	0.58	3.90	24.49
MF16	Right	1.05	0.35	3.21	40.50
SM1	Right	0.87	0.51	2.16	34.47
TF1	Right	0.70	0.62	1.63	22.36
TF6	Right	0.73	0.46	1.70	32.78
MF7	Right	0.93	0.67	3.27	32.88
TF10	Right	0.74	0.51	1.78	29.23
TF11	Right	0.70	0.94	4.73	12.08
FB4	Left	0.95	0.67	3.72	21.41
MF6	Left	0.95	0.51	3.24	34.06
MF10	Left	0.93	0.63	4.01	24.27
TF18	Left	0.89	0.73	6.95	11.04
TF8	Left	0.81	0.51	4.14	23.30
TF7	Left	0.93	0.68	5.98	21.68
TF14	Left	0.74	0.78	5.23	18.26
TF17	Left	0.88	0.54	2.68	23.07
FN3	Left	0.72	0.40	10.62	12.51
ACB71	Left	0.74			
TF25	Left	0.76	0.54	2.53	19.42
FB4	Right	1.09	0.56	9.32	19.34
MF6	Right	1.02	0.50	4.65	27.43
MF10	Right	0.86	0.46	2.86	25.55
TF18	Right	0.88	0.89	7.42	11.86
TF8	Right	0.88	0.36	4.18	31.19
TF7	Right	0.78	0.51	5.11	16.36
TF14	Right	0.82	0.83	3.90	14.22
TF17	Right	0.83	0.68	3.25	27.07
FN3	Right	0.78	0.89	3.50	15.64
ACB71	Right	0.75	0.47	1.05	35.98
TF25	Right	0.69	0.47	1.74	23.09

Table B.10. Mechanical indentation data for medial covered (site 2) in 6 month group.

Rabbit	Limb	Thickness (mm)	E_m (MPa)	E_f (MPa)	k_0 ($m^4/(Ns)^* 10^{-12}$)
RSOCO4	Left	0.50	0.32	1.93	15.29
RSOLAB	Left	0.60	0.73	4.23	8.71
FM1	Left	0.53	0.50	2.08	6.90
MF15	Left	0.56	0.45	1.42	18.13
MF17	Left	0.56	1.04	16.98	4.35
MF16	Left	0.61	0.51	4.24	12.96
SM1	Left	0.56	0.82	2.61	8.61
TF1	Left	0.54	0.62	1.44	12.62
TF6	Left	0.53	0.54	3.52	11.61
MF7	Left	0.73	0.94	3.15	14.74
TF10	Left	0.67	1.01	10.27	6.52
TF11	Left	0.57	0.80	3.59	9.62
RSOCO4	Right	0.63	0.47	2.97	11.74
RSOLAB	Right	0.60	0.68	13.42	5.81
FM1	Right	0.67	0.80	6.86	5.62
MF15	Right	0.72	0.46	2.26	12.86
MF17	Right	0.67	1.36	51.75	2.97
MF16	Right	0.83	0.71	3.35	10.63
SM1	Right	0.56	0.60	0.98	14.31
TF1	Right	0.59	0.66	5.11	6.56
TF6	Right	0.46	0.56	4.59	7.69
MF7	Right	0.59	0.71	2.29	11.78
TF10	Right	0.57	0.85	7.78	7.50
TF11	Right	0.55	0.63	3.96	8.66
FB4	Left	0.56	0.72	10.26	7.26
MF6	Left	0.57	0.92	14.80	6.44
MF10	Left	0.60	0.62	9.58	8.20
TF18	Left	0.61	1.02	10.87	4.55
TF8	Left	0.63	0.67	4.41	11.60
TF7	Left	0.48	0.49	5.91	7.57
TF14	Left	0.53	0.41	3.22	15.52
TF17	Left	0.59	0.74	3.51	10.61
FN3	Left	0.54	1.00	7.24	6.98
ACB71	Left	0.67	0.65	2.29	12.21
TF25	Left	0.57	0.77	11.96	6.90
FB4	Right	0.56	0.54	2.10	10.82
MF6	Right	0.56	2.64	29.23	1.47
MF10	Right	0.47	0.49	4.72	9.11
TF18	Right	0.52	0.98	2.97	7.07
TF8	Right	0.61	0.36	4.83	12.14
TF7	Right	0.53	0.41	5.66	8.96
TF14	Right	0.55	0.83	1.95	12.01
TF17	Right	0.66	0.88	5.33	9.60
FN3	Right	0.52	1.13	8.29	4.78
ACB71	Right	0.69	0.59	2.30	11.18
TF25	Right	0.48	0.95	25.72	3.56

Table B.11. Mechanical indentation data for lateral uncovered (site 3) 6 month group.

Rabbit	Limb	Thickness (mm)	E_m (MPa)	E_f (MPa)	k_0 ($m^4/(Ns)^* 10^{-12}$)
RSOCO4	Left	0.72	0.45	9.26	8.18
RSOLAB	Left	0.66	0.68	13.46	4.76
FM1	Left	0.63	0.93	7.99	3.98
MF15	Left	0.60	0.73	11.14	5.23
MF17	Left	0.49	0.99	16.57	2.67
MF16	Left	0.68	0.53	5.22	15.11
SM1	Left	0.93	1.33	15.63	5.88
TF1	Left	0.79	1.08	17.46	4.72
TF6	Left	0.76	0.87	14.28	6.31
MF7	Left	0.84	0.97	15.76	8.56
TF10	Left	0.76	0.96	12.07	7.53
TF11	Left	0.75	1.54	23.82	3.30
RSOCO4	Right	0.81	0.44	11.89	10.59
RSOLAB	Right	0.72	0.87	18.11	4.70
FM1	Right	0.64	1.04	11.91	4.85
MF15	Right	0.44	0.46	2.30	10.77
MF17	Right	0.49	1.25	24.15	2.24
MF16	Right	0.86	0.70	14.64	7.54
SM1	Right	0.76	0.83	7.82	7.59
TF1	Right	0.85	0.89	12.55	7.37
TF6	Right	0.74	1.02	16.68	5.24
MF7	Right	0.78	0.91	16.20	7.71
TF10	Right	0.76	1.41	18.50	4.44
TF11	Right	0.69	1.73	18.41	3.55
FB4	Left	0.67	0.90	14.92	3.62
MF6	Left	0.71	0.68	7.73	9.55
MF10	Left	0.72	0.80	16.98	4.41
TF18	Left	0.69	1.03	11.20	5.12
TF8	Left	0.57	0.79	13.39	6.22
TF7	Left	0.55	0.69	7.08	4.56
TF14	Left	0.62	1.32	16.69	4.08
TF17	Left	0.70	0.71	9.35	9.08
FN3	Left	0.78	1.12	18.81	4.61
ACB71	Left	0.78	0.56	1.55	19.03
TF25	Left	0.56	1.26	29.76	2.40
FB4	Right	0.58	0.86	10.77	4.28
MF6	Right	0.79	0.70	8.09	10.67
MF10	Right	0.69	0.82	15.09	5.99
TF18	Right	0.63	0.79	9.98	5.05
TF8	Right	0.78	0.72	23.16	6.60
TF7	Right	0.79	0.75	10.34	7.49
TF14	Right	0.62	1.00	11.83	4.01
TF17	Right	0.75	1.05	13.99	5.74
FN3	Right	0.70	0.97	14.22	6.18
ACB71	Right	0.80	0.65	13.28	7.63
TF25	Right	0.51	1.66	42.67	1.98

Table B.12. Mechanical indentation data for lateral covered (site 4) in 6 month group.

Rabbit	Limb	Thickness (mm)	E_m (MPa)	E_f (MPa)	k_0 ($m^4/(Ns)^* 10^{-12}$)
RSOCO4	Left	0.40	12.60	135.94	0.30
RSOLAB	Left	0.41	0.95	34.45	2.72
FM1	Left	0.38	1.04	21.65	2.27
MF15	Left	0.37	3.03	38.13	1.07
MF17	Left	0.35	3.74	33.71	1.34
MF16	Left	0.44	3.93	65.22	1.34
SM1	Left	0.57	1.51	15.65	2.53
TF1	Left	0.45	0.92	4.64	5.54
TF6	Left	0.52	1.78	48.77	2.11
MF7	Left	0.43	1.34	36.18	3.01
TF10	Left	0.46	1.18	21.58	3.09
TF11	Left	0.48	1.55	30.68	2.33
RSOCO4	Right	0.32	14.84	28.70	0.69
RSOLAB	Right	0.33	1.74	32.06	1.73
FM1	Right	0.40	1.34	35.98	2.32
MF15	Right	0.53	5.65	128.79	0.94
MF17	Right	0.39	3.89	78.62	0.99
MF16	Right	0.46	2.13	52.60	1.56
SM1	Right	0.49	1.36	43.97	1.93
TF1	Right	0.50	1.10	5.43	5.01
TF6	Right	0.50	1.10	31.91	2.68
MF7	Right	0.50	1.38	47.94	3.15
TF10	Right	0.44	1.27	26.60	3.30
TF11	Right	0.45	2.04	16.02	2.95
FB4	Left	0.36	1.56	21.09	1.74
MF6	Left	0.43	2.71	59.45	1.14
MF10	Left	0.34	1.35	37.41	2.26
TF18	Left	0.39	1.25	24.93	1.95
TF8	Left	0.34	0.94	37.22	2.26
TF7	Left	0.31	3.55	18.92	1.50
TF14	Left	0.47	1.28	40.80	2.22
TF17	Left	0.51	1.19	10.49	3.72
FN3	Left	0.42	1.19	14.28	2.13
ACB71	Left	0.47	0.93	14.83	2.18
TF25	Left	0.37	3.81	96.45	1.15
FB4	Right	0.28	1.81	21.92	2.18
MF6	Right	0.36	0.94	8.99	3.23
MF10	Right	0.33	1.31	23.53	2.29
TF18	Right	0.39	1.40	16.64	1.84
TF8	Right	0.33	1.61	31.74	1.48
TF7	Right	0.32	1.37	16.98	2.37
TF14	Right	0.49	1.45	49.48	2.25
TF17	Right	0.47	1.06	9.91	4.40
FN3	Right	0.41	1.10	20.99	2.36
ACB71	Right	0.47	0.73	25.94	3.14
TF25	Right	0.37	3.12	85.04	1.44

Table B.13. Mechanical indentation data for medial uncovered (site 1) in the 1 year group.

Rabbit	Limb	Thickness (mm)	E_m (MPa)	E_f (MPa)	k_0 ($m^4/(Ns)*10^{-12}$)
A3	Left	0.92	0.70	4.67	19.78
MF12	Left	0.81	0.75	4.77	19.40
FN1	Left	0.82	0.69	2.74	22.07
FB3	Left	0.86	0.99	7.26	10.17
CKDOC	Left	0.84	0.97	11.54	6.85
A2	Left	0.95	0.91	10.59	8.66
B2	Left	0.76	0.69	7.66	11.19
TF21	Left	0.96	0.71	8.28	11.93
MF9	Left	0.81	0.75	5.53	11.08
CKSAM	Left	0.77	0.96	6.45	8.98
TF24	Left	0.80	0.80	7.05	9.71
A3	Right	0.98	0.77	6.88	19.72
MF12	Right	0.78	0.99	6.62	10.07
FN1	Right	0.72	0.55	1.97	23.31
FB3	Right	0.84	0.95	6.03	12.66
CKDOC	Right	0.68	0.84	4.32	10.53
A2	Right	0.88	0.83	6.38	11.24
B2	Right	0.78	0.67	5.59	15.98
TF21	Right	0.83	0.67	3.74	23.04
MF9	Right	0.71	0.72	3.49	14.85
CKSAM	Right	0.70	1.05	3.13	12.93
TF24	Right	0.74	0.85	4.98	9.51
BCW2	Left	0.90	0.57	5.58	16.30
GM1	Left	0.64	0.73	2.58	17.35
AB1	Left	0.62	0.44	0.73	34.32
FN2	Left	0.75	1.03	3.93	13.30
TF5	Left	0.77	0.73	2.45	20.25
TF23	Left	0.86	0.71	3.36	31.63
TF27	Left	0.86	0.62	6.95	18.97
543RL	Left	0.89	1.38	14.63	6.67
551RF	Left	0.89	0.72	4.87	19.03
TF35	Left	1.00	0.59	6.03	20.18
BCW2	Right	0.89	0.67	7.61	11.34
GM1	Right	0.70	0.67	2.12	20.13
AB1	Right	0.62	0.42	1.00	26.79
FN2	Right	0.72	0.94	2.39	20.21
TF5	Right	0.91	0.86	4.04	17.89
TF23	Right	0.83	0.55	2.82	31.70
TF27	Right	0.87	0.79	7.16	15.03
543RL	Right	0.97	1.45	12.19	8.80
551RF	Right	0.86	0.70	4.63	16.80
TF35	Right	0.99	0.58	4.99	23.64

Table B.14. Mechanical indentation data for medial covered (site 2) in the 1 year group.

Rabbit	Limb	Thickness (mm)	E_m (MPa)	E_f (MPa)	k_0 ($m^4/(Ns)^* 10^{-12}$)
A3	Left	0.60	0.77	3.26	10.72
MF12	Left	0.64	0.87	7.84	8.04
FN1	Left	0.50	0.75	2.64	7.83
FB3	Left	0.55	0.88	4.35	8.95
CKDOC	Left	0.47	0.60	1.00	14.73
A2	Left	0.62	0.82	1.78	12.44
B2	Left	0.50	0.48	1.94	12.68
TF21	Left	0.64	0.71	1.75	16.20
MF9	Left	0.52	1.19	15.48	4.45
CKSAM	Left	0.51	0.56	3.43	8.38
TF24	Left	0.57	0.69	11.79	5.92
A3	Right	0.63	0.73	4.06	10.81
MF12	Right	0.61	0.87	6.42	9.09
FN1	Right	0.53	0.60	1.16	13.67
FB3	Right	0.66	1.03	5.45	11.26
CKDOC	Right	0.47	0.87	13.76	4.05
A2	Right	0.62	0.81	5.24	7.35
B2	Right	0.55	0.58	3.13	10.25
TF21	Right	0.62	0.57	2.75	11.54
MF9	Right	0.50	1.31	19.42	3.77
CKSAM	Right	0.54	0.75	2.78	6.86
TF24	Right	0.53	0.79	14.13	4.43
BCW2	Left	0.55	0.63	3.10	10.85
GM1	Left	0.55	1.22	7.22	4.74
AB1	Left	0.51	0.46	0.50	28.29
FN2	Left	0.52	0.80	1.93	12.92
TF5	Left	0.56	0.67	2.54	9.26
TF23	Left	0.67	1.00	10.09	6.42
TF27	Left	0.54	0.66	9.00	6.54
543RL	Left	0.73	1.28	5.81	9.55
551RF	Left	0.59	0.91	7.86	5.29
TF35	Left	0.74	0.69	2.96	16.89
BCW2	Right	0.55	0.65	2.60	10.70
GM1	Right	0.55	1.02	3.70	8.81
AB1	Right	0.48	0.51	0.89	16.67
FN2	Right	0.60	1.16	2.83	12.97
TF5	Right	0.58	0.80	2.10	9.38
TF23	Right	0.69	0.72	6.26	9.79
TF27	Right	0.60	0.75	4.69	7.51
543RL	Right	0.61	1.60	6.79	6.29
551RF	Right	0.61	0.99	9.03	5.92
TF35	Right	0.68	0.90	9.41	5.95

Table B.15. Mechanical indentation data for lateral uncovered (site 3) in the 1 year group.

Rabbit	Limb	Thickness (mm)	E_m (MPa)	E_f (MPa)	k_0 ($m^4/(Ns)*10^{-12}$)
A3	Left	0.82	0.99	17.88	4.97
MF12	Left	0.57	0.87	7.84	8.04
FN1	Left	0.61	0.92	7.88	7.88
FB3	Left	0.66	1.58	19.07	2.68
CKDOC	Left	0.60	0.94	13.72	3.33
A2	Left	0.73	0.85	13.11	4.93
B2	Left	0.80	0.81	12.10	8.46
TF21	Left	0.81	0.72	13.84	7.21
MF9	Left	0.70	1.44	13.84	4.45
CKSAM	Left	0.75	0.93	6.59	11.82
TF24	Left	0.81	1.26	14.28	5.12
A3	Right	0.82	1.13	20.24	4.52
MF12	Right	0.68	1.35	18.45	3.87
FN1	Right	0.68	0.84	14.25	5.52
FB3	Right	0.62	1.61	23.02	3.19
CKDOC	Right	0.63	0.88	13.67	4.57
A2	Right	0.70	1.04	15.82	4.54
B2	Right	0.84	0.92	11.71	8.01
TF21	Right	0.83	0.75	19.72	5.65
MF9	Right	0.72	1.43	16.43	4.21
CKSAM	Right	0.63	0.81	15.15	4.58
TF24	Right	0.79	1.32	8.89	6.68
BCW2	Left	0.78	0.58	14.73	6.28
GM1	Left	0.65	1.24	5.39	6.27
AB1	Left	0.65	0.99	8.19	9.15
FN2	Left	0.67	1.56	11.01	4.00
TF5	Left	0.69	1.41	22.67	2.81
TF23	Left	0.74	1.03	16.03	8.51
TF27	Left	0.70	0.99	13.36	5.29
543RL	Left	0.82	1.47	16.82	5.79
551RF	Left	0.84	1.02	15.02	6.63
TF35	Left	0.71	1.00	13.14	6.11
BCW2	Right	0.65	0.55	21.62	4.58
GM1	Right	0.64	1.43	11.86	4.37
AB1	Right	0.63	0.78	6.83	12.66
FN2	Right	0.63	1.52	15.99	3.30
TF5	Right	0.77	1.34	10.46	5.84
TF23	Right	0.68	1.00	25.51	3.96
TF27	Right	0.75	1.03	16.31	5.14
543RL	Right	0.80	1.37	18.13	5.44
551RF	Right	0.81	0.85	14.56	6.70
TF35	Right	0.85	1.04	14.70	7.31

Table B.16. Mechanical indentation data for lateral covered (site 4) in the 1 year group.

Rabbit	Limb	Thickness (mm)	E_m (MPa)	E_f (MPa)	k_0 ($m^4/(Ns)^* 10^{-12}$)
A3	Left	0.40	1.86	49.88	1.96
MF12	Left	0.35	1.59	59.31	2.02
FN1	Left	0.48	1.02	11.99	3.09
FB3	Left	0.49	1.85	30.84	1.61
CKDOC	Left	0.38	2.22	75.14	1.92
A2	Left	0.33	4.91	70.30	1.44
B2	Left	0.45	2.19	85.39	1.75
TF21	Left	0.54	1.03	24.78	2.81
MF9	Left	0.44	1.54	33.02	2.04
CKSAM	Left	0.42	1.18	65.57	2.19
TF24	Left	0.56	1.32	32.28	2.46
A3	Right	0.53	1.62	48.28	1.78
MF12	Right	0.42	1.25	30.32	4.17
FN1	Right	0.45	0.80	17.17	3.57
FB3	Right	0.38	1.94	39.44	1.99
CKDOC	Right	0.39	1.79	69.32	1.94
A2	Right	0.38	2.63	57.64	1.25
B2	Right	0.46	0.88	18.78	3.53
TF21	Right	0.46	0.98	38.96	2.55
MF9	Right	0.43	1.89	37.54	1.47
CKSAM	Right	0.39	5.20	85.41	1.81
TF24	Right	0.50	1.22	26.79	2.49
BCW2	Left	0.41	1.52	61.12	1.66
GM1	Left	0.48	1.61	51.19	1.50
AB1	Left	0.49	0.88	15.64	3.81
FN2	Left	0.45	1.37	17.61	2.96
TF5	Left	0.41	1.76	58.75	1.73
TF23	Left	0.45	1.97	34.65	2.37
TF27	Left	0.53	1.19	27.90	2.50
543RL	Left	0.52	1.59	20.25	2.62
551RF	Left	0.54	1.39	25.24	2.50
TF35	Left	0.40	2.66	34.29	1.32
BCW2	Right	0.41	0.81	67.18	1.96
GM1	Right	0.48	1.82	30.10	1.64
AB1	Right	0.45	1.30	41.76	1.94
FN2	Right	0.46	1.13	6.98	5.18
TF5	Right	0.46	1.55	57.36	1.84
TF23	Right	0.43	2.08	72.25	2.04
TF27	Right	0.46	0.94	22.79	3.39
543RL	Right	0.50	2.12	14.59	3.98
551RF	Right	0.55	1.33	26.96	2.57
TF35	Right	0.50	2.34	53.31	1.69

APPENDIX C

RAW DATA FROM CHAPTER FOUR

Table C.1. Cell viability data for the impacted (left) and unimpacted (right) limbs of animals with acutely torn ACL

RABBIT TF41														
sample	**sup.**	**%**	**mid.**	**%**	**deep**	**%**	**Total live**	**% live**	**sup.**	**mid.**	**deep**	**Total Dead**	**% Dead**	**Total**
LFL1	345	90.31	619	86.09	369	89.78	1333	88.16	37	100	42	179	11.84	1512
LFL 3	281	72.42	658	92.68	359	85.27	1298	85.45	107	52	62	221	14.55	1519
LFM 1	228	59.84	437	77.21	226	77.93	891	72.03	153	129	64	346	27.97	1237
LFM 2	271	44.65	715	89.38	320	78.43	1306	71.96	336	85	88	509	28.04	1815
LTL 3	536	91.78	688	84.31	505	82.25	1729	85.85	48	128	109	285	14.15	2014
LTL 4	437	75.87	641	66.56	480	80.27	1558	72.91	139	322	118	579	27.09	2137
LTM 3	292	49.83	635	76.88	346	55.54	1273	62.56	294	191	277	762	37.44	2035
LTM 4	208	53.47	504	74.67	366	62.24	1078	65.25	181	171	222	574	34.75	1652
RFL 2	251	91.27	546	98.20	305	94.72	1102	95.58	24	10	17	51	4.42	1153
RFL 3	371	94.40	739	89.36	375	88.44	1485	90.33	22	88	49	159	9.67	1644
RFM 1	433	98.86	794	99.13	434	95.59	1661	98.11	5	7	20	32	1.89	1693
RFM 4	363	94.04	857	97.61	552	96.67	1772	96.57	23	21	19	63	3.43	1835
RTL 1	509	91.88	746	96.63	503	96.55	1758	95.18	45	26	18	89	4.82	1847
RTL 3	554	89.64	830	95.07	489	83.73	1873	90.27	64	43	95	202	9.73	2075
RTM 1	315	83.55	308	90.06	284	80.91	907	84.77	62	34	67	163	15.23	1070
RTM 3	399	96.61	484	95.65	565	89.54	1448	93.42	14	22	66	102	6.58	1550

Table C.1 Continued.

RABBIT TF36														
sample	sup.	%	mid.	%	deep	%	Total live	% live	sup.	mid.	deep	Total Dead	% Dead	Total
LFL1	233	55.48	689	85.27	362	78.02	1284	75.89	187	119	102	408	24.11	1692
LFL4	163	41.27	588	86.60	329	78.15	1080	72.24	232	91	92	415	27.76	1495
LFM2	239	65.12	478	63.23	221	72.22	938	65.64	128	278	85	491	34.36	1429
LFM4	153	54.45	341	42.41	254	67.37	748	51.16	128	463	123	714	48.84	1462
LTL1	318	67.37	558	79.71	263	67.78	1139	73.01	154	142	125	421	26.99	1560
LTL 2	336	50.83	724	74.95	319	51.87	1379	61.51	325	242	296	863	38.49	2242
LTM 1	191	38.59	580	76.62	290	50.61	1061	58.14	304	177	283	764	41.86	1825
LTM 2	363	68.49	548	79.54			911	74.73	167	141		308	25.27	1219
RFL 2	162	35.06	619	83.31	374	78.90	1155	68.79	300	124	100	524	31.21	1679
RFL 4	210	44.12	586	84.80	222	64.53	1018	67.37	266	105	122	493	32.63	1511
RFM1	179	69.38	587	96.55	276	84.15	1042	87.27	79	21	52	152	12.73	1194
RFM 3	259	76.18	661	92.97	294	75.77	1214	84.36	81	50	94	225	15.64	1439
RTL 1	327	64.24	567	65.40	409	63.41	1303	64.47	182	300	236	718	35.53	2021
RTL 3	415	78.15	439	60.30	154	49.20	1008	64.12	116	289	159	564	35.88	1572
RTM 1	280	52.83	469	76.63	378	73.68	1127	68.10	250	143	135	528	31.90	1655
RTM 3	227	54.70	215	66.77	214	55.73	656	58.52	188	107	170	465	41.48	1121

Table C.2. Pressure film data from ACL tear rabbit

Specimen	NSUQ3R
Lateral Plateau	
Test	1 (1059N)
# Pixels =	1127
Area =	32.266
Ave Pressure	27.5058
Ave Force =	887.5
Max. Pressure	50.87
Min. Pressure	10.1
Percent of total	46.3%
Medial Plateau	
# Pixels =	1580
Area =	45.2354
Ave Pressure =	22.725
Ave Force =	1027.98
Max. Pressure	48.37
Min. Pressure	10.1
Percent of total	53.7%
Medium Total Force	1915.48

Table C.3. Gross morphological scoring for the traumatic and transected animals

	Transected						Tramatic					
	TF40		TF42		TF47		TF16		TF19		TF34	
	Femur	Tibia	Femur	Tibia	Femur	Tibia	Femur	Tibia	Femur	Tibia	Femur	Tibia
LM	4	2	2	3	2	2	4	4	4	4	4	4
RM	2	2	1	2	1	2	1	2	1	2	2	2
LL	2	1	2	1	2	3	3	3	3	4	3	2
RL	2	2	1	2	1	1	1	2	1	2	1	1

Table C.4. Impact loads and injuries from trial cadaver tests.

Cadaver Drop Test			
Rabbit	**Height (cm)**	**Load**	**Injury**
LB737	60	1008	None
RSOA04 L	60	1332	None
RSOA04 R	60	1264	None
RSOTO6	60	920	Partial ACL & Posterior L meniscus
AF1	70	1130	None
BC268		1215	None
FB2		874	Tibia Fracture at boot
GM3		883	None
WE	80	858	None
RSOO94	90	979	Tibia Fracture at boot
BC108	80	844	L meniscal tear
AC5	90	656	None - Lower weight
BB1 L	80	650	Fractured Tibia
BB1 R	75	645	Fractured Tibia
MG1 L	120	1227.8	Fractured Tibial Plateau - ACL Avulsion
MG1 R	110	715	Tibia Fracture at boot
MF2 L	110	1442	Fractured Tibial Plateau - ACL Avulsion
MF2 R	100	1062	None
RSOA17 La	110	670	None
RSOA17 Lb	130	907	None
RSOA17 Lc	130	945	None
RSOA17 Ra	110	1086	None
RSOA17 Rb	110	1022	None
BU63 L	110	850	Torn Acl - 1.33 kg mass used
GN1	70	960	Torn ACL and L meniscus
MF5 L	70	1264	Fractured Tibia at boot
MF5 R	65	1134	None
RSOI6 L	70	1108	Fractured tibial plateau
RSOI6 R	65	1213	None
TF9 L	70	935	Fractued Tibial Plateau, partial ACL tear, torn L meniscus
TF9 Ra	60	845	None
TF9 Rb	70	920	None
TF9 Rc	75	900	Tibial plateau fracture, torn M meniscus, ACL tear, Fibula fracture
FF1 L	70	894	PCL tear torn M&L meniscus
FF1 Ra	75	879	None
FF1 Rb	75	856	None
FF1 Rc	75	1038	None
FF1 Rd	75	911	None
FF1 Re	75	985	Torn ACL, torn M meniscus
W	70	1223	Torn ACL

Table C.4 Continued

Cadaver Drop Test			
Rabbit	**Height (cm)**	**Load**	**Injury**
NFUQ3 La	120	984	None
NFUQ3 Lb	130	1073	Fractured Tibial Plateau - ACL Avulsion
NFUQ3 R	130	1059	Torn ACL - Torn L meniscus
RSOF2	100	1081	Torn ACL - Torn L&M mensicus
AC	100	1229	Torn ACL - Torn L&M mensicus
TF3 L	80	976	Torn ACL - Torn L&M mensicus
TF3 R	80	784	Torn ACL - Torn L&M mensicus
SF2 La	70	888	None
SF2 Lb	70	992	
SF2 Lc	70	936	
SF2 Ld	65	1041	
SF2 Le	70	1010	Torn ACL - Torn L meniscus
SF2 R	70	759	Torn ACL - Torn L meniscus
TF2 L	70	1084	Torn ACL - Torn M meniscus
TF2 R	70	964	None
TF32	70	1119	Torn ACL
TF41	70	1010	Torn ACL - Torn L&M mensicus
544	70	1076	Torn ACL
BF738	70	857	Torn ACL
TF19		950	
TF16		912	
TF34		928	

Table C.5. Isolated joint ACL failure tests performed in the Instron.

Isolated Joints			
Rabbit	**Input Load (N)**	**Actual Load (N)**	**Injury**
K211	2000	630.54	Femur Fracture
MF1	2000	1150	None
FE1	1500	1235	None
BU64	1000	883	
BU64	1200	1071	
BU64	1400	1181	
BU64	1600	1275	
BU64	1800	1514	Tibial plateau fracture
MG3	1200	934	
MG3	1500	1180	None
MG3B	1500	1164	None
TP	1500	1375	None
426 L	500	463	
426 L	700	635	
426 L	900	792	
426 L	1100	979	
426 L	1300	1154	
426 L	1500	1312	
426 L	1700	1453	Torn ACL, M & L meniscal tears posterior
426 R	500	487	
426 R	700	677	
426 R	900	822	
426 R	1100	997	
426 R	1300	1181	
426 R	1500	1363	Femur Fracture
T24B L	500	250	
T24B L	700	380	
T24B L	900	550	
T24B L	1100	720	
T24B L	1300	850	
T24B L	1500	1050	
T24B L	1700	1230	
T24B L	1900	1290	ACL Avulsion & Tibial plateau fracture
T24B R	500	230	
T24B R	700	340	
T24B R	900	450	
T24B R	1100	620	
T24B R	1300	780	
T24B R	1500	810	Torn ACL - small fracture at posterior TP
A1 L	500	265	
A1 L	700	420	
A1 L	900	570	
A1 L	1100	720	
A1 L	1300	900	

Table C.5 Continued

Isolated Joints			
Rabbit	**Input Load (N)**	**Actual Load (N)**	**Injury**
A1 L	1500	1050	
A1 L	1700	1200	
A1 L	1900	1350	ACL Tear and TP fracture
A1 R	500	215	
A1 R	700	320	
A1 R	900	455	
A1 R	1100	600	
A1 R	1300	750	
A1 R	1500	900	
A1 R	1700	1050	
A1 R	1900	1175	TP fracture
M57 R	500	280	
M57 R	700	410	
M57 R	900	540	
M57 R	1100	700	
M57 R	1300	650	ACL Tear
M57 L	500	280	
M57 L	700	410	
M57 L	900	560	
M57 L	1100	700	
M57 L	1300	850	
M57 L	1500	950	ACL Tear - Midsubstance
M51 L	300	176	
M51 L	500	317	
M51 L	700	682	
M51 L	900	912	
M51 L	1100	1100	
M51 L	1300	1300	
M51 L	1500	1492	ACL Tear - buckethandle tears of M&L meniscus
M51 R	300	170	
M51 R	500	320	
M51 R	700	481	
M51 R	900	634	
M51 R	1100	827	
M51 R	1300	1038	
M51 R	1500	1262	
M51 R	1700	1423	
M51 R	1900	1568	ACL Tear

Table C.5 Continued

Isolated Joints			
Rabbit	Input Load (N)	Actual Load (N)	Injury
M49 R	300	210	
M49 R	500	350	
M49 R	700	510	
M49 R	900	700	
M49 R	1100	920	
M49 R	1300	1110	
M49 R	1500	1300	
M49 R	1700	1500	
M49 R	1900	1448	ACL Tear
M49 L	500	350	
M49 L	700	500	
M49 L	900	690	
M49 L	1100	850	
M49 L	1300	1090	
M49 L	1500	1250	
M49 L	1700	1448	ACL Tear - Partial
MG2	2000	1031	Partial ACL Tear

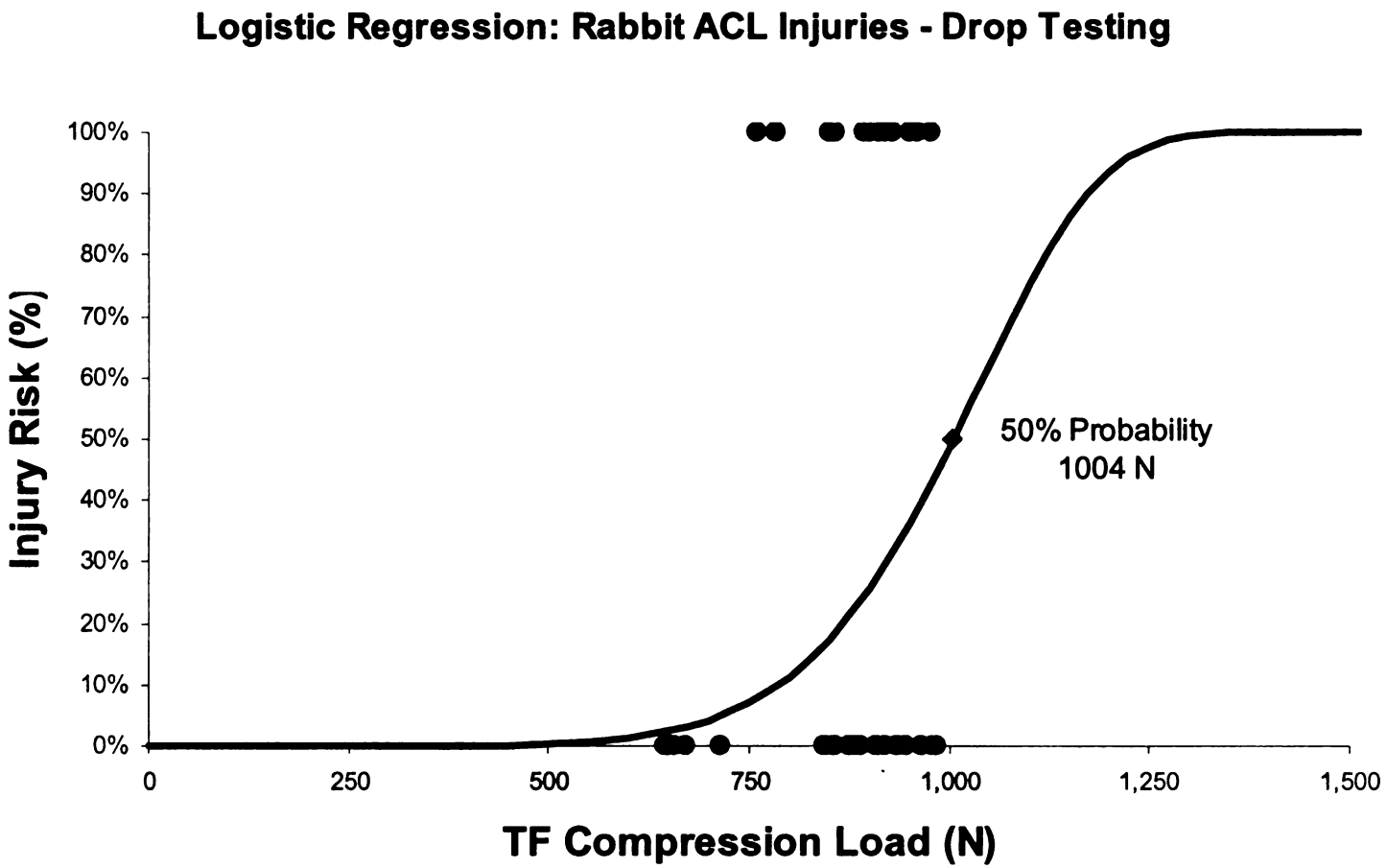

Figure C.1. Survival analysis of ACL failure trials indicating probability of ACL failure at a given load

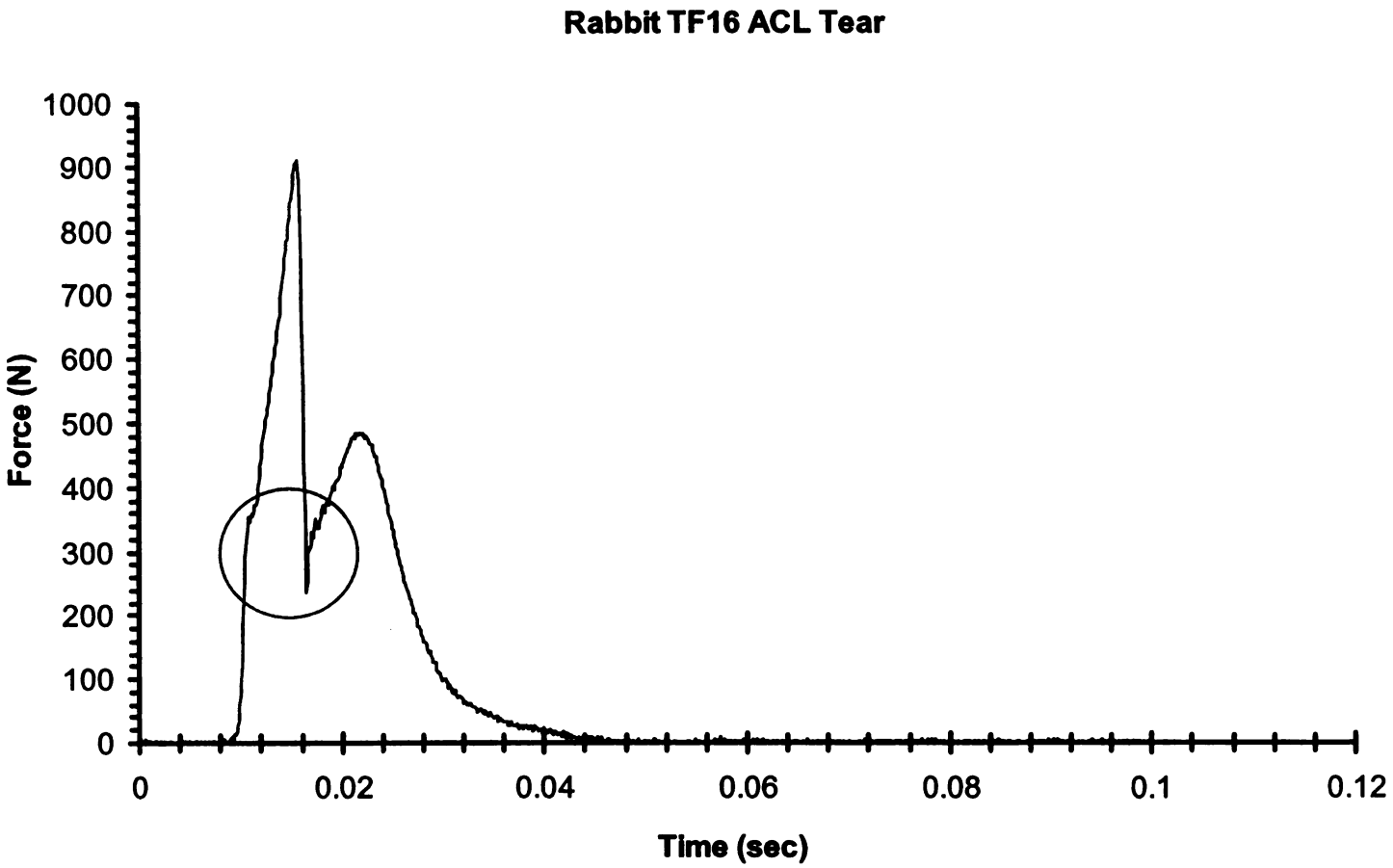

Figure C.2. Sample force versus time plot for an ACL failure experiment. The circled portion indicates ACL failure.

APPENDIX D

RAW DATA FROM CHAPTER FIVE

Table D.1. Cell viability analysis of 1-day controls (% dead cells).

1-DAY CONTROL								
	LFL	RFL	LFM	RFM	LTL	RTL	LTM	RTM
BF733	32.85	13.51	13.66	23.41	26.48	34.99		32.02
BF733	21.61	19.87	35.46	18.46	28.96	22.97		50.86
BF733	25.93	27.14	17.41	20.82	27.98	27.34		
DB1	18.70	13.46	8.75	17.86	32.20	7.03	24.02	14.08
DB1	9.13	11.30	9.77	9.00	16.87	9.39	23.06	28.47
DB1	11.96	13.81	7.92	6.95	11.27	11.35	36.67	23.60
TF31	23.14	17.75	16.64	17.99	7.50	9.56	27.76	29.15
TF31	34.49	20.83	19.50	24.10	17.75	13.84	28.25	21.24
TF31	24.13	10.23	31.02	11.99	24.24	8.52	32.94	21.82
TF31	37.37	22.58	18.88	11.20	20.84	13.72	28.92	15.07
TF30	30.62	27.14	24.91	34.57	38.61	37.31	39.65	17.20
TF30	35.43	29.39	29.09	41.41	43.92	21.73	48.58	19.39
TF30	27.19	27.96		13.64	54.26	25.42	29.61	
TF28	24.40	9.72	11.02	11.17	23.28	11.68	21.27	16.84
TF28	16.31	10.14	24.95	5.20	15.32	10.04	43.46	14.50
TF28	18.48	10.42	6.04	8.91	30.09	6.25	17.38	12.16
Average	24.48	17.83	18.33	17.29	26.22	16.95	30.89	22.60
St. Dev	8.34	7.21	9.11	9.96	12.13	10.01	9.09	10.17

Table D.2. Cell viability analysis of 4-day controls (% dead cells).

4-DAY CONTROL								
	LFL	RFL	LFM	RFM	LTL	RTL	LTM	RTM
532RF	24.60	4.01	27.30	5.79	21.32	6.27	16.54	13.43
532RF	21.60	6.26	24.57	3.32	4.88	10.74	9.63	7.45
532RF	17.73	7.36	13.84	13.26	12.29	8.09	17.10	3.99
BF731	31.59	26.54	39.97	17.01	46.97	25.76	52.15	26.76
BF731	44.51	21.91	47.52	30.83	45.15		37.33	41.91
BF731	37.74	29.06	30.53	25.47			29.88	36.40
62881	17.83	9.34	16.97	14.48	15.35	25.04	28.07	24.26
62881	18.45	12.33	13.68	10.82	19.49	19.18	35.08	15.71
62881	16.43	12.21	8.18	8.27	25.69	19.73	31.44	10.67
TF45	21.22	16.36	29.23	26.00	32.22	13.13	16.11	8.97
TF45	20.33	22.12	25.88	17.84	29.15	11.83	23.12	11.73
TF45	19.13	14.71	32.02	19.99	37.41	7.96	33.09	14.46
TF39	47.78	31.85	22.44	30.60	29.86	17.12	44.29	27.19
`TF39	45.75	33.42	22.77	31.36	36.70	17.36	35.60	22.88
TF39	39.17	23.85	18.36		45.41	27.89	42.54	17.52
ZIB5	57.02	21.42	28.75	33.84	54.39	38.68	38.61	37.25
ZIB5	54.54	25.89	49.96	26.27	45.39	37.65	41.98	45.51
ZIB5	55.97	36.68	30.29	23.09	51.79	37.23	51.19	29.75
Average	32.85	19.74	26.79	19.90	32.56	20.23	32.43	21.99
St. Dev	14.92	9.88	11.11	9.54	14.62	10.86	12.23	12.45

Table D.3. Cell viability analysis of 4-Day P188 (% dead cells).

4-Day P188								
	LFL	**RFL**	**LFM**	**RFM**	**LTL**	**RTL**	**LTM**	**RTM**
STID	9.58	12.96	13.34	21.81	22.60	24.11	15.15	28.57
STID	20.81	13.10	16.82	11.83	23.13	36.32	27.16	29.13
STID		14.92	16.91	15.82	16.41	25.09	27.23	
TF36	14.42	12.56	10.45	11.02	16.80	16.55	31.15	17.46
TF36	20.26	13.58	12.01	14.62	15.27	21.47	43.23	21.15
TF36	15.03	10.70		8.64	21.41	20.48		12.41
DB4	14.76	14.14	6.57	5.21		16.38		
DB4	10.37	17.24	5.17	11.94		12.57		
DB4	9.69	13.34	11.81	17.65		13.26		
TF37	14.13	11.14	7.48	4.48	23.37	12.22	28.13	16.24
TF37	16.45	9.95	17.58	8.81	17.47	8.61	24.20	14.51
TF37	12.56	13.73	12.51	4.68	20.74	12.01	24.45	18.66
BF739	21.49	20.93	27.95	19.52	27.92			
BF739	20.89	11.43	21.63	23.19	18.51			
BF739	21.58	16.31	23.33	29.28	25.04			
TF46	18.64	18.95	13.72	11.70	16.59	17.49	13.07	27.80
TF46	22.18	16.10	12.50	16.72	17.08	19.13	15.96	11.14
TF46	19.63	22.17	12.08	14.39	19.75	26.83	12.44	18.89
Average	16.62	14.63	14.23	13.96	20.14	18.84	23.83	19.63
St. Dev	4.41	3.43	5.99	6.72	3.71	7.19	9.24	6.38

Table D.4. Zonal cell viability data of 1-day controls (% dead cells).

	1 Day											
	LFL			LFM			LTL			LTM		
	Sup.	Mid.	Deep	Sup.	Mid.	Deep	Sup.	Mid.	Deep	Sup.	Mid.	Deep
BF733	84.01	57.74	66.19	89.28	86.27	83.33	82.59	63.58	81.20			
	58.15	81.47	88.79	59.32	72.49	50.00	81.60	61.76	74.69			
	67.58	81.75	66.76	87.32	82.61	77.70	82.35	61.27	80.40			
Average	**69.92**	**73.65**	**73.91**	**78.64**	**80.46**	**70.34**	**82.18**	**62.21**	**78.76**			
DB1	90.00	88.17	63.26	96.09	96.34	94.52	95.11	89.68	95.64	80.16	77.18	70.61
	80.77	92.46	96.77	90.28	96.96	82.30	92.16	58.82	61.29	84.32	70.28	76.50
	71.65	90.91	92.13	81.19	92.06	94.75	92.37	78.28	83.84	73.90	84.45	79.51
				88.27	94.59	91.80	94.46	88.67	83.91	70.07	73.83	42.97
Average	**80.81**	**90.51**	**84.05**	**88.96**	**94.99**	**90.84**	**93.52**	**78.86**	**81.17**	**77.11**	**76.44**	**67.40**
TF28	41.06	88.00	90.91	89.00	90.18	86.73	82.13	69.68	80.78	85.21	81.55	68.32
	79.36	81.09	92.31	73.56	85.15	62.12	92.86	86.04	72.78	46.13	59.31	61.67
	72.05	78.37	92.31	93.21	96.73	89.98	55.67	87.84	61.28	80.23	83.98	82.85
Average	**64.16**	**82.49**	**91.84**	**85.26**	**90.69**	**79.61**	**76.88**	**81.19**	**71.61**	**70.52**	**74.94**	**70.95**
TF30	64.26	68.26	74.87	61.17	83.14	75.13	66.55	62.12	52.08	24.46	76.18	85.07
	60.60	69.47	59.21	54.73	76.85	76.26	41.28	59.42	65.87	16.03	79.80	40.93
	63.37	88.18	57.08				47.49	42.02	51.88	56.68	92.07	56.99
Average	**62.74**	**75.30**	**63.72**	**57.95**	**80.00**	**75.70**	**51.77**	**54.52**	**56.61**	**32.39**	**82.68**	**61.00**
TF31	62.89	86.34	71.33	81.48	86.61	79.87	89.53	94.21	92.42	79.69	75.54	64.65
	68.79	56.13	77.56	83.51	88.72	64.32	76.76	83.58	86.11	79.56	68.82	69.39
	62.96	80.75	81.89	83.04	84.06	39.03	78.19	73.40	77.57	78.42	63.86	60.90
	58.47	67.36	56.74	88.51	81.64	0.00	75.33	83.73	75.94	77.17	70.40	68.32
Average	**63.28**	**72.64**	**71.88**	**84.14**	**85.26**	**45.80**	**79.95**	**83.73**	**83.01**	**78.71**	**69.66**	**65.82**
Overall Ave.	**68.18**	**78.92**	**77.08**	**78.99**	**86.28**	**72.46**	**76.86**	**72.10**	**74.23**	**64.68**	**75.93**	**66.29**
St. Dev	7.62	7.54	10.98	12.33	6.51	16.69	15.37	12.95	10.76	21.82	5.36	4.13

Table D.4 Continued

	1 Day											
	RFL			RFM			RTL			RTM		
BF733	Sup.	Mid.	Deep	Sup.	Mid.	Deep	Sup.	Mid.	Deep	Sup.	Mid.	Deep
	79.53	93.79	78.76	59.45	85.74	77.80	62.78	69.82	59.89	71.54	69.92	61.86
	61.60	90.84	83.57	70.19	91.90	73.03	74.46	79.87	74.78	47.14	50.00	49.56
Average	64.58	81.07	67.05	64.22	85.84	80.14	60.26	84.35	69.75			
DB1	**68.57**	**88.57**	**76.46**	**64.62**	**87.83**	**76.99**	**65.83**	**78.02**	**68.14**	**59.34**	**59.96**	**55.71**
	76.00	91.86	82.95	65.70	83.41	92.56	96.13	93.41	89.14	65.85	95.75	87.26
	88.76	91.61	82.19	62.90	87.66	90.80	89.64	92.87	86.97	57.48	81.44	66.11
	65.63	90.04	92.50	88.28	94.55	87.50	81.68	94.28	85.52	84.62	77.21	70.41
Average	86.22	94.20	97.73	86.43	93.46	96.85	85.87	89.41	84.62			
TF28	**79.15**	**91.93**	**88.84**	**75.83**	**89.77**	**91.93**	**88.33**	**92.49**	**86.56**	**69.32**	**84.80**	**74.59**
	76.94	96.53	95.29	80.84	92.68	87.82	93.67	85.82	86.72	90.11	90.15	72.88
	81.91	92.16	90.43	92.21	96.62	93.72	88.75	94.60	84.77	91.60	82.37	83.51
Average	75.94	95.93	94.03	88.11	94.20	88.82	95.15	93.48	92.51	85.25	94.43	82.67
TF30	**78.27**	**94.87**	**93.25**	**87.05**	**94.50**	**90.12**	**92.52**	**91.30**	**88.00**	**88.99**	**88.98**	**79.69**
	79.39	71.34	70.04	72.73	66.80	55.88	46.25	69.73	66.41	84.56	87.72	73.02
	79.09	72.33	56.99	46.20	60.99	63.53	87.04	82.98	60.20	83.50	87.20	71.37
Average	83.96	77.30	45.19	90.98	89.33	76.42	71.71	89.95	43.48			
TF31	**80.81**	**73.66**	**57.41**	**69.97**	**72.37**	**65.28**	**68.34**	**80.89**	**56.70**	**84.03**	**87.46**	**72.19**
	63.20	94.94	79.84	84.50	90.01	69.64	95.01	88.97	87.34	87.64	83.41	45.61
	54.87	89.14	87.97	92.99	82.00	54.70	88.00	90.08	78.56	87.61	83.31	69.27
	79.57	91.53	92.08	91.70	90.98	78.59	92.62	90.48	91.98	80.66	77.52	77.91
Average	50.22	86.28	88.73	91.22	93.56	79.84	81.41	90.92	83.92	84.79	85.77	83.70
	61.97	**90.47**	**87.16**	**90.10**	**89.14**	**70.69**	**89.26**	**90.11**	**85.45**	**85.18**	**82.50**	**69.12**
Overall Ave.	**73.75**	**87.90**	**80.62**	**77.51**	**86.72**	**79.00**	**80.86**	**86.56**	**76.97**	**77.37**	**80.74**	**70.26**
St. Dev	8.14	8.29	14.37	10.90	8.41	11.75	12.70	6.62	13.92	12.55	11.88	9.00

Table D.5. Zonal cell viability data of 4-day controls (% dead cells).

	4 Day Control											
	LFL			LFM			LTL			LTM		
	Sup.	Mid.	Deep	Sup.	Mid.	Deep	Sup.	Mid.	Deep	Sup.	Mid.	Deep
ZIB5	36.70	41.64	53.72	62.73	90.40	50.00	26.61	53.46	63.47	55.16	67.81	60.00
	33.15	57.76	34.37	55.56	57.49	29.70	58.32	49.24	57.80	52.49	79.96	41.73
	16.11	49.69	56.16	57.20	86.58	47.92	19.75	66.53	56.34	22.41	73.99	51.57
Average	**28.65**	**49.70**	**48.09**	**58.50**	**78.16**	**42.54**	**34.89**	**56.41**	**59.20**	**43.35**	**73.92**	**51.10**
TF45	56.19	90.36	87.29	51.95	93.10	59.72	56.89	72.78	72.70	70.40	94.24	84.18
	63.73	86.71	81.34	64.36	91.62	58.11	61.55	70.87	80.09	66.72	87.64	71.33
	68.79	86.20	82.84	34.72	80.97	78.02	34.55	80.56	67.41	77.55	74.32	48.10
Average	**62.90**	**87.75**	**83.82**	**50.34**	**88.56**	**65.28**	**51.00**	**74.74**	**73.40**	**71.56**	**85.40**	**67.87**
532RF	74.87	70.98	82.48	77.08	56.85	93.25	79.05	86.12	57.25	73.14	90.51	83.45
	79.27	72.81	88.38	76.58	64.90	92.13	94.48	94.34	97.02	82.80	92.99	94.33
	90.53	82.99	78.53	89.80	84.51	85.59	96.68	89.10	75.92	88.48	77.67	83.85
Average	**81.56**	**75.59**	**83.13**	**81.15**	**68.76**	**90.32**	**90.07**	**89.85**	**76.73**	**81.47**	**87.06**	**87.21**
62881	57.08	92.16	89.95	93.76	84.77	66.83	79.07	89.48	81.92	85.63	64.33	69.58
	70.93	82.71	88.72	90.63	88.08	78.79	78.17	77.14	86.80	82.38	60.67	54.49
	75.38	87.48	84.00	86.40	92.77	94.85	83.53	71.17	68.97	79.19	62.75	68.78
Average	**67.80**	**87.45**	**87.56**	**90.27**	**88.54**	**80.16**	**80.26**	**79.26**	**79.23**	**82.40**	**62.58**	**64.28**
BF731	44.37	75.17	80.51	63.16	65.87	49.67	34.55	62.54	53.57	26.70	68.55	40.46
	40.94	68.88	45.95	52.94	60.71	37.04	58.72	56.26	48.64	54.49	77.03	49.88
	36.63	74.68	59.56	69.74	71.25	66.74				84.26	78.02	48.57
Average	**40.65**	**72.91**	**62.00**	**61.95**	**65.94**	**51.15**	**46.63**	**59.40**	**51.11**	**55.15**	**74.53**	**46.30**
TF39	41.30	62.18	46.36	63.19	88.85	73.55	46.17	76.38	77.01	63.53	50.42	55.64
	13.57	76.45	57.41	48.38	90.83	82.12	57.28	73.63	57.25	29.45	86.92	71.40
	51.83	71.64	51.73	64.07	92.08	79.63	40.85	63.36	53.70	51.06	59.84	59.95
Average	**35.57**	**70.09**	**51.83**	**58.55**	**90.58**	**78.43**	**48.10**	**71.12**	**62.65**	**48.01**	**65.73**	**62.33**
Overall Ave.	**52.85**	**73.92**	**69.41**	**66.79**	**80.09**	**67.98**	**58.49**	**71.80**	**67.05**	**63.66**	**74.87**	**63.18**
St. Dev	20.89	14.00	17.57	15.41	10.82	18.41	21.60	12.50	11.11	17.09	9.95	14.37

Table D.5 Continued.

	4 Day Control											
	RFL			RFM			RTL			RTM		
	Sup.	Mid.	Deep	Sup.	Mid.	Deep	Sup.	Mid.	Deep	Sup.	Mid.	Deep
ZIB5	69.77	87.46	71.88	44.72	75.66	73.24	46.86	69.50	62.17	38.21	70.90	78.02
	60.84	83.31	67.67	57.89	89.11	46.93	58.30	77.43	46.38	35.70	67.37	57.12
	47.89	75.50	56.60	71.31	84.77	66.84	61.60	77.15	44.96	61.55	83.37	68.10
Average	**59.50**	**82.09**	**65.38**	**57.98**	**83.18**	**62.34**	**55.58**	**74.69**	**51.17**	**45.15**	**73.88**	**67.75**
TF45	75.94	85.60	85.29	69.94	80.08	67.03	95.42	89.85	73.27	91.01	94.06	85.09
	58.80	85.31	76.06	61.49	91.37	81.36	89.89	89.68	84.47	83.96	92.36	88.93
	81.82	88.19	83.18	62.99	91.04	73.91	95.36	97.12	79.09	69.98	94.17	88.65
Average	**72.19**	**86.37**	**81.51**	**64.81**	**87.50**	**74.10**	**93.56**	**92.22**	**78.94**	**81.65**	**93.53**	**87.56**
532RF	95.19	94.93	98.00	96.23	92.31	95.88	82.27	96.89	99.57	86.78	87.53	85.58
	92.42	92.93	95.71	96.93	95.33	98.38	88.99	90.06	87.80	97.73	94.62	83.59
	97.62	90.65	90.43	95.74	92.09	66.47	82.07	95.12	95.70	97.93	98.77	92.02
Average	**95.08**	**92.84**	**94.72**	**96.30**	**93.24**	**86.91**	**84.45**	**94.02**	**94.35**	**94.15**	**93.64**	**87.06**
62881	84.52	92.51	91.14	78.25	91.75	80.98	69.89	76.60	77.63	70.18	75.06	80.69
	86.29	89.60	85.26	72.88	94.84	94.51	81.41	75.30	91.83	78.38	86.26	84.05
	85.71	89.46	86.19	93.63	95.25	84.23	86.22	75.71	80.50	89.72	94.60	80.12
Average	**85.51**	**90.52**	**87.53**	**81.59**	**93.95**	**86.57**	**79.17**	**75.87**	**83.32**	**79.42**	**85.30**	**81.62**
BF731	74.77	80.89	59.09	82.61	94.41	59.60	70.20	83.61	62.75	71.92	88.28	57.48
	75.70	9.00	70.74	55.22	79.11	63.32				64.69	62.76	45.61
	43.37	84.32	74.56	88.29	81.99	53.64				61.37	74.68	50.00
Average	**64.62**	**58.07**	**68.13**	**75.37**	**85.17**	**58.85**	**70.20**	**83.61**	**62.75**	**65.99**	**75.24**	**51.03**
TF39	35.23	84.36	68.27	55.76	87.75	51.30	62.22	89.61	85.79	81.45	81.78	57.98
	48.48	73.37	67.94	53.87	89.23	49.21	71.17	83.17	89.54	85.55	83.15	64.58
	62.04	81.58	77.89				65.27	75.90	70.99	63.90	86.56	89.04
Average	**48.59**	**79.77**	**71.36**	**54.81**	**88.49**	**50.26**	**66.22**	**82.89**	**82.11**	**76.97**	**83.83**	**70.53**
Overall Ave.	**70.91**	**81.61**	**78.11**	**71.81**	**88.59**	**69.84**	**74.86**	**83.88**	**75.44**	**73.89**	**84.24**	**74.26**
St. Dev	17.13	12.54	11.69	15.73	4.30	15.17	13.62	8.02	15.66	16.73	8.53	14.08

Table D.6. Zonal cell viability data of 4-P188 (% dead cells).

	4 Day P-188											
	LFL			LFM			LTL			LTM		
	Sup.	Mid.	Deep	Sup.	Mid.	Deep	Sup.	Mid.	Deep	Sup.	Mid.	Deep
TF46	70.59	81.13	63.62	90.23	91.15	77.31	85.81	82.66	83.04	73.82	92.76	88.89
	79.55	90.46	70.00	86.17	89.39	85.47	72.19	86.79	84.47	81.76	90.51	79.57
	67.10	84.73	74.00	87.00	89.66	85.97	91.38	76.75	79.05	76.19	93.57	89.13
	70.81	88.98	74.21									
Average	**72.01**	**86.33**	**70.46**	**87.80**	**90.07**	**82.92**	**83.13**	**82.07**	**82.19**	**77.26**	**92.28**	**85.86**
TF37	85.57	91.83	75.14	94.91	90.40	93.72	78.97	81.12	68.93	83.27	63.45	73.67
	78.53	90.90	73.96	84.51	88.74	73.03	92.73	85.21	66.36	77.94	88.58	58.26
	85.40	90.62	84.11	84.49	90.30	85.29	73.65	85.11	75.66	85.29	71.47	73.20
Average	**83.17**	**91.12**	**77.74**	**87.97**	**89.81**	**84.02**	**81.78**	**83.81**	**70.31**	**82.17**	**74.50**	**68.38**
DB4	89.91	92.38	71.21	95.22	91.51	95.53						
	84.36	91.61	90.82	93.92	93.32	98.37						
	87.50	89.41	94.55	95.62	86.06	87.47						
Average	**87.26**	**91.13**	**85.53**	**94.92**	**90.30**	**93.79**						
BF739	82.48	75.51	79.32	87.63	76.79	49.23	73.08	80.41	53.44			
	79.93	76.57	82.79	86.63	81.76	60.43	79.73	87.96	68.22			
	72.36	86.81	69.41	84.43	76.06	65.80	75.84	77.81	65.76			
Average	**78.26**	**79.63**	**77.17**	**86.23**	**78.20**	**58.49**	**76.21**	**82.06**	**62.47**			
TF36	89.58	82.74	85.75	93.00	86.46	91.09	75.38	89.32	81.74	73.62	64.22	69.84
	78.61	86.33	69.63	81.48	90.14	90.63	72.93	93.38	79.90		65.66	59.63
	89.58	88.14	75.68	28.99	84.36	76.10	80.06	76.47	80.29			
Average	**85.92**	**85.74**	**77.02**	**67.82**	**86.99**	**85.94**	**76.12**	**86.39**	**80.64**	**73.62**	**64.94**	**64.73**
STID	88.13	92.04	88.44	83.80	91.72	79.15	80.26	81.02	68.07	60.45	95.76	88.10
	67.23	81.45	85.06	78.51	85.19	83.54	67.48	77.48	82.65	50.89	89.55	65.91
				79.06	87.19	79.50	82.49	88.41	75.66	58.17	91.31	53.40
Average	**77.68**	**86.75**	**86.75**	**80.46**	**88.03**	**80.73**	**76.75**	**82.30**	**75.46**	**56.50**	**92.21**	**69.13**
Overall Ave.	**80.72**	**86.78**	**79.11**	**84.20**	**87.23**	**80.98**	**78.80**	**83.33**	**74.22**	**72.39**	**80.98**	**72.03**
St. Dev	5.78	4.25	6.07	9.26	4.61	11.90	3.38	1.86	8.05	11.15	13.58	9.42

Table D.6 Continued.

	4 Day P-188											
	RFL			RFM			RTL			RTM		
	Sup.	Mid.	Deep	Sup.	Mid.	Deep	Sup.	Mid.	Deep	Sup.	Mid.	Deep
TF46	72.22	81.91	84.93	73.30	94.69	91.95	65.35	89.17	83.95	79.53	80.00	59.10
	69.59	92.87	78.90	80.97	89.18	73.60	67.33	87.44	80.10	80.26	95.53	86.21
	77.17	78.22	77.44	71.12	92.66	83.13	68.75	77.00	68.80	82.72	79.86	80.96
Average	**72.99**	**84.33**	**80.42**	**75.13**	**92.18**	**82.89**	**67.14**	**84.54**	**77.62**	**80.84**	**85.13**	**75.42**
TF37	92.55	93.62	73.44	96.11	95.14	95.58	90.37	88.58	83.84	91.55	87.16	72.61
	89.31	93.45	66.61	97.30	93.71	82.82	92.31	93.18	88.03	86.87	81.88	88.46
	85.96	86.43	86.27	95.47	96.38	93.82	95.64	91.85	74.08	77.21	84.82	80.30
	88.70	91.99	87.83									
Average	**89.13**	**91.37**	**78.54**	**96.29**	**95.08**	**90.74**	**92.77**	**91.20**	**81.99**	**85.21**	**84.62**	**80.46**
DB4	86.78	90.84	79.59	92.86	94.87	96.12	85.41	79.50	88.70			
	56.04	91.31	88.73	88.35	93.13	78.25	94.07	82.94	89.15			
	83.57	85.66	90.36	71.37	83.30	76.99	89.25	88.72	80.00			
Average	**75.47**	**89.27**	**86.23**	**84.19**	**90.44**	**83.79**	**89.58**	**83.72**	**85.95**			
BF739	73.42	80.27	81.82	69.83	89.17	71.38						
	83.18	9.00	86.61	74.71	82.22	66.82						
	84.98	87.89	74.73	61.21	75.65	67.11						
Average	**80.53**	**59.05**	**81.05**	**68.58**	**82.34**	**68.44**						
TF36	85.47	89.66	85.44	86.89	93.70	82.95	62.75	90.80	89.81	80.68	85.47	79.58
	83.33	91.22	81.67	82.91	92.49	77.90	70.61	84.91	76.92	76.16	78.60	81.29
	86.05	90.05	92.08	91.46	92.83	88.95	72.46	85.47	80.00	88.37	87.64	86.58
Average	**84.95**	**90.31**	**86.40**	**87.08**	**93.01**	**83.27**	**68.61**	**87.06**	**82.24**	**81.73**	**83.90**	**82.48**
STID	87.50	95.77	70.66	83.37	91.49	48.88	82.04	86.37	47.77	45.51	75.71	78.06
	84.94	97.06	67.28	81.46	95.41	81.57	68.03	67.87	47.60	42.90	80.54	75.64
	82.77	96.58	62.65	83.61	92.26	68.24	81.95	68.99	77.48			
Average	**85.07**	**96.47**	**66.86**	**82.81**	**93.05**	**66.23**	**77.34**	**74.41**	**57.62**	**44.21**	**78.13**	**76.85**
Overall Ave.	**81.36**	**85.14**	**79.92**	**82.35**	**91.02**	**79.23**	**79.09**	**84.19**	**77.08**	**73.00**	**82.95**	**78.80**
St. Dev	6.20	13.36	7.15	9.61	4.51	9.68	11.76	6.19	11.28	19.29	3.25	3.24